Crystal Form and Defect Analysis of Pharmaceutical Materials

This dissertation is submitted for the degree of Doctor of Philosophy

Mark Eddleston

Clare College

July 2011

Declaration

The work described in this thesis was performed under the supervision of Prof. W. Jones in the Department of Chemistry at the University of Cambridge. This dissertation is the result of my own work and includes nothing which is the outcome of work done in collaboration except where specifically indicated in the text.

This thesis is not substantially the same as any that I have submitted or will be submitting for a degree, diploma or other qualification at this or any other University.

The work submitted is identical to that which was examined, except as required by the examiners by way of correction, and does not exceed the 60,000 word limit.

_____

Mark Eddleston
November 2011

Acknowledgements

I wish to thank my supervisor, Bill Jones, for giving me the opportunity to study for a PhD, for guiding me to interesting and fruitful areas of research, for invariably providing helpful suggestions during my studies and for making the whole process a really enjoyable one.

I am also grateful to Erica Bithell, Graeme Day, Katarzyna Hejczyk and Andrew Cassidy, whose contributions to this body of work have been invaluable, and to Saranja Sivachelvam for being a great summer project student (a thoroughly deserving Young Chemist of the Year!). I thank Graham Sharp for TEM training and for always being both helpful and cheerful.

I have been fortunate enough to work with many wonderful people in the Materials Chemistry Group over the years. Their friendships mean as much to me as the PhD which they have helped me to complete.

Life outside the lab has been equally enjoyable thanks to all of my friends and family, with particular mention to Alex Eberlin for countless stress-relieving evenings out to watch football.

This thesis is dedicated to my parents, whose care and support throughout the years is the reason that I have managed to achieve this doctorate, to my brother Jonathan, and to my wife, Madzia, for filling my world with warmth and happiness.

Contents

Abbreviations

AFM	Atomic force microscopy
API	Active pharmaceutical ingredient
BFDH	Bravais, Friedel, Donnay and Harker
BIPY	Bipyridyl
CSD	Cambridge Structural Database
CSP	Crystal structure prediction
DCM	Dichloromethane
DMF	N,N-dimethylformamide
DMSO	Dimethylsulphoxide
DSC	Differential scanning calorimetry
FT-IR	Fourier transform infra-red
HSM	Hot stage microscopy
NMR	Nuclear magnetic resonance
OM	Optical microscopy
PLM	Polarised light microscopy
R_1	Crystal structure R-factor.
SEM	Scanning electron microscopy
SSNMR	Solid-state nuclear magnetic resonance
TEM	Transmission electron microscopy
TGA	Thermogravimetric analysis
THF	Tetrahydrofuran
VBA	Visual basic for applications
VT-XRPD	Variable temperature X-ray powder diffraction
XRPD	X-ray powder diffraction

Summary

The main finding that is reported in this thesis is that transmission electron microscopy (TEM), a technique widely used for the study of inorganic specimens, can also be used to obtain useful information about pharmaceutical materials. The combination of high magnification imaging and diffraction capability with this technique enabled identification of the crystal form of samples, mapping of crystal habit to crystal structure, characterisation of pharmaceutical nanomaterials and identification of crystal defects, and often yielded information that could not be obtained with conventional analytical methods. Atomic force microscopy was used to obtain complementary information from the surfaces of samples.

A novel approach for the determination of crystal structures was developed and used to obtain the structure of a new crystal form (polymorph) of the pharmaceutically active compound theophylline. A set of potential crystal structures of theophylline was generated *'in silico'*, using crystal structure prediction (CSP) methods. TEM electron diffraction was then used to determine which of these potential structures corresponded to the new crystal form. The major advantage of this approach is that just a small number of electron diffraction patterns are required for the crystal structure determination. These patterns can be collected before a significant amount of electron beam damage occurs in a sample, enabling the strength of TEM as a tool for characterising small amounts of sample to be exploited.

The methods that are routinely used to prepare cocrystals of pharmaceuticals are grinding, crystallisation from solution, slurrying and thermal methods. In this study, three alternative approaches to cocrystal formation were developed which overcome limitations with the more commonly used methods, and also offer potential advantages for the scale up of cocrystals. During this work, a number of polymorphic cocrystal systems were identified.

Crystals of the compounds caffeine, theophylline, carbamazepine and aspirin were prepared with an unusual tubular crystal morphology. It is demonstrated that the growth of these tubular crystals occurs under diffusion limited conditions.

1 Introduction

1.1 Context

"There is nothing we can do today to prevent a hurricane from striking any community or polymorphism from striking any drug"

- Dr Eugene Sun, Abbott Laboratories[1]

Understanding the solid state behaviour of a pharmaceutical compound is an integral part of the drug development process.[2] The importance of this understanding is highlighted by the drug product NORVIR, a treatment for AIDS, which had to be withdrawn from the market due to the unexpected crystallisation of a new solid form of the active ingredient ritonavir.[3] The above quote was given by a scientist working on NORVIR shortly after this withdrawal, and his use of the hurricane analogy probably alludes to the devastation experienced by the patients who were suddenly left without a supply of their vital medicine, and the turmoil within Abbott Laboratories as the scientists sought to understand the implications of this unexpected solid state behaviour of ritonavir.

This chapter gives an overview of the roles of solid state chemistry in the pharmaceutical industry. It covers the different types of crystal forms that are investigated, methods that are employed to screen for these forms and analytical techniques that are used to identify and characterise them. Particular attention will be paid to one particular type of crystal form - the cocrystal.

Limitations and difficulties associated with the screening methods and analytical techniques are known, and these provided motivation for the experimental work described in the subsequent chapters of the thesis. An overview of the aims of the investigation is given at the end of the introduction.

1.2 Solid Forms of Pharmaceutical Compounds

The development of a pharmaceutical product involves several stages. Initially, a decision is made about which illness(es) a company will aim to treat. A specific stage of the disease pathway which might be disrupted by a drug molecule, often activation or inhibition of an enzyme, is then identified. In general, the subsequent lead identification phase involves testing the *in-vitro* activity of a vast library of small organic molecules against a relevant biological marker. Compounds that show a response will be modified systematically to optimise their activity (lead optimisation) and one final molecule will be selected for drug development. This active pharmaceutical ingredient (API) will be formulated along with several excipients into a drug product such as a tablet for oral administration or a dry powder for inhalation, and simultaneously subjected to clinical trials to assess toxicity and efficacy *in-vivo*. An application for permission to market the drug can then be made to the relevant authorities. This process typically takes around 10 years to complete[4] and costs approximately $1Bn. For every drug product that makes it to market, it is estimated that 10 fail during the development process.[5]

The solid state behaviour of a pharmaceutical is not usually investigated until after the lead optimisation phase, when a single drug molecule (or at most 2 or 3 molecules) has been selected. A suitable solid form of the drug is then chosen and will be used throughout the formulation and clinical trial stages of development.

It is common that multiple different solid forms of a pharmaceutical compound are identified during drug development, including polymorphs, hydrates, solvates, salts, cocrystals and amorphous phases.[6] The crystalline forms are shown schematically in Figure 1.1.

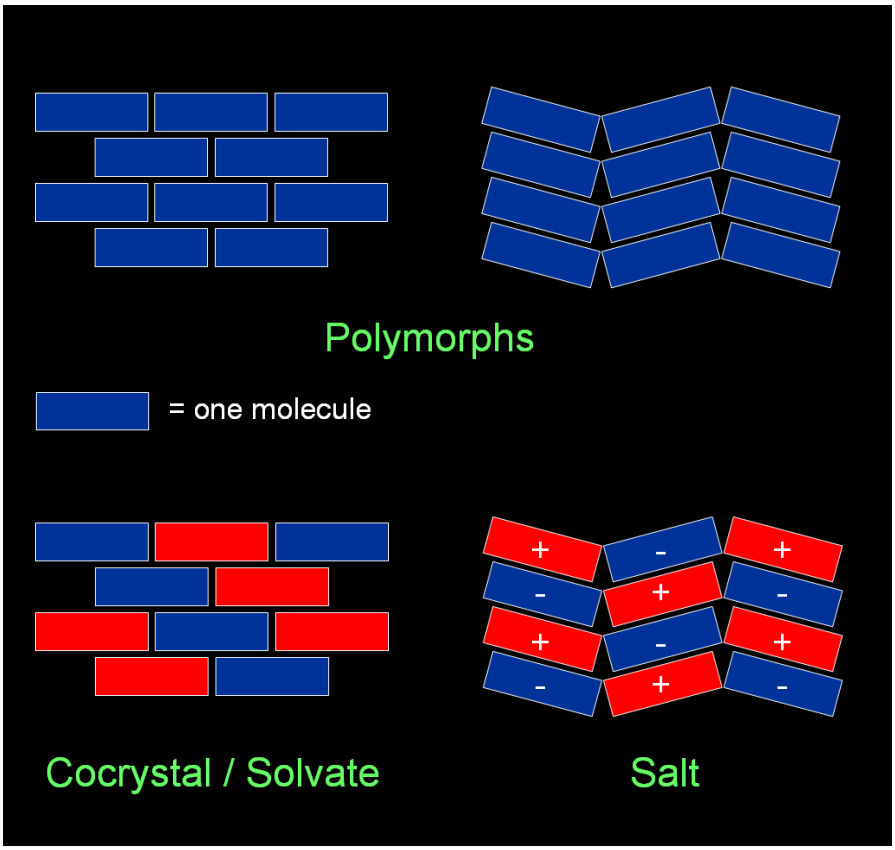

Figure 1.1 Schematic showing the different types of crystal forms of pharmaceutical compounds. Different crystal packing arrangements of the same API are known as polymorphs. APIs can also form multi-component crystals. In cocrystals and solvates the molecules are neutral, in salts the molecules are charged.

Polymorphism is the ability of a compound to form multiple different crystal structures,[7] and a majority of pharmaceutical compounds exhibit polymorphism.[6,8-10] Water and other solvents can also be incorporated into a crystal lattice along with the drug molecule leading to the formation of hydrates and solvates (pseudopolymorphs). These polymorphs and pseudopolymorphs have different properties, and may have different bioavailablities,[11] meaning that a different amount would need to be given to a patient in order to deliver a therapeutic dose. It is therefore extremely important to control the polymorphic form of a pharmaceutical compound in a drug product.

Pharmaceuticals are often large, hydrophobic organic molecules with low aqueous solubility, and the current trend is towards larger and less soluble molecules.[12] Low

solubility can lead to low bioavailability,[13] and it may not be possible to obtain a therapeutic dose within patients. For APIs with ionisable functional groups this problem can be overcome by preparing salts,[14,15] which may have aqueous solubilities that are several orders of magnitude greater than that of the neutral compound.

In the case of ritonavir, the drug product was designed around Form I, the only polymorph that had been identified at the time. The product was formulated by dissolving ritonavir in an ethanol/water mixture and encasing the solution within a semi-solid capsule which patients would take orally. At some point, however, it was observed that a solid was precipitating in the capsules. The solid was found to be a second polymorph of ritonavir, a form which had a greater lattice energy than Form I, making it more stable and less soluble. Most importantly, the bioavailability of Form II was significantly lower than that of Form I, meaning that patients were no longer receiving the required therapeutic dose of ritonavir when taking the semi-solid capsules, necessitating the withdrawal of the product from the market.[3]

1.2.1 Discovery and Preparation of Pharmaceutical Solid Forms

Each drug molecule in development is screened thoroughly to identify all of the solid phases that it will form. Not only is this polymorph screening required by the regulatory authorities to prevent situations similar to that of ritonavir, it is also in the interest of the pharmaceutical company developing the active compound from an IP point of view. Any new solid form that is identified may have beneficial properties which would enable them to be patented, extending the period during which the company has exclusive rights to market the compound (and can recoup the vast amounts of money that were spent in developing the drug). Patenting all solid forms of a drug is also important as it prevents the possibility of competitors finding these forms and obtaining their own IP rights to the compound.

Thermal screening methods exploit the fact that for many drug compounds the relative thermodynamic stability of polymorphs varies with temperature. For example, the stable phase of caffeine at room temperature, Form II, is less stable than the other known polymorph of caffeine, Form I, at temperatures above 150 °C.[16] This kind of

polymorphic relationship is referred to as enantiotropic, and the polymorphic form which is stable at room temperature can be either heated or cooled to induce a phase transition to a different polymorph. The other possibility, where one polymorph is the most thermodynamically stable form at all temperatures below the melting point of the compound, is termed monotropic. A second method of thermally accessing different polymorphs is to make use of crystallisation kinetics. Heating the amorphous form of a compound (which can be obtained by quench cooling the melt, or by using freeze/spray-drying) can yield metastable polymorphs, as it is often metastable forms that are the first to crystallise.[17] For example, a new, metastable polymorph of RS-ibuprofen was recently prepared by crystallisation from the amorphous phase.[18]

Crystallisation from solution is a complex process involving supersaturation, nucleation and crystal growth.[12,19,20] The solvent which is used during crystallisation can influence the crystal form that is obtained through kinetic, thermodynamic and/or specific intermolecular interaction effects.[19] For this reason, solution crystallisation screens are widely used to investigate polymorphism, and will typically involve a large set of solvents selected to have as wide a range of properties as possible.[21] Conditions such as level of supersaturation, temperature and evaporation rate may also be varied.[19]

A second type of screen, which also uses solvent properties to direct formation of different polymorphs, is slurrying. Here, the amount of solvent that is used in the experiments is less than that required to dissolve all of the solid that is used as input material, meaning that the drug is present both as a solid and as a solute. The slurry is then subjected to thermal cycles to cause dissolution and re-crystallisation and promote a change in the crystal form of the solid. One limitation of the slurrying technique is that there may be a seeding effect due to the presence of the crystalline input material. Seeding is a process where molecules in a supersaturated solution crystallise on the surface of existing crystals (causing them to grow) rather than nucleating and forming crystals of a different phase.[4,22] For this reason, the crystal form that is present at the start of a slurry experiment may persist, even if it is not the most thermodynamically stable phase under the solvent conditions used in the experiment.

In order to increase the range of crystallisation conditions that are investigated in solution and slurry polymorph screens, high throughput approaches can be used.[19,23] This will typically involve a robot capable of solid and/or liquid handling, and experiments performed in 96 or 384 well plates, with automated analysis of the resulting samples.[24]

Although solution and thermal polymorph screening methods are the most frequently used, there are many other approaches that can be employed such as sublimation, crystallisation with supercritical CO_2, epitaxial crystal growth and application of pressure to crystals.[9,25]

When screening for salt forms of an API, suitable acids / bases are selected, for regulatory reasons, from a small number of pharmaceutically acceptable counterions.[15] In order for a stable salt to form it is generally necessary for there to be a pKa difference of at least 2 units between the acidic and basic groups of the salt forming molecules.[26] Just like the free form of the active compound, these salts may have polymorphic and pseudopolymorphic forms, and so polymorph screens are also conducted on salts.[27]

Polymorph and salt screening is usually performed on a small scale, typically just a few milligrams of solid per experiment, since the drug substance is not being synthesised in large quantities at the point in the drug development process that screening is conducted. Though a variety of screening techniques are employed in identifying new phases, solution crystallisation is the optimum method for the large-scale manufacture of a drug substance.[4] It may be necessary to add seed crystals of the desired polymorph of a drug to a crystallisation in order to generate this form in preference to other polymorphs.[4,22]

1.2.2 Selection of the Optimum Solid Form

All of the solid forms that are identified during polymorph and salt screening will be characterised to determine if they are anhydrous or solvated phases, and to measure their properties. An ideal solid form will have high purity, and a solubility / dissolution rate sufficient for the therapeutic dose of the compound to be achieved in the body. It will have low hygroscopicity to prevent problems of inconsistent dosing due to variable water content, and a melting point high enough to avoid melting during drug product manufacturing processes such as tableting. The crystal habit should not be needle-like or plate-like as this can cause problems with filtration, drying and handling, and if the form is taken orally it should not have an unpleasant taste. Whereas the properties of different polymorphs of an API tend to be similar, salt forms often have more diverse properties. An ideal salt form will incorporate a non-toxic counterion that has a low molecular weight, as the inclusion of a counterion increases the mass of the tablet or capsule that the patient must swallow without contributing to the therapeutic action of the drug.[28]

The final choice of solid form for use in a drug product will take into account not only these properties, but also solid state stability. A solid form with an ideal solubility profile may be a poor candidate for development if it will rapidly convert to a more stable, less soluble polymorph. For example, an amorphous phase of a pharmaceutical can be expected to have an enhanced intrinsic dissolution rate over crystalline forms, but it is a thermodynamically metastable phase and may well be liable to crystallise.[29] Similarly, solvates are not generally considered suitable for use in a drug product as over time the solvent molecules may leave the crystal lattice and evaporate, resulting in a form change.[12,24] The one exception to this rule is hydrates. Hydrates may be stable under normal atmospheric conditions if water in the crystal lattice is in equilibrium with water in the atmosphere.[4]

Solid forms of pharmaceutical compounds need to be physically and chemically stable during drug product manufacturing processes such as milling and tableting, and during storage under conditions of high temperature and humidity (40°C / 75% RH),[30] mimicking conditions that might be encountered in a bathroom cabinet or car glove

box on a hot day. In practice, a wide range of techniques and storage conditions are used in order to thoroughly understand the conditions under which solid forms of a pharmaceutical compound will inter-convert.

Though Dr Eugene Sun has suggested that nothing can be done to prevent polymorphism from striking a drug, in practise, the more work that is put in to discovering all of the possible solid forms of a drug, and understanding the transformations between these forms, the less likely it is that problems such as those encountered with ritonavir will re-occur.

1.2.3 Cocrystals as Novel Pharmaceutical Forms

Recently, cocrystals containing pharmaceutically active molecules have been investigated as a way of improving the properties of drug molecules, building on cocrystallisation studies with organic molecules that were conducted by many groups including that of Etter.[31,32] The first systematic studies of pharmaceutical cocrystals were performed by the groups of Caira, who prepared cocrystals of aspirin and 4-aminosalicylic acid with sulfadimidine,[33] and Zaworotko, who cocrystallised RS-ibuprofen, RS-flurbiprofen and aspirin with 4,4-bipyridine,[34] and also prepared a variety of cocrystals of carbamazepine.[35] There has been increasing interest ever since, but single component and salt forms of an API are still far more prevalent in drug products. Only two cocrystal forms of a drug molecule have been marketed to date, a caffeine:citric acid cocrystal and darunavir ethanolate, though other cocrystal forms are currently undergoing clinical trials.

Cocrystals contain two or more neutral molecules in a crystal lattice (see Figure 1.1). There is debate in the literature as to whether or not the molecules are required to be solids at room temperature,[12,36] but as this seems to be a rather arbitrary requirement (a solid form containing DMSO could be a cocrystal on a cold winter's morning and not a cocrystal on a warm summer's afternoon), solvates and hydrates will be classified as cocrystals in this thesis. From a pharmaceutical perspective, cocrystal forms that comprise coformers that are solids at room temperature are preferred to solvates as they are likely to be more stable, and so more suitable for development.[12]

1.2.3.1 Advantages of Cocrystals

It is a relatively common occurrence that none of the polymorphic forms of an API in development are suitable for use in a drug product, and that salt forms are either impossible (as the molecule has no ionisable functional groups), or are also unsuitable. Free forms of an API often exhibit low bioavailability, whereas salts can be hygroscopic and prone to hydration problems. In these cases, cocrystallisation may provide a strategy for form development. The first example of cocrystal formation being used to improve the properties of an API is that of the prevention of hydrate formation in caffeine. Trask et al showed that cocrystals of caffeine with dicarboxylic acids showed a greater stability to hydrate formation than the free form of caffeine.[37] Subsequently, cocrystallisation has been used to modify many other properties such as chemical stability,[38] propensity for polymorphism,[39] tableting behaviour[40] and melting point.[35,41]

There have been many studies on the solubility of cocrystals, and though the thermodynamic aqueous solubility of an API is not always improved significantly by cocrystallisation (as in solution the cocrystal is dissociated and the API can crystallise),[36] improvements in the kinetic solubility and dissolution rate have been observed.[42-44] For example, the dissolution rate and solubility of certain cocrystals of itraconazole were shown to be equivalent to amorphous itraconazole.[45] There is evidence of a 'spring and parachute' effect[13] in the solubility-time profile of many cocrystals. They initially dissolve to a concentration much greater than the thermodynamic solubility of the API, and subsequently the concentration decreases slowly, not reaching the thermodynamic solubility of the API for an hour or more.[36] This may be long enough to have a significant improvement on the bioavailability of the API.[42,44]

1.2.3.2 Screening for Cocrystals

Currently, cocrystallisation is not an entirely predictable process.[46-48] Not every selected pair of molecules will form a cocrystal, and the propensity for different pharmaceutical molecules to cocrystallise varies greatly. For example, there are over 40 reported carbamazepine cocrystals in the Cambridge Structural Database (CSD), formed with molecules containing a range of functional groups, whereas for other molecules such as artemisinin preparing any cocrystal is a challenge.[49] Additionally, the ratio of coformers in the crystal form does not have to be 1:1. 2:1 and 1:2 stoichiometries are also common.[34,45,50]

The first stage of cocrystal screening with an API is the selection of coformers which may be expected to cocrystallise with the API. These compounds must be non-toxic, and will typically be one of the pharmaceutically acceptable salt formers or a compound on the Generally Regarded as Safe (GRAS) list.[12,46,51] The selection is usually made by studying the functional groups that are present in the API, and identifying coformers with complimentary functionalities that would be expected to form strong hydrogen bonds with the API.[32,35,52] The CSD is a useful resource for assessing the frequency with which different types of hydrogen bonding interactions (supramolecular synthons) occur in crystal structures.[47,52,53]

Each API / coformer pair is then screened experimentally. A simple approach is to crystallise an equi-molar ratio of the two compounds by evaporation from a range of solvents. Although such solution based approaches are desirable for scale-up and manufacturing,[46] and have been used successfully for cocrystallisation,[54] often the cocrystal formers crystallise as separate phases due to the difference in their solubilities.[46,55-57] For this reason, solution approaches are not ideal for cocrystal screening as a negative result does not necessarily indicate that the two coformers will not form a cocrystal.

Another method that has been used to prepare cocrystals is slurrying,[58,59] which is a way of avoiding the problem of differences in the solubility of cocrystal formers as neither coformer is fully dissolved,[58] though there can be issues with seeding (as

described in Section 1.2.1). Seeding may prevent two compounds from nucleating as a cocrystal phase even if this phase is thermodynamically favourable. Slurrying is also much less suitable for the manufacture of cocrystals on a large scale than solution crystallisation.[60]

Cocrystals have also been prepared by grinding coformers in the solid state, which again avoids solubility problems.[55,57] The grinding can be done by hand using a mortar and pestle, or more energetically with a mechanical ball mill. The addition of a small amount of liquid to the grinding vessel (liquid assisted grinding) has also been shown to increase the likelihood and rate of cocrystallisation.[61] There is debate in the literature as to the mechanism by which cocrystallisation occurs during grinding,[62] with amorphous intermediates, vapour diffusion and intermediate liquid (melt) phases all being postulated.[56,63,64] A key advantage of grinding is that it is a quick and simple technique to use, furthermore, a recent study showed that some cocrystals of nicotinamide that were prepared by grinding could not be obtained (at least without further experimentation) from solution crystallisations.[50] As with slurrying, there is potentially a seeding effect in grinding, though this has not been investigated in detail. Grinding is not a convenient and reproducible way of manufacturing a solid form of a drug on a large scale.[48,54]

Another approach to cocrystal screening is to crystallise a mixture of API and coformer from the melt either by the Kofler method[65] or by differential scanning calorimetry.[66] Cocrystals of many APIs, including RS-ibuprofen,[67] have been prepared in this manner, and the related technique of hot melt extrusion can be used to perform melt cocrystallisation on a large scale.[68] This approach, however, can only be applied to the small percentage of pharmaceutical compounds which do not undergo degradation on melting.

Other techniques that have been used to prepare cocrystals are sonication, spray drying and supercritical CO_2 crystallisation.[69-72]

1.3 Identification and Characterisation of Pharmaceutical Solid Forms

The standard technique for characterising samples that are generated during API solid form screening experiments, and for monitoring the solid state behaviour of crystal forms, is X-ray powder diffraction (XRPD).[73] Every peak in an XRPD trace corresponds to Bragg diffraction from one set of crystal planes, and as different crystal forms have unique sets of crystal plane spacings, their X-ray powder diffraction patterns are different, and can be used as a 'fingerprint' of the form. XRPD analysis is a quick and easy way of determining if new phases have been obtained from screening experiments. The minimum amount of sample that is required for an XRPD trace is approximately 1 mg.

Another indication that a new crystal form has been obtained, or that a solid form transformation has occurred, is a change in crystal morphology. There are several microscopy techniques that can be used to observe such changes, the simplest of which is optical microscopy (OM) / polarised light microscopy (PLM). If necessary, higher magnifications can be achieved by using scanning electron microscopy (SEM), a technique which yields images of the surfaces of crystals rather than the bulk. SEM is also useful for measuring particle size, which is linked to the dissolution rate of crystals. Atomic force microscopy (AFM) is a relatively new imaging technique for pharmaceutical analysis.[74] A sharp tip on a small metal cantilever is run over the surface of a sample and if there is a change in the height of the sample surface (or in the force of interaction with the probe) this causes the cantilever to bend. The bending of the cantilever is monitored and can be used to generate an image showing surface features.[75] AFM is so sensitive that atomic resolution is possible.[76]

The existence of new API phases can also be determined thermally, as different crystal forms have different melting points. Differential scanning calorimetry (DSC), which measures changes in the enthalpy of a sample during heating, can be used as a sensitive way of measuring the melting point of samples. It is also a tool that can be applied to screening for any form changes that occur on heating or cooling a sample. Raman spectroscopy and solid-state NMR (SSNMR) are also sensitive to differences

in crystal structure, if there are variations in the intermolecular interactions that are present, and are frequently used to identify different forms of APIs. However, the differences between the Raman and SSNMR spectra of different polymorphs of a compound are often subtle,[77] making these techniques more suitable for monitoring solid-form transitions in well understood systems rather than for finding new phases during screening. Raman analysis of pharmaceuticals is also associated with problems such as fluorescence, which can give rise to noisy spectra, and sample heating which can cause form changes.[78,79] Raman microscopy is used to generate images which show the distribution of different crystal forms across a sample, and has a resolution of a few micrometers.[78]

Difficulties can arise with these techniques when analysing mixtures of forms as spectra are made more complicated by multiple sets of overlapping peaks, and it may be impossible to detect all of the phases that are present in a sample. The limit of detection of a minor phase in a mixture of two crystal forms has been determined to be between 0.1 and 1 % for XRPD, as low as 0.9 % for Raman spectroscopy and 0.1 % for DSC.[80-82]

For any new form that is identified during screening experiments, further analysis must be performed to determine the nature of the form. Ideally, the crystal structure would be solved using single crystal X-ray diffraction (SXD), giving the unit cell dimensions for the crystal form and the position of each of the atoms and molecules in the unit cell. For typical laboratory single-crystal diffractometers this requires a high quality crystal with a reasonably isotropic morphology, such as a block or prism, and a large size (~200 μm), but it is not always possible to grow such a crystal.[57,83] With the latest generation of diffractometers structures are possible from crystals several times smaller than this and at a synchrotron a crystal of just 1 μm^3 may be sufficient. If small crystallite sizes or anisotropic crystal morphologies such as needles or plates prevent the use of SXD analysis, crystal structures can sometimes be determined from XRPD traces using structural solution algorithms, or by comparison with output from crystal structure prediction.[57,84] SSNMR analysis can also provide limited information about crystal structures such as the number of molecules in the asymmetric unit (number of non-symmetry equivalent molecules in the unit cell).[25]

Frequently, it is not possible to solve the crystal structure of a new crystal form, but it is still important to determine if it is a single component (polymorph) phase of the API, or a salt / cocrystal, and to ensure that the molecular structure of the API has remained unchanged (i.e. that the new form is not a degradant of the API). This information can be obtained by ^{1}H NMR spectroscopy. When solvated forms are obtained, thermogravimetric analysis (TGA) is used to determine stoichiometries by accurately measuring weight losses due to evolution of solvent during heating.

An overview of the characteristics of the main pharmaceutical analytical techniques is shown in Table 1.1. Transmission electron microscopy (TEM), though a technique that has not found widespread use in pharmaceutical analysis, has also been included as it was identified as a tool which could fill some of the gaps in the pharmaceutical characterisation toolkit.

Table 1.1 A table showing features of the analytical techniques routinely used for pharmaceutical analysis.

Analytical technique	Bulk / Individual crystal	Surface / Entire crystal	Imaging Resolution	Crystal structure information
XRPD	Bulk	-	-	√
SXD	Individual crystal	Entire crystal	-	√
DSC / TGA	Bulk	-	-	X
SSNMR	Bulk	-	-	~
Raman / IR	Bulk	-	-	X
Raman imaging	Individual crystal	Surface	Low	X
Optical microscopy	Individual crystal	Entire crystal	Low	X
SEM	Individual crystal	Surface	Medium	X
AFM	Individual crystal	Surface	High	X
TEM	Individual crystal	Entire crystal	High	√

1.4 Introduction to Transmission Electron Microscopy (TEM)

Transmission electron microscopy has been developed as an analytical tool for over 50 years and is widely used for the characterisation of inorganic samples such as metals and minerals.[85-90] A photograph of a TEM instrument is shown in Figure 1.2. A coherent beam of electrons is generated at the top of the instrument and passes down the column, through the sample, and is focussed on a screen at the bottom. Samples for TEM are prepared on a circular mesh grid, usually made of a metal such as copper, approximately 3 mm in diameter. The grid is then placed into a sample holder and inserted into the instrument. Only a small region of the sample grid is viewed at any one time, but the grid can be moved within the instrument so that the whole area of the grid can be analysed.

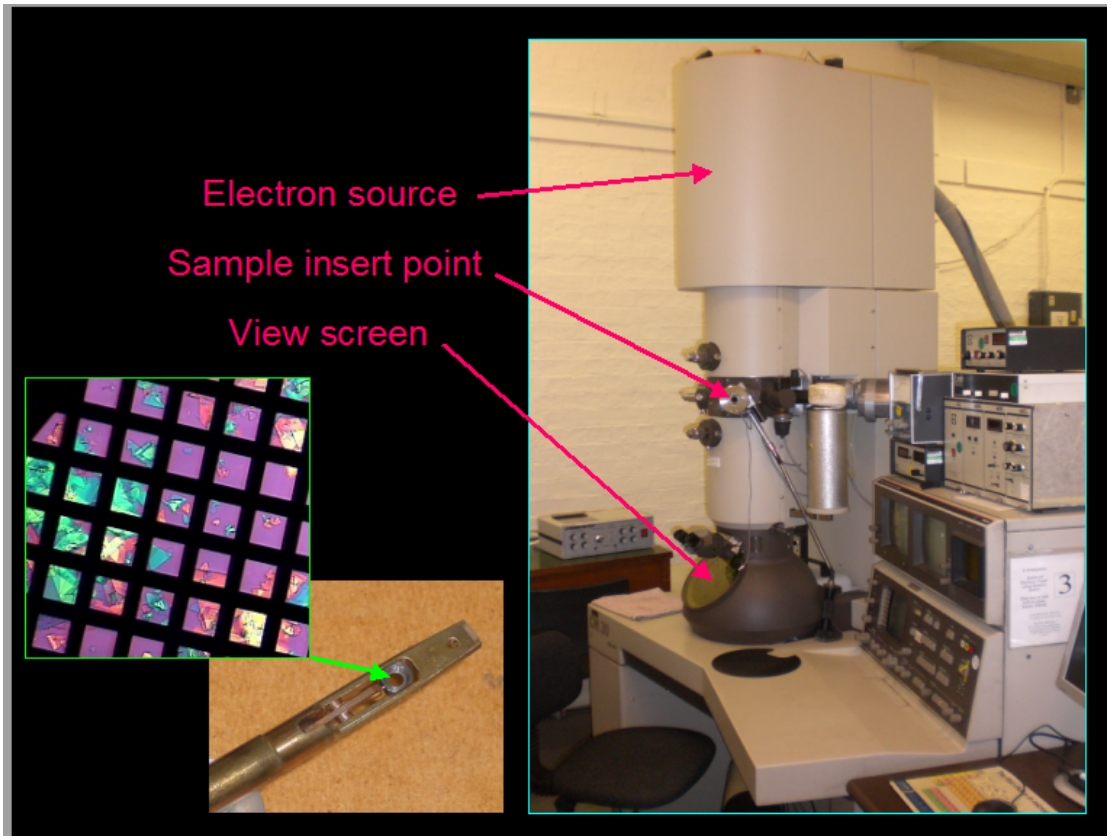

Figure 1.2 Pictures of a TEM sample grid (left), sample holder (bottom left) and instrument (right).

Some of the electrons will pass straight through the sample, while others will be scattered. Electrons can be focussed with lenses to form an image, and the scattering gives rise to contrast in the image through differences in sample thickness, density and composition. The technique has a high spatial resolution, better than 0.1 nm for modern aberration-corrected instruments, allowing direct imaging of the crystal lattice.[91] This ability, however, will require the specimen not to be charged or damaged by the incident beam (see later).

Transmission electron microscopes also have a diffraction mode. Electron diffraction from crystalline materials is analogous to X-ray diffraction, but as the wavelength of electrons is of the order of two magnitudes shorter than that of X-rays (0.0197 Å at 300 kV) the Bragg scattering angles are correspondingly smaller. Diffraction patterns are usually obtained by aligning the electron beam with a crystallographic axis. Because samples are not perfectly flat, and Bragg angles are small, the resulting diffraction pattern will contain reflections from each of the crystal planes that are perpendicular to the crystallographic axis. Electron diffraction patterns from each (non symmetry related) crystallographic axis of each different crystal structure are unique, and can therefore be used to identify crystal forms and measure the orientation of crystals with respect to the electron beam. It is also possible to solve crystal structures by combining diffraction patterns, but the process is not as straightforward as with single crystal X-ray diffraction due to difficulties in obtaining accurate reflection intensities.[92] Electron diffraction patterns can be obtained from very small amounts of sample (< 1 fg).[93]

Changing between imaging and diffraction modes in a TEM is easily achieved by varying the current through the electron lenses. Corresponding image and diffraction data from samples can therefore be readily obtained, and is a particular strength of the technique.

1.4.1 Application of Transmission Electron Microscopy to the Analysis of Pharmaceutical Samples

A majority of the few literature examples of TEM analysis of pharmaceutical samples report imaging of liposomal, micellular and polymeric formulations of an API.[94-96] The use of TEM to study the solid form of an API has been very limited. Crystals of the compounds dipyridamole[95] and taxol have been imaged,[97] as have defects in liquid crystals of fenoprofen,[98] and there has been an electron diffraction study on roxifiban,[99] but the full potential of the technique has yet to be fully appreciated. There are two main reasons for this. The first relates to sample preparation: because of the strong interaction of the electron beam with the sample[90] it is required that specimens be very thin (<<500 nm even for light, organic compounds).[100] It is difficult to prepare crystals of this size, and while thin films of metals and minerals can be prepared from larger crystals by focussed ion beam milling or mechanical polishing, the fragile nature of pharmaceutical molecules makes this impractical. The second concern is the inherent susceptibility of an organic material to electron beam damage.[100] In an electron beam, crystals of organic compounds are prone to bending, amorphisation, sublimation and even melting. Despite these problems, many TEM studies of organic compounds have been made.[93,100-102]

Assuming that these difficulties could be overcome with pharmaceutical samples, there are several potential advantages of characterisation with TEM. Firstly, the resolution possible with TEM imaging is approximately an order of magnitude greater than with SEM. Also, the entire volume of particles is analysed with TEM making it complimentary to SEM, and also AFM, which image the surfaces of samples. Electron diffraction patterns could be used as a 'fingerprint tool' to identify the solid phase of a pharmaceutical compound, just as XRPD traces are used currently, but could be obtained from far less material (just a single crystallite). As crystals can be analysed one by one during TEM analysis, all of the phases present in mixtures could be identified, even if they are present in low proportions. This would be aided by the TEM imaging mode, as crystals of the different forms that are present in a sample could be distinguished by their different morphologies. Also, image (real space) and diffraction (reciprocal space) information about pharmaceutical crystals could be

combined making it possible to map crystal structure to crystal habit. This information is important when trying to modify crystal habit, and currently requires the use of single crystal X-ray diffraction. Finally, TEM could be an ideal technique for the characterisation of pharmaceutical nanoparticles, yielding a range of useful information such as particle size distribution, particle morphology and crystal phase. Interest in sub-micron sized particles of pharmaceuticals is increasing due to enhanced properties such as solubility.[103-106] Characterisation of pharmaceutical nanoparticles is not straightforward, and TEM would compliment the methods that are currently used such as SEM, IR and dynamic light scattering.[107-109]

In general, TEM has moved away from simple imaging and diffraction analysis towards approaches such as aberration-corrected high resolution imaging, electron tomography and scanned probe methods which give directly interpretable images or yield three dimensional data.[93,110] However, because these methods require high signal to noise ratios, and therefore high electron doses, it is unlikely that they will be applicable to pharmaceutical samples.

1.5 Crystal Defects and their Influence on Solid State Chemistry

Crystals are defined as collections of atoms or molecules that are arranged into an ordered, 3-dimensional repeating lattice, with the simplest repeating section referred to as the unit cell. In real crystals, however, the ordering is not perfect, resulting in defects.

Interstitial defects, where there is either a molecule missing from a lattice site, or an additional molecule included in a non-lattice site, exist in large numbers in all crystals. The presence of linear defects such as edge dislocations and screw dislocations, and planar defects such as stacking faults, will vary depending on the crystal form (see Chapter 9 for more detailed information about crystal defects). Linear and planar defects in crystals can be imaged by TEM, or by AFM if they are emergent at a crystal surface.[111,112]

The defects that are present in inorganic crystals are well understood,[85,113] and have been correlated to bulk properties such as metal fatigue and conductivity in superconductors.[114,115] Furthermore, defects have been linked to the solid form stability of inorganic materials. It has been shown that defects are sites in crystals at which chemical reactions and transformations, such as polymorphic transitions and hydrate formation, are initiated.[116-119] For example, Thomas et al demonstrated that the dehydration of nickel sulphate hexahydrate in single crystals occurs at regions of the crystal surface where defects are found.[120] Also, defects have been shown to influence the rate at which polymorphic transitions (from a metastable polymorph to a more stable one) occur.[121] The transition process involves two steps. Firstly, a nucleation step where atoms/molecules locally re-organise into the structure found in the more stable polymorph. Secondly, there is propagation of the more stable phase throughout the crystal from the nucleation point. The propagation stage is rapid, often proceeding at a rate greater than the speed of sound. In contrast, the nucleation step has a large energy barrier associated with straining or breaking intermolecular interactions, and the rate is usually several orders of magnitude slower. Sometimes nucleation occurs at just one point in a crystal during a conversion.[121] Crystal defects can have a very significant affect on the rate of nucleation as in the local area around a defect the atoms/molecules are arranged differently than in the bulk crystal. Depending on the type of defect, the local arrangement of atoms/molecules may be similar to that in the stable polymorph, in which case the kinetic barrier to nucleation of this polymorph would be lower in this region, and nucleation more rapid. In a martensitic transformation, the polymorphic conversion occurs at an interface (defect surface) which is crystallographically coherent for the two phases.[117]

These studies would suggest that defects should be a key concern for the pharmaceutical industry, given the serious consequences of unexpected polymorphic conversions in pharmaceutical compounds[3] and indeed, the potential importance of defects has been recognised.[122-124] In addition, Byrn et al have demonstrated that crystal defects can have an influence on pharmaceutical solid-state behaviour by showing that introducing defects into crystals of caffeine monohydrate caused them to dehydrate more rapidly.[125] It is, therefore, surprising that the amount and nature of defects in crystals of a pharmaceutical compound is very rarely well understood, or even studied at all, during drug development within the pharmaceutical industry,[123]

especially as processes that are routinely used in the manufacture of pharmaceutical products such as milling, drying and tableting introduce defects into crystals.[123,126,127]

The few literature examples of defects in pharmaceutical crystals being observed and characterised have involved the use of chemical etching, X-ray topography or atomic force microscopy.[124,128,129] Additionally, defect content in crystals has been calculated using X-ray diffraction, X-ray density measurements and grazing incident diffraction.[123,126,127,130]

The primary reason that defects are not routinely studied in pharmaceutical materials could be the very limited application of TEM, the ideal technique for characterising defects, to pharmaceutical analysis. TEM has been used to study defects in crystals of other organic compounds such as anthracene,[131] pyrene[100] and p-terphenyl,[132] suggesting that defect analysis in pharmaceuticals should be possible. Furthermore, it was possible to determine that polymorphic conversions in 1,8-dichloro-10-methylanthracene, p-dichlorobenzene and pyrene are martensitic in character, initiating at crystal defects.[133-135]

1.6 Project Aims and Thesis Outline

Experimental work was directed to four main areas of research.

1.6.1 Cocrystals

The first aim of the study on cocrystals was to investigate alternative cocrystallisation methods which avoid the coformer solubility problems associated with solution cocrystallisations and that could be used for preparing cocrystals on a large scale. Also, a seeding effect in grinding experiments was studied. This work is described in Chapter 3.

During this investigation, and while preparing samples for TEM analysis, several polymorphic cocrystals were identified. These observations are summarised in Chapter 4, and insights into strategies for screening for polymorphs of cocrystals are presented.

1.6.2 Characterisation of Pharmaceutical Materials by Transmission Electron Microscopy

The initial goal was to determine how much of a hindrance sample preparation and beam damage are to the analysis of pharmaceutical materials by TEM, and to develop strategies for reducing these problems. The basic applications of TEM were then explored with pharmaceutical samples (Chapter 5).

The next aim was to use TEM to identify the crystal form of pharmaceutical compounds and distinguish between different polymorphs. Examples are given in Chapter 6.

A strategy for solving the crystal structure of new crystal forms, through a combination of crystal structure prediction and TEM, was devised. An investigation was conducted in order to determine if this strategy was effective in practice. The method was then used to identify a new polymorph of the compound theophylline (Chapter 7).

A further objective was to assess the potential of TEM for the analysis of sub-micron sized crystallites of APIs and to investigate changes in particle size and morphology during grinding experiments. This work is described in Chapter 8.

1.6.3 Analysis of Defects in Pharmaceutical Crystals

The primary objective was to observe and identify defects in pharmaceutical crystals by TEM. Another aim was to use AFM as a complimentary technique for observing defects at the surfaces of crystals.

Once defects were identified, it was hoped that they could be linked to the solid-state behaviour of pharmaceutical compounds (Chapter 9).

1.6.4 Tubular Crystals of Pharmaceutical Compounds

While preparing samples for TEM analysis tubular crystals of pharmaceutical compounds including caffeine and aspirin were isolated. This unexpected, but interesting, phenomenon is described in Chapter 10.

1.7 References

1. Sun E. Statement given at a press conference on behalf of Abbott Laboratories during the Ritonavir crisis. Quoted in a research summary for Professor Joel Bernstein http://www.uwa.edu.au/__data/assets/pdf_file/0004/635026/Joel_Bernstein_Research_Summary.pdf.

2. Byrn S., Pfeiffer R., Ganey M., Hoiberg C., Poochikian G. Pharmaceutical solids: a strategic approach to regulatory considerations. *Pharm. Res.*, 1995, 12(7), 945-954.

3. Bauer J., Spanton S., Henry R., Quick J., Dziki W., Porter W., Morris J. Ritonavir: an extraordinary example of conformational polymorphism. *Pharm. Res.*, 2001, 18(6), 859-866.

4. Hilfiker R., Blatter F., von Raumer M. 2006. Relevance of solid-state properties for pharmaceutical products. In Hilfiker R, editor Polymorphism, Weinheim, Germany: Wiley-VCH Verlag GmbH & Co. pp 1-19.

5. Variankaval N., Cote A. S., Doherty M. F. From form to function: crystallization of active pharmaceutical ingredients. *AIChE J.*, 2008, 54(7), 1682-1688.

6. Stahly G. P. Diversity in Single- and Multiple-Component Crystals. The Search for and Prevalence of Polymorphs and Cocrystals. *Cryst. Growth Des.*, 2007, 7(6), 1007-1026.

7. Bernstein J. 2008. Crystal Polymorphism. In Novoa JJ, Braga D, Addadi L, editors. Engineering of Crystalline Materials Properties: Springer. p 87-109.

8. Verbeeck R. K., Kanfer I., Walker R. B. Generic substitution: The use of medicinal products containing different salts and implications for safety and efficacy. *Eur. J. Pharm. Sci.*, 2006, 28(1-2), 1-6.

9. Haleblian J., McCrone W. Pharmaceutical applications of polymorphism. *J Pharm Sci*, 1969, 58(8), 911-929.

10. Grunenberg A. Polymorphism and thermal analysis of pharmaceuticals. *Pharm. Unserer Zeit*, 1997, 26(5), 224-231.

11. Singhal D., Curatolo W. Drug polymorphism and dosage form design: a practical perspective. *Adv. Drug Delivery Rev.*, 2004, 56(3), 335-347.

12. Blagden N., de Matas M., Gavan P. T., York P. Crystal engineering of active pharmaceutical ingredients to improve solubility and dissolution rates. *Adv. Drug Delivery Rev.*, 2007, 59(7), 617-630.

13. Clarke H. D., Arora K. K., Bass H., Kavuru P., Ong T. T., Pujari T., Wojtas L., Zaworotko M. J. Structure-Stability Relationships in Cocrystal Hydrates: Does the Promiscuity of Water Make Crystalline Hydrates the Nemesis of Crystal Engineering? *Cryst. Growth Des.*, 2010, 10(5), 2152-2167.

14. Lam K.-W., Xu J.-J., Ng K.-M., Wibowo C., Lin G., Luo K. Q. Pharmaceutical Salt Formation Guided by Phase Diagrams. *Ind. Eng. Chem. Res.*, 2010, 49(24), 12503-12512.

15. Stahl P. H., Wermuth C. G. Handbook of Pharmaceutical Salts: Properties, Selection, and Use. Verlag Helvetica Chimica Acta, Wiley-VCH, (Eds.) 2002.

16. Cesaro A., Starec G. Thermodynamic properties of caffeine crystal forms. *J. Phys. Chem.*, 1980, 84(11), 1345-1346.

17. Burley J. C., Duer M. J., Stein R. S., Vrcelj R. M. Enforcing ostwald's rule of stages: Isolation of paracetamol forms III and II. 2007, 31(5), 271-276.

18. Dudognon E., Danede F., Descamps M., Correia N. T. Evidence for a New Crystalline Phase of Racemic Ibuprofen. *Pharm. Res.*, 2008, 25(12), 2853-2858.

19. Miller J. M., Rodriguez-Hornedo N., Blackburn A. C., Macikenas D., Collman B. M. Solvent systems for crystallization and polymorph selection. *Biotechnol.: Pharm. Aspects*, 2007, 6, 53-109.

20. Lee A. Y., Myerson A. S. Particle engineering: fundamentals of particle formation and crystal growth. *MRS Bull.*, 2006, 31(11), 881-886.

21. Allesoe M., Rantanen J., Aaltonen J., Cornett C., van den Berg F. Solvent subset selection for polymorph screening. *J. Chemom.*, 2008, 22(11-12), 621-631.

22. Nichols G., Frampton C. S. Physicochemical Characterization of the Orthorhombic Polymorph of Paracetamol Crystallized from Solution. *J. Pharm. Sci.*, 1998, 87(6), 684-693.

23. Gardner C. R., Almarsson O., Chen H., Morissette S., Peterson M., Zhang Z., Wang S., Lemmo A., Gonzalez-Zugasti J., Monagle J., Marchionna J., Ellis S., McNulty C., Johnson A., Levinson D., Cima M. Application of high throughput technologies to drug substance and drug product development. *Comput. Chem. Eng.*, 2004, 28(6-7), 943-953.

24. Morissette S. L., Almarsson O., Peterson M. L., Remenar J. F., Read M. J., Lemmo A. V., Ellis S., Cima M. J., Gardner C. R. High-throughput crystallization: polymorphs, salts, co-crystals and solvates of pharmaceutical solids. *Adv. Drug Delivery Rev.*, 2004, 56(3), 275-300.

25. Rodriguez-Spong B., Price C. P., Jayasankar A., Matzger A. J., Rodriguez-Hornedo N. General principles of pharmaceutical solid polymorphism. A supramolecular perspective. *Adv. Drug Delivery Rev.*, 2004, 56(3), 241-274.

26. Childs S. L., Stahly G. P., Park A. The salt-cocrystal continuum: the influence of crystal structure on ionization state. *Mol. Pharmaceutics*, 2007, 4(3), 323-338.

27. Saal C. Pharmaceutical salts optimization of solubility or even more? *Am. Pharm. Rev.*, 2010, 13(2), 18-22.

28. Kumar L., Amin A., Bansal A. K. Salt selection in drug development. *Pharm. Technol.*, 2008, 32(3), 128-146.

29. Matteucci M. E., Miller M. A., Williams 3rd R. O., Johnston K. P. Highly supersaturated solutions of amorphous drugs approaching predictions from configurational thermodynamic properties. *J Phys Chem B*, 2008, 112(51), 16675-16681.

30. U.S. Food and Drug Administration (FDA). Q1A(R2) Stability Testing of New Drug Substances and Products. 2003, (2).

31. Stahly G. P. A Survey of Cocrystals Reported Prior to 2000. *Cryst. Growth Des.*, 2009, 9(10), 4212-4229.

32. Etter M. C. Hydrogen bonds as design elements in organic chemistry. *J. Phys. Chem.*, 1991, 95(12), 4601-4610.

33. Caira M. R. Molecular complexes of sulfonamides. 2. 1:1 Complexes between drug molecules: sulfadimidine-acetylsalicylic acid and sulfadimidine-4-aminosalicylic acid. *J. Crystallogr. Spectrosc. Res.*, 1992, 22(2), 193-200.

34. Walsh R. D. B., Bradner M. W., Fleischman S., Morales L. A., Moulton B., Rodriguez-Hornedo N., Zaworotko M. J. Crystal engineering of the composition of pharmaceutical phases. *Chem. Commun.*, 2003, (2), 186-187.

35. Fleischman S. G., Kuduva S. S., McMahon J. A., Moulton B., Bailey Walsh R. D., Rodriguez-Hornedo N., Zaworotko M. J. Crystal Engineering of the Composition of Pharmaceutical Phases: Multiple-Component Crystalline Solids Involving Carbamazepine. *Cryst. Growth Des.*, 2003, 3(6), 909-919.

36. Schultheiss N., Newman A. Pharmaceutical Cocrystals and Their Physicochemical Properties. *Cryst. Growth Des.*, 2009, 9(6), 2950-2967.

37. Trask A. V., Motherwell W. D. S., Jones W. Pharmaceutical cocrystallization: Engineering a remedy for caffeine hydration. *Cryst. Growth Des.*, 2005, 5(3), 1013-1021.

38. Nangia A., Nanubolu J. B., Sanphui P. 2010. Stable cocrystals of temozolomide. Application: IN: (India).

39. Hickey M. B., Peterson M. L., Scoppettuolo L. A., Morrisette S. L., Vetter A., Guzman H., Remenar J. F., Zhang Z., Tawa M. D., Haley S., Zaworotko M. J., Almarsson O. Performance comparison of a co-crystal of carbamazepine with marketed product. *Eur. J. Pharm. Biopharm.*, 2007, 67(1), 112-119.

40. Karki S., Friscic T., Fabian L., Laity P. R., Day G. M., Jones W. Improving mechanical properties of crystalline solids by cocrystal formation: new compressible forms of paracetamol. *Adv. Mater. (Weinheim, Ger.)*, 2009, 21(38-39), 3905-3909.

41. Forrest J. O., George N., Burton R. C., Parmar M. M., Tandy M. D., Buttar S. M., Frampton C. S., Brown A. S. C., Chorlton A. P. 2010. Cocrystals of propiconazole and cocrystal forming compound. Application: WO: (Syngenta Ltd., UK).

42. Shan N., Zaworotko M. J. The role of cocrystals in pharmaceutical science. *Drug Discovery Today*, 2008, 13(9/10), 440-446.

43. Good D. J., Rodriguez-Hornedo N. Solubility Advantage of Pharmaceutical Cocrystals. *Cryst. Growth Des.*, 2009, 9(5), 2252-2264.

44. McNamara D. P., Childs S. L., Giordano J., Iarriccio A., Cassidy J., Shet M. S., Mannion R., O'Donnell E., Park A. Use of a glutaric acid cocrystal to improve oral bioavailability of a low solubility API. *Pharm. Res.*, 2006, 23(8), 1888-1897.

45. Remenar J. F., Morissette S. L., Peterson M. L., Moulton B., MacPhee J. M., Guzman H. R., Almarsson O. Crystal engineering of novel cocrystals of a triazole drug with 1,4-dicarboxylic acids. *J. Am. Chem. Soc.*, 2003, 125(28), 8456-8457.

46. Thayer A. M. Form and Function. *C&EN News*, 2007, 85(25).

47. Peterson M. L., Hickey M. B., Zaworotko M. J., Almarsson O. Expanding the Scope of Crystal form Evaluation in Pharmaceutical Science. *J. Pharm. Pharm. Sci.*, 2006, 9(3), 317-326.

48. Li Z., Yang B.-S., Jiang M., Eriksson M., Spinelli E., Yee N., Senanayake C. A Practical Solid Form Screen Approach to Identify a Pharmaceutical Glutaric Acid Cocrystal for Development. *Org. Process Res. Dev.*, 2009, 13(6), 1307-1314.

49. Karki S., Friscic T., Fabian L., Jones W. New solid forms of artemisinin obtained through cocrystallisation. *CrystEngComm*, 2010, 12(12), 4038-4041.

50. Karki S., Friscic T., Jones W. Control and interconversion of cocrystal stoichiometry in grinding: stepwise mechanism for the formation of a hydrogen-bonded cocrystal. *CrystEngComm*, 2009, 11(3), 470-481.

51. Friscic T., Jones W. Benefits of cocrystallization in pharmaceutical materials science: an update. *J. Pharm. Pharmacol.*, 2010, 62(11), 1547-1559.

52. Desiraju G. R. Supramolecular synthons in crystal engineering - a new organic synthesis. *Angew. Chem., Int. Ed. Engl.*, 1995, 34(21), 2311-2327.

53. Shattock T. R., Arora K. K., Vishweshwar P., Zaworotko M. J. Hierarchy of Supramolecular Synthons: Persistent Carboxylic Acid.Pyridine Hydrogen Bonds in Cocrystals That also Contain a Hydroxyl Moiety. *Cryst. Growth Des.*, 2008, 8(12), 4533-4545.

54. Sheikh A. Y., Abd. Rahim S., Hammond R. B., Roberts K. J. Scalable solution cocrystallization: case of carbamazepine-nicotinamide I. *CrystEngComm*, 2009, 11(3), 501-509.

55. Chiarella R. A., Davey R. J., Peterson M. L. Making Co-Crystals - The Utility of Ternary Phase Diagrams. *Cryst. Growth Des.*, 2007, 7(7), 1223-1226.

56. Friscic T., Jones W. Recent Advances in Understanding the Mechanism of Cocrystal Formation via Grinding. *Cryst. Growth Des.*, 2009, 9(3), 1621-1637.

57. Karki S., Fabian L., Friscic T., Jones W. Powder x-ray diffraction as an emerging method to structurally characterize organic solids. 2007, 9(16), 3133-3136.

58. Zhang G. G. Z., Henry R. F., Borchardt T. B., Lou X. Efficient co-crystal screening using solution-mediated phase transformation. *J. Pharm. Sci.*, 2007, 96(5), 990-995.

59. Bucar D. K., Henry R. F., Lou X. C., Borchardt T. B., Zhang G. G. Z. A "hidden" co-crystal of caffeine and adipic acid. 2007, (5), 525-527.

60. Gagniere E., Mangin D., Puel F., Bebon C., Klein J.-P., Monnier O., Garcia E. Cocrystal Formation in Solution: In Situ Solute Concentration Monitoring of the Two Components and Kinetic Pathways. *Cryst. Growth Des.*, 2009, 9(8), 3376-3383.

61. Shan N., Toda F., Jones W. Mechanochemistry and co-crystal formation: effect of solvent on reaction kinetics. *Chem. Commun.*, 2002, (20), 2372-2373.

62. Chadwick K., Davey R., Cross W. How does grinding produce co-crystals? Insights from the case of benzophenone and diphenylamine. *CrystEngComm*, 2007, 9(9), 732-734.

63. Jayasankar A., Somwangthanaroj A., Shao Z. J., Rodriguez-Hornedo N. Cocrystal Formation during Cogrinding and Storage is Mediated by Amorphous Phase. *Pharm. Res.*, 2006, 23(10), 2381-2392.

64. Nguyen K. L., Friscic T., Day G. M., Gladden L. F., Jones W. Terahertz time-domain spectroscopy and the quantitative monitoring of mechanochemical cocrystal formation. *Nat. Mater.*, 2007, 6(3), 206-209.

65. Alkhalil A., Nanubolu J. B., Roberts C. J., Aylott J. W., Burley J. C. Confocal Raman Microscope Mapping of a Kofler Melt. *Cryst. Growth Des.*, 2011, 11(2), 422-430.

66. Lu E., Rodriguez-Hornedo N., Suryanarayanan R. A rapid thermal method for cocrystal screening. *CrystEngComm*, 2008, 10(6), 665-668.

67. Berry D. J., Seaton C. C., Clegg W., Harrington R. W., Coles S. J., Horton P. N., Hursthouse M. B., Storey R., Jones W., Friscic T., Blagden N. Applying Hot-Stage Microscopy to Co-Crystal Screening: A Study of Nicotinamide with Seven Active Pharmaceutical Ingredients. *Cryst. Growth Des.*, 2008, 8(5), 1697-1712.

68. Dhumal Ravindra S., Kelly Adrian L., York P., Coates Phil D., Paradkar A. Cocrystalization and simultaneous agglomeration using hot melt extrusion. *Pharm Res*, 2010, 27(12), 2725-2733.

69. Childs S. L., Mougin P., Stahly B. C. 2005. Screening for solid pharmaceutical forms by ultrasound crystallization and cocrystallization using ultrasound. Application: WO: (S.S.C.I., Inc., USA).

70. Friscic T., Childs S. L., Rizvi S. A. A., Jones W. The role of solvent in mechanochemical and sonochemical cocrystal formation: a solubility-based approach for predicting cocrystallisation outcome. *CrystEngComm*, 2009, 11(3), 418-426.

71. Alhalaweh A., Velaga S. P. Formation of Cocrystals from Stoichiometric Solutions of Incongruently Saturating Systems by Spray Drying. *Cryst. Growth Des.*, 2010, 10(8), 3302-3305.

72. Padrela L., Rodrigues M. A., Velaga S. P., Matos H. A., Gomes de Azevedo E. Formation of indomethacin-saccharin cocrystals using supercritical fluid technology. *Eur. J. Pharm. Sci.*, 2009, 38(1), 9-17.

73. Byrn S. R., Bates S., Ivanisevic I. Regulatory aspects of X-ray powder diffraction, part 1. *Am. Pharm. Rev.*, 2005, 8(3,5), 55-59,137-141.

74. Turner Y. T. A., Roberts C. J., Davies M. C. Scanning probe microscopy in the field of drug delivery. *Adv. Drug Delivery Rev.*, 2007, 59(14), 1453-1473.

75. Binnig G., Quate C. F., Gerber C. Atomic force microscope. *Phys. Rev. Lett.*, 1986, 56(9), 930-933.

76. Binnig G., Gerber C., Stoll E., Albrecht T. R., Quate C. F. Atomic resolution with atomic force microscope. *Europhys. Lett.*, 1987, 3(12), 1281-1286.

77. Mehrens S. M., Kale U. J., Qu X. Statistical analysis of differences in the Raman spectra of polymorphs. *J. Pharm. Sci.*, 2005, 94(6), 1354-1367.

78. McGoverin C. M., Rades T., Gordon K. C. Recent pharmaceutical applications of raman and terahertz spectroscopies. *J. Pharm. Sci.*, 2008, 97(11), 4598-4621.

79. Vankeirsbilck T., Vercauteren A., Baeyens W., Van der Weken G., Verpoort F., Vergote G., Remon J. P. Applications of Raman spectroscopy in pharmaceutical analysis. *TrAC, Trends Anal. Chem.*, 2002, 21(12), 869-877.

80. Campbell Roberts S. N., Williams A. C., Grimsey I. M., Booth S. W. Quantitative analysis of mannitol polymorphs. X-ray powder diffractometry-exploring preferred orientation effects. *J. Pharm. Biomed. Anal.*, 2002, 28(6), 1149-1159.

81. Giron D. Monitoring polymorphism of drugs, an on-going challenge- part 1. *Am. Pharm. Rev.*, 2008, 11(1), 66, 68-71.

82. Nemet Z., Kis G. C., Pokol G., Demeter A. Quantitative determination of famotidine polymorphs: X-ray powder diffractometric and Raman spectrometric study. *J. Pharm. Biomed. Anal.*, 2009, 49(2), 338-346.

83. Vogt F. G. A multi-disciplinary approach to the solid-state analysis of pharmaceuticals. *Am. Pharm. Rev.*, 2008, 11(5), 50-57.

84. Harris K. D. M. Modern applications of powder X-ray diffraction in pharmaceutical sciences. *Am. Pharm. Rev.*, 2004, 7(2), 86-91.

85. Hirsch P., Cockayne D., Spence J., Whelan M. 50 years of TEM of dislocations. Past, present and future. *Philos. Mag.*, 2006, 86(29-31), 4519-4528.

86. Wilkes P. Solid State Chemistry in Metallurgy. Cambridge: Cambridge University Press, 1973, p 393-418.

87. McLaren A. C. Transmission Electron Microscopy of Minerals and Rocks, (2nd ed.). Cambridge: Cambridge University Press, 1991.

88. Champness P. E. Transmission electron microscopy in earth science. *Annu. Rev. Earth Planet. Sci.*, 1977, 5, 203-226.

89. Czichos H., Saito T., Smith L. Springer Handbook of Materials Measurement Methods. Springer, (Eds.) 2006, p 187-205.

90. Reimer L., Kohl H. Transmission Electron Microscopy: Physics of Image Formation, (5th ed.). New York: Springer, 2008.

91. Urban K. W. Is science prepared for atomic-resolution electron microscopy? *Nat. Mater.*, 2009, 8(4), 260-262.

92. Vincent R., Midgley P. A. Double conical beam-rocking system for measurement of integrated electron diffraction intensities. *Ultramicroscopy*, 1994, 53(3), 271-282.

93. Thomas J. M., Midgley P. A. High-resolution transmission electron microscopy: the ultimate nanoanalytical technique. *Chem. Commun.*, 2004, (11), 1253-1267.

94. Almgren M., Edwards K., Karlsson G. Cryo transmission electron microscopy of liposomes and related structures. *Colloids Surf., A*, 2000, 174(1-2), 3-21.

95. Tang Y., Liu Shiyong Y., Armes Steven P., Billingham Norman C. Solubilization and controlled release of a hydrophobic drug using novel micelle-forming ABC triblock copolymers. *Biomacromolecules*, 2003, 4(6), 1636-1645.

96. Kim I.-S., Kim S.-H. Development of polymeric nanoparticulate drug delivery systems: evaluation of nanoparticles based on biotinylated poly(ethylene glycol) with sugar moiety. *Int. J. Pharm.*, 2003, 257(1-2), 195-203.

97. Liu Y., Yang Z., Du J., Yao X., Zheng X., Lei R., Liu J., Hu H., Li H. Interaction of Taxol with intravenous immunoglobulin: An inhibition of Taxol from crystallizing in aqueous solution. *Int. Immunopharmacol.*, 2008, 8(3), 390-400.

98. Rades T., Mueller-Goymann C. C. Electron and light microscopical investigation of defect structures in mesophases of pharmaceutical substances. *Colloid Polym. Sci.*, 1997, 275(12), 1169-1178.

99. Li Z. G., Harlow R. L., Foris C. M., Li H., Ma P., Vickery R. D., Maurin M. B., Toby B. H. New applications of electron diffraction in the pharmaceutical industry: Polymorph determination by using a combination of electron diffraction and synchrotron X-ray powder diffraction techniques. *Microsc. Microanal.*, 2002, 8(2), 134-138.

100. Jones W., Thomas J. M. Applications of electron microscopy to organic solid-state chemistry. *Prog. Solid State Chem.*, 1979, 12(2), 101-124.

101. Schmidt M. U., Bruehne S., Wolf A. K., Rech A., Bruening J., Alig E., Fink L., Buchsbaum C., Glinnemann J., van de Streek J., Gozzo F., Brunelli M., Stowasser F., Gorelik T., Mugnaioli E., Kolb U. Electron diffraction, X-ray powder diffraction and pair-distribution-function analyses to determine the crystal structures of Pigment Yellow 213, C23H21N5O9. *Acta Crystallogr., Sect. B: Struct. Sci.*, 2009, B65(2), 189-199.

102. Kolb U., Gorelik T. E., Mugnaioli E., Stewart A. Structural Characterization of Organics Using Manual and Automated Electron Diffraction. *Polym. Rev.*, 2010, 50(3), 385-409.

103. Katteboinaa S., Chandrasekhar P V. S. R., Balaji S. Drug nanocrystals: a novel formulation approach for poorly soluble drugs. *Int. J. PharmTech Res.*, 2009, 1(3), 682-694.

104. Colombo I., Grassi G., Grassi M. Drug mechanochemical activation. *J. Pharm. Sci.*, 2009, 98(11), 3961-3986.

105. Zhang H., Wang D., Butler R., Campbell Neil L., Long J., Tan B., Duncalf David J., Foster Alison J., Hopkinson A., Taylor D., Angus D., Cooper Andrew I., Rannard Steven P. Formation and enhanced biocidal activity of water-dispersable organic nanoparticles. *Nat Nanotechnol*, 2008, 3(8), 506-511.

106. Bucar D.-K., Macgillivray Leonard R. Preparation and reactivity of nanocrystalline cocrystals formed via sonocrystallization. *J Am Chem Soc*, 2007, 129(1), 32-33.

107. Czichos H., Saito T., Smith L. Springer Handbook of Materials Measurement Methods. Springer, (Eds.) 2006, p 159-171.

108. Signorell R., Kunzmann M. K., Suhm M. A. FTIR investigation of non-volatile molecular nanoparticles. *Chem. Phys. Lett.*, 2000, 329(1,2), 52-60.

109. Chu B., Liu T. Characterization of nanoparticles by scattering techniques. *J. Nanopart. Res.*, 2000, 2(1), 29-41.

110. Midgley P. A., Dunin-Borkowski R. E. Electron tomography and holography in materials science. *Nat. Mater.*, 2009, 8(4), 271-280.

111. Armigliato A. Analysis of crystal defects by transmission electron microscopy. *Mater. Chem.*, 1979, 4(3), 453-471.

112. McPherson A. Atomic force microscopy applications in macromolecular crystallography. *Acta Crystallogr., Sect. D: Biol. Crystallogr.*, 2001, D57(8), 1053-1060.

113. Williams D. B., Carter C. B. Transmission electron microscopy. A textbook for materials science. New York: Plenum Press, 1996.

114. Ma B.-T., Laird C. Dislocation structures of copper single crystals for fatigue tests under variable amplitudes. *Mater. Sci. Eng., A*, 1998, 102(2), 247-258.

115. Van Tendeloo G. TEM characterization of structural defects. *NATO ASI Ser., Ser. B*, 1996, 355(Stability of Materials), 473-507.

116. Thomas J. M. Topography and topology in solid state chemistry. *Philos. Trans. R. Soc. London, Ser. A*, 1974, 277(1268), 251-287.

117. Bhadeshia H. K. D. H. 2001. Martensitic Transformation. In Buschow K, Cahn RW, Flemings MC, Lischner B, Kramer EJ, Mahajan S, editors. Encyclopedia of Materials Science: Science and Technology: Pergamon press, Elsevier Science. pp 5203-5206.

118. Mnyukh Y. V. Polymorphic transitions in crystals: nucleation. *J. Cryst. Growth*, 1976, 32(3), 371-377.

119. Thomas J. M., Williams J. O. Dislocations and the reactivity of organic solids. *Prog. Solid State Chem.*, 1971, 6, 119-154.

120. Thomas J. M., Renshaw G. D. Role of dislocations in the dehydration of nickel sulfate hexahydrate. II. Topographical studies by use of optical microscopy. *J. Chem. Soc. A*, 1969, (18), 2753-2755.

121. Kitaigorodskii A. I., Mnyukh Y. V., Asadov Y. G. Relations for single-crystal growth during polymorphic trans- formation. *Phys. Chem. Solids*, 1965, 26(3), 463-472.

122. Chamarthy S. P., Pinal R. The nature of crystal disorder in milled pharmaceutical materials. *Colloids Surf., A*, 2008, 331(1-2), 68-75.

123. Byard S. J., Jackson S. L., Smail A., Bauer M., Apperley D. C. Studies on the crystallinity of a pharmaceutical development drug substance. *J. Pharm. Sci.*, 2005, 94(6), 1321-1335.

124. Prasad K. V. R., Ristic R. I., Sheen D. B., Sherwood J. N. Dissolution kinetics of paracetamol single crystals. *Int. J. Pharm.*, 2002, 238(1-2), 29-41.

125. Byrn S. R., Lin C.-T. The effect of crystal packing and defects on desolvation of hydrate crystals of caffeine and L-(-)-1,4-cyclohexadiene-1-alanine. *J. Am. Chem. Soc.*, 1976, 98(13), 4004-4005.

126. Huttenrauch R., Keiner I. Producing lattice defects by drying processes. *Int. J. Pharm.*, 1979, 2(1), 59-60.

127. Koivisto M., Heinaenen P., Tanninen V. P., Lehto V.-P. Depth Profiling of Compression-Induced Disorders and Polymorphic Transition on Tablet Surfaces with Grazing Incidence X-ray Diffraction. *Pharm. Res.*, 2006, 23(4), 813-820.

128. Vasilchenko M. A., Shakhtshneider T. P., Naumov D. Y., Boldyrev V. V. The morphology of etch pits during thermal treatment of drugs and its dependence on the features of their crystallochemical structure. *J. Therm. Anal. Calorim.*, 1999, 57(1), 157-164.

129. Gliko O., Reviakine I., Vekilov P. G. Stable equidistant step trains during crystallization of insulin. *Phys. Rev. Lett.*, 2003, 90(22), 1-4.

130. Bates S., Kelly R. C., Ivanisevic I., Schields P., Zografi G., Newman A. W. Assessment of defects and amorphous structure produced in raffinose pentahydrate upon dehydration. *J. Pharm. Sci.*, 2007, 96(5), 1418-1433.

131. Parkinson G. M., Thomas J. M., Goringe M. J., Smith D. A. Planar faults in crystalline anthracene. *Chem. Phys. Lett.*, 1979, 63(3), 436-437.

132. Jones W., Thomas J. M., Williams J. O., Hobbs L. W. Electron microscopic studies of extended defects in organic molecular crystals. I. p-Terphenyl. *J. Chem. Soc., Faraday Trans. 2*, 1975, 71(1), 138-145.

133. Jones W., Thomas J. M., Williams J. O. Electron and optical microscopic studies of a stress-induced phase transition in 1,8-dichloro-10-methylanthracene. *Philos. Mag.*, 1975, 32(1), 1-11.

134. Reynolds P. A. Martensitic phase transitions in molecular crystals - p-dichlorobenzene. *Acta Crystallogr., Sect. A*, 1977, A33(1), 185-191.

135. Jones W., Cohen M. D. Transmission electron microscopic study of the low temperature phase transformation in pyrene. *Mol. Cryst. Liq. Cryst.*, 1977, 41(4), 103-107.

2 Analytical and Experimental Methods

2.1 Analytical Methods

2.1.1 X-ray Powder Diffraction

XRPD analysis was performed on a Philips X'Pert Diffractometer equipped with an X'celerator RTMS detector using CuKα radiation at a wavelength of 1.5406 Å. Data were collected between 3 and 50 °2θ at ambient temperature. A step size of 0.0167 °2θ was used and a collection time of 5 minutes.

Typically, 20 mg of solid was used for analysis and pressed gently on a glass slide to give a level surface.

XRPD overlays are plotted with an arbitrary intensity scale and were generated using X'Pert Highscore software.

2.1.2 Single Crystal X-ray Diffraction

Data were collected at 180 K (unless stated) on a Nonius Kappa CCD diffractometer equipped with an Oxford Cryosystems cooling device using MoKα radiation. Data collections and structure solutions were performed by Dr. J. E. Davis of the Department of Chemistry, University of Cambridge.

2.1.3 Generation of Simulated XRPD Traces from Crystal Structures

Simulated XRPD diffractograms were generated with Mercury v2.0 software from structures published in the Cambridge Structural Database.

2.1.4 Crystal Morphology Prediction

Morphology predictions were generated with Mercury v2.0 software from structures in the CSD using the Bravais, Friedel, Donnay and Harker (BFDH) model.

2.1.5 Optical Microscopy / Polarized Light Microscopy and Video Analysis

Optical images and videos were collected on a Leica DM1000 transmission microscope, with and without a polarizing filter, using Studio Capture software. Samples were prepared for analysis on glass slides.

2.1.6 Scanning Electron Microscopy

SEM images were obtained with a JEOL JSM-5510LV instrument unless stated.

Samples were prepared on a sticky carbon sample mount placed on a brass SEM stub and sputter coated with platinum to reduce charging during analysis.

2.1.7 Transmission Electron Microscopy

Transmission electron microscopy characterisation was performed at room temperature on a Philips CM30 instrument operating at 300 kV (unless stated), and data were collected on photographic films which were scanned in order to generate digital images. A double tilt sample holder was used and the samples supported on holey-carbon films on 400 mesh copper grids. The images presented in this thesis are bright field images (unless stated otherwise). Electron diffraction patterns were recorded using a selected area aperture to focus on a region of interest, and were indexed by comparison with known crystal structures. The positions of reflections in experimental diffraction patterns were measured using Motic Images Plus 2.0 software. These values were converted to d-spacings and matched to calculated values

for known structures, giving both the composition of the sample and the zone axis of the diffraction pattern. The experimental diffraction pattern was then compared with a simulated diffraction pattern (based on a kinematic model of electron diffraction) of the given zone axis generated using CrystalMaker SingleCrystal v1.3 software from crystal structures published in the Cambridge Structural Database (CSD) to ensure a match. In practice, some diffraction patterns, especially those from high index zone axes, could not be unambiguously indexed. If a crystal form had no reported crystal structure, electron diffraction patterns were compared with a PXRD trace of the form by plotting reflections on a 2θ scale.

A liquid nitrogen filled sample holder was used for work at sub-ambient temperatures.

2.1.8 Atomic Force Microscopy

AFM images were recorded using a Veeco Instruments Multimode atomic force microscope, operated by a Nanoscope IIIa controller, interfaced with a Quadrex extender module. Samples were prepared on a glass slide or mica coverslip attached to a stainless steel AFM sample disc using a sticky tab. Samples were imaged using either a J scanner (150 μm maximum scan size) or an E scanner (13 μm maximum scan size) in tapping mode (unless stated). Data were analysed using NanoscopeTM software version 6 and images were flattened prior to analysis.

2.1.9 Differential Scanning Calorimetry

DSC thermograms were recorded in a nitrogen atmosphere using a Mettler Toledo STARe DSC822e/700 calorimeter. STARe software was used for data acquisition and analysis. The heating rate was typically 10 °C.min^{-1}. Endotherms are plotted as downward peaks unless stated. Samples were prepared by weighing typically 1-5 mg of solid into a 40 μl aluminum pan. Pans were then sealed using a cold weld. When analysing solvates, a pinhole was made in the pan lid. An empty 40 μl aluminium pan was used as a reference.

2.1.10 Thermogravimetric Analysis

TGA analysis was performed in air in a Mettler Toledo TGA/SDTA851e/SF/1100 instrument. STARe software was used for data acquisition and analysis. The heating rate was typically 10 °C.min^{-1}. 5 to 20 mg of sample was analysed in a 100 µl aluminum pan.

2.2 Experimental Methods

All chemicals were purchased from Sigma-Aldrich and used as received.

2.2.1 Grinding in a Ball Mill

Ball milling was performed in a Retsch MM200 grinder for 30 minutes at a frequency of 30 Hz. The grinding was done in a metal vial with two 7 mm diameter metal balls. For liquid assisted grinding 20 µl of nitromethane was also added. Typically, experiments were performed on a 300 mg scale.

2.2.2 Freeze-Drying

Solutions for freeze-drying were prepared by dissolving compound(s) in water or t-butanol in a round bottom flask. The solutions were rapidly frozen by cooling the flask in an acetone/dry ice bath or in liquid nitrogen. A Virtis Advantage 2.0 EL instrument and Leybold vacuum pump were used for freeze-drying, with the round bottom flasks held on nozzles on the outside of the instrument.

2.2.3 Crystal Structure Prediction

Crystal structure prediction (CSP) was performed by Dr Graeme Day and Dr Katarzyna Hejczyk of the Department of Chemistry, University of Cambridge.

The methodology used for crystal structure prediction of theophylline is given here as an example. The molecule was built from scratch and then fully optimised using DFT and gaussian03. 50,000 structures were generated with CrystPred (constrained to the space groups P1, P-1, $P2_1$, $P2_12_12_1$, $P2_1/c$, Pbcn, Pbca, Pnma, $Pna2_1$, $Pca2_1$, C2, Cc, C2/c and R-3) and minimised using a point charges model in DMACryst. The generated structures were re-minimised using atomic multipoles, and finally the lowest energy structures (within 10kJ/mol energy of the global minimum) were recalculated in order to obtain the final symmetry.

3 Alternative Cocrystallisation Methods

3.1 Introduction

There is an opportunity to develop new methods for preparing cocrystals of pharmaceutical compounds to overcome the difficulties associated with current approaches (which are described in Section 1.2.3.2 and listed in Table 3.1).

Table 3.1 A table listing limitations with current cocrystallisation methods.

Cocrystallisation method	Problems / Limitations
Solution crystallisation	Coformers often crystallise separately due to solubility differences
Slurrying	Seeding effect. Not suitable for production on a large scale
Grinding	Seeding effect. Not suitable for production on a large scale
Crystallisation from the melt	Many pharmaceuticals chemically degrade on melting

A preliminary aim of this work was to study the seeding effect that may occur in grinding experiments. Cocrystal formation by grinding is thought to proceed via an amorphous intermediate phase. However, if crystalline input material is used in the grinding experiment, any amorphous phase that is generated could crystallise on the surfaces of the input crystals, rather than nucleating as a new crystal phase, and the crystalline phases that were initially present could persist rather than converting to a more stable cocrystal form. This is analogous to the seeding effect that is often observed in slurries, and would be an important consideration when screening for cocrystals of an API by grinding. Three possible alternative approaches to cocrystal formation were then identified which had the potential to avoid problems with seeding, and with differences in coformer solubility, and could also be used to prepare cocrystals on a large scale.

3.1.1 Cocrystallisation by Freeze-Drying

The first method to be investigated was freeze-drying (lyophillisation). Freeze-drying is a technique where a solution of a compound in water, or other solvent with a suitable triple point, is prepared and rapidly frozen. The frozen solution is then held under a high vacuum causing the solvent to sublime, leaving the solute which forms a low density, often amorphous, powder. Though freeze-drying is a technique primarily used to prepare amorphous forms,[1] if the glass transition temperature of these forms is at or below ambient temperature, they will be liable to spontaneous crystallisation.[1,2] The rationale for using freeze-drying as a cocrystallisation method is that if a solid amorphous mixture of two coformers can be prepared, the kinetic barrier of having crystalline seeds of the two cocrystal formers is avoided, and the chance of forming a cocrystal is maximised. Freeze-drying is also routinely used to prepare pharmaceutical solid forms and formulations on an industrial scale.[3]

The compounds selected for freeze-drying investigations were caffeine and theophylline, well studied cocrystal formers.[4-6] Caffeine is a stimulant present in tea and coffee. Theophylline, a compound that is used to treat asthma and COPD, has a similar molecular structure to caffeine, and is also found in tea.

3.1.2 Cocrystallisation at the Interface between Solvent Layers

The principle difficulty with preparing cocrystals from solution is that the two cocrystal formers often have very different solubilities, and therefore precipitate as separate phases. An alternative cocrystallisation method was proposed that actually exploits these differences in solubility. The strategy was to prepare two saturated solutions, one of a hydrophilic compound in water, and one of a hydrophobic compound in an organic solvent which is immiscible with water. One of these solutions would then be layered onto the other. If a cocrystal of the two compounds is more thermodynamically stable, and hence less soluble, than one of the individual coformers, there would be a driving force for it to crystallise at the solvent interface (See Figure 3.1).

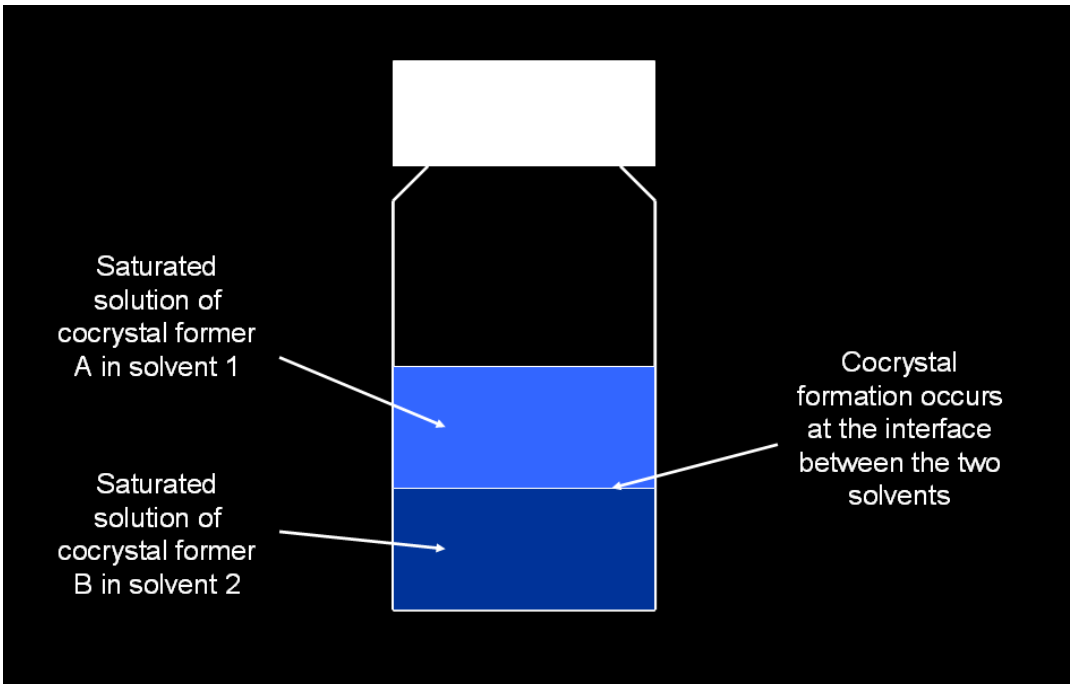

Figure 3.1 A schematic showing the experimental set-up for preparing cocrystals at a solvent interface.

The primary advantage of this technique is that by starting with saturated solutions of the coformers, the possibility of crystallising either of them in preference to a cocrystal phase is avoided. A possible limitation is that the individual coformers must be strongly hydrophobic/hydrophilic or they would be able to diffuse across the solvent interface, leading to sub-saturated solutions, and reducing the driving force for the cocrystal to precipitate at the solvent interface.

The phenazine:mesaconic acid cocrystal[7] was selected for initial investigation work. This cocrystal has been used previously as a model system for studying cocrystal formation by grinding[8] and was chosen for this study as phenazine is a strongly hydrophobic molecule, while mesaconic acid is hydrophilic (aqueous solubilities have been measured to be 0.025 $mg.ml^{-1}$ and 26.3 $mg.ml^{-1}$ respectively).[9] The crystallisation at a solvent interface method was then applied to a pharmaceutical system, the 1:1 caffeine:1-hydroxy-2-naphthoic acid cocrystal.[10]

Cocrystal formation at an interface of two solutions has been mentioned in a patent by Childs.[11] However, the described method involves the mixing of two different solutions and so differs significantly from the approach detailed here, where mixing is deliberately avoided. Crystallisation between layers of immiscible solvents is not a new technique, but to the knowledge of the author it has not been applied to cocrystallisation of pharmaceutical compounds.

3.1.3 Cocrystallisation by Salt Swapping

It was hypothesised that the large difference in aqueous solubility between salt forms and neutral forms of compounds could be exploited to give a method for preparing cocrystals from solution, even when the solubilities of the two coformers are different.

The strategy was to mix a saturated aqueous solution of the hydrochloride salt of one cocrystal former with a saturated aqueous solution of the sodium salt of a second cocrystal former (in equimolar quantities). On mixing the two solutions, a salt swap would occur, with the strongest conjugate base and conjugate acid (chloride ions and sodium ions respectively) associating and causing the two coformers to exchange a proton and neutralise. Both coformers would then be in a highly supersaturated state due to the lower aqueous solubility of the neutral forms, and would be expected to precipitate simultaneously giving an opportunity for cocrystallisation.

The main drawback to this cocrystallisation technique is that both the API and coformer must have an ionisable functional group.

The 2:1 RS-ibuprofen:4,4-Bipy cocrystal[12] was chosen for investigating this preparation method. RS-ibuprofen is a non-steroidal anti-inflammatory drug used in pain relief and has been reported to form a sodium salt.[13] 4,4-Bipy has previously been prepared as a dihydrochloride salt.[14] A schematic of the expected salt swap reaction is shown in Figure 3.2.

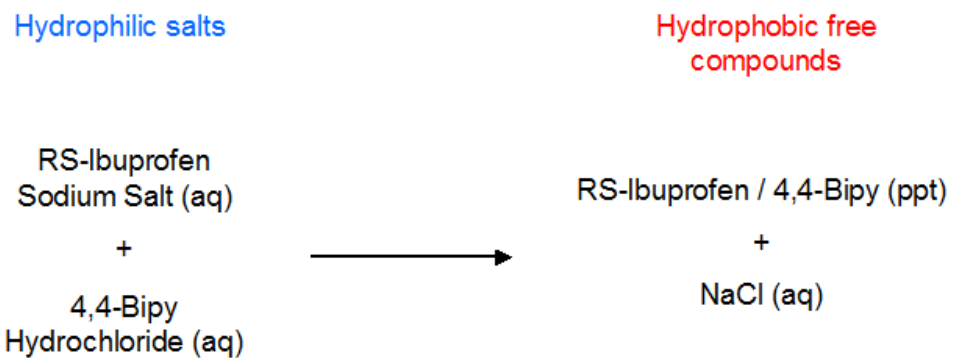

Figure 3.2 A schematic showing the expected salt swap reaction that would occur on mixing aqueous solutions of RS-ibuprofen and 4,4-bipyridyl dihydrochloride.

3.2 Experimental

Saturated solutions for cocrystallisation at a solvent interface were generated by preparing slurries of the two cocrystal formers in appropriate solvents and leaving them to equilibrate for 24 hours. The saturated solution with the lowest density was layered onto the second saturated solution in a vial, which was then capped and stored under ambient conditions.

Planetary ball milling was performed with a Fritsch planetary mill at Universite Lille 1. The grinding was done in a zirconium dioxide vessel with seven 15 mm diameter zirconium dioxide balls at a rotation speed of 400 rpm. Experiments were performed on a 1 g scale.

See Section 2.2.2 for details of the freeze-drying method.

3.3 Results and Discussion

3.3.1 Investigation of the Seeding Effect in Grinding Experiments

A seeding effect was observed during competitive grinding experiments with caffeine, theophylline and glutaric acid.

Both caffeine and theophylline form 1:1 cocrystals with glutaric acid (two polymorphs of the caffeine:glutaric acid cocrystal have been reported).[5,15] These three compounds were ground in a 1:1:1 molar ratio, with nitromethane, to see which of the two cocrystals would be obtained. Caffeine and glutaric acid cocrystallised, leaving the theophylline unconverted (Figure 3.3). It is unclear whether the caffeine:glutaric acid cocrystal is thermodynamically more favourable than the theophylline:glutaric acid cocrystal, or whether it was just the first cocrystal form to nucleate.

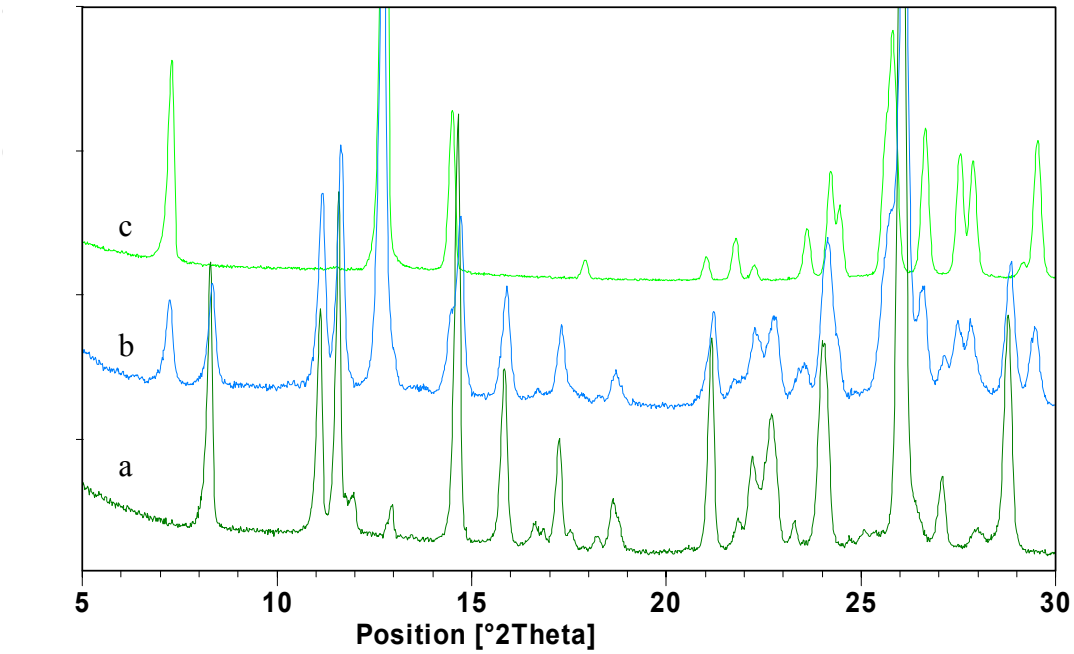

Figure 3.3 XRPD analysis of caffeine, theophylline and glutaric acid ground in a 1:1:1 molar ratio, with 20 µl of nitromethane. (a) Reference trace of the 1:1 caffeine:glutaric acid cocrystal. (b) XRPD trace of a sample prepared by grinding caffeine, theophylline and glutaric acid. (c) Reference trace of theophylline Form II.

The procedure was then modified so that the compounds were ground in a step-wise manner. In the first step, two of the coformers were ground together. In the second step, the third coformer was added and grinding repeated. This is shown schematically in Figure 3.4.

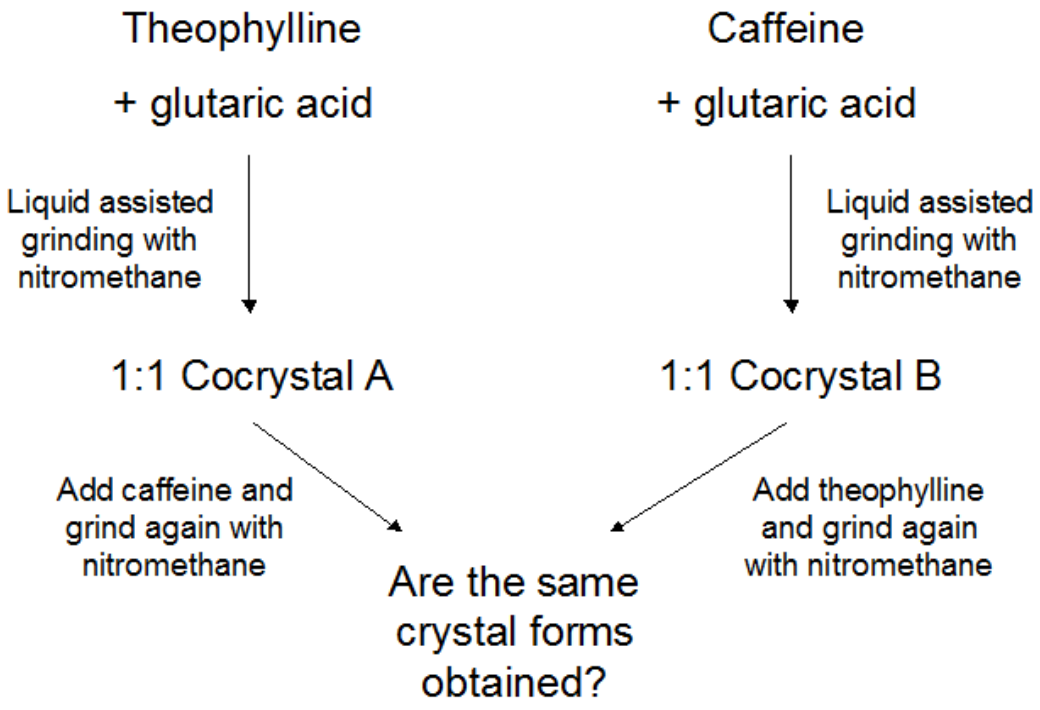

Figure 3.4 Schematic outlining an investigation into competitive grinding with the compounds caffeine, theophylline and glutaric acid.

In the first step-wise experiment, caffeine and glutaric acid were ground together in an equimolar ratio, with 20 µl of nitromethane, to give a 1:1 cocrystal. One mole equivalent of theophylline was then added, and liquid assisted grinding repeated. The resulting solid was analysed by XRPD (Figure 3.5) and found to be a mixture of theophylline and the two known polymorphs of the caffeine:glutaric acid cocrystal.

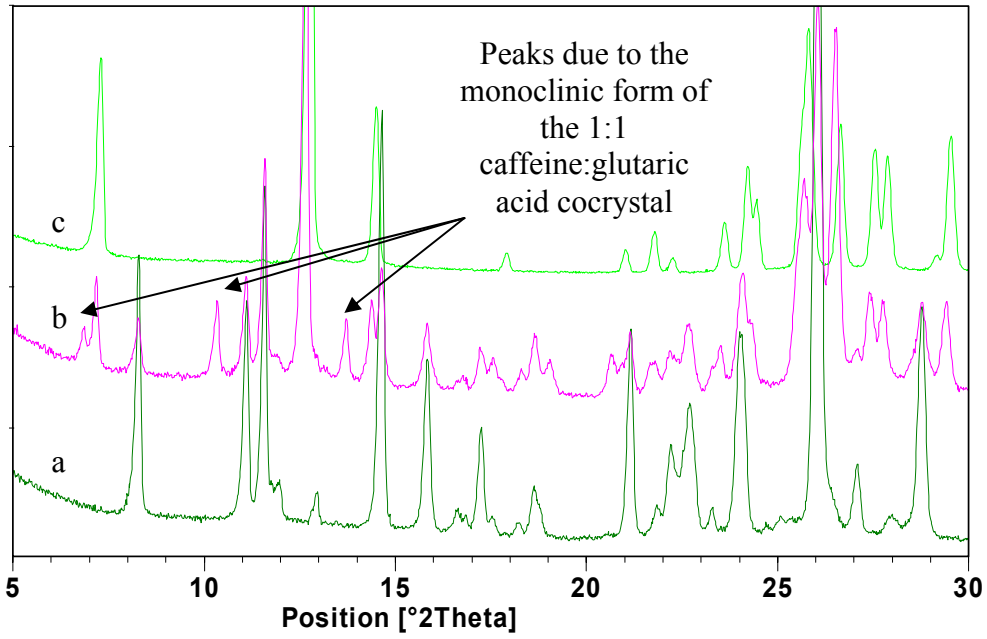

Figure 3.5 XRPD analysis of caffeine ground with glutaric acid and then ground again with theophylline. (a) Caffeine ground with glutaric acid. (b) The same sample after grinding with 1 equivalent of theophylline. (c) Reference trace of theophylline Form II.[16]

In a second experiment, theophylline and glutaric acid were ground together in an equimolar ratio, with 20 µl of nitromethane, to give a 1:1 cocrystal. One mole equivalent of caffeine was then added, and liquid assisted grinding repeated. The resulting solid was analysed by XRPD (Figure 3.6) and found to be a mixture of caffeine and the theophylline:glutaric acid cocrystal.

In this second experiment, the same ratio of the three compounds were ground together as in the first experiment, but the outcome was different. The outcome was influenced by the order in which the compounds were ground together, and it can be concluded that in at least one of the two experiments, the thermodynamically favourable products were not obtained. This result demonstrates that a kinetic seeding effect may occur in grinding experiments (under conditions that are typically used when grinding pharmaceuticals).

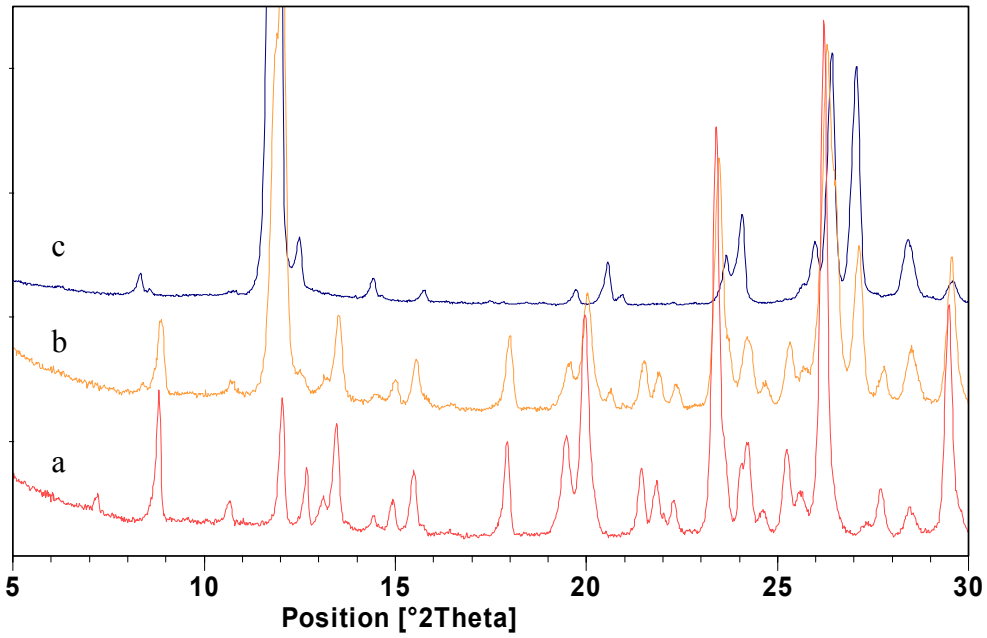

Figure 3.6 XRPD analysis of theophylline ground with glutaric acid and then ground again with caffeine. (a) Theophylline ground with glutaric acid. (b) The same sample after grinding with 1 equivalent of caffeine. (c) Reference trace of caffeine Form II.

As a further extension to this investigation, a third experiment was conducted where caffeine and theophylline were ground together in an equimolar ratio, with 20 µl of nitromethane. A new crystal form, a 1:1 cocrystal of caffeine and theophylline, was obtained. One mole equivalent of glutaric acid was then added, and liquid assisted grinding repeated. The resulting solid was analysed by XRPD (Figure 3.7) and found to be a mixture of glutaric acid and the caffeine:theophylline cocrystal. In this third experiment, even though caffeine, theophylline and glutaric acid were again ground together in a 1:1:1 molar ratio, the outcome was different to that in the two previous experiments. This further demonstrated a seeding effect in grinding.

These findings differ from those of Caira et al who investigated competitive grinding experiments with a set of sulfadimidine:carboxylic acid cocrystals.[17] They found that grinding any of these sulfadimidine cocrystals with one equivalent of anthranilic acid resulted in the formation of the sulfadimidine:anthranilic acid cocrystal.

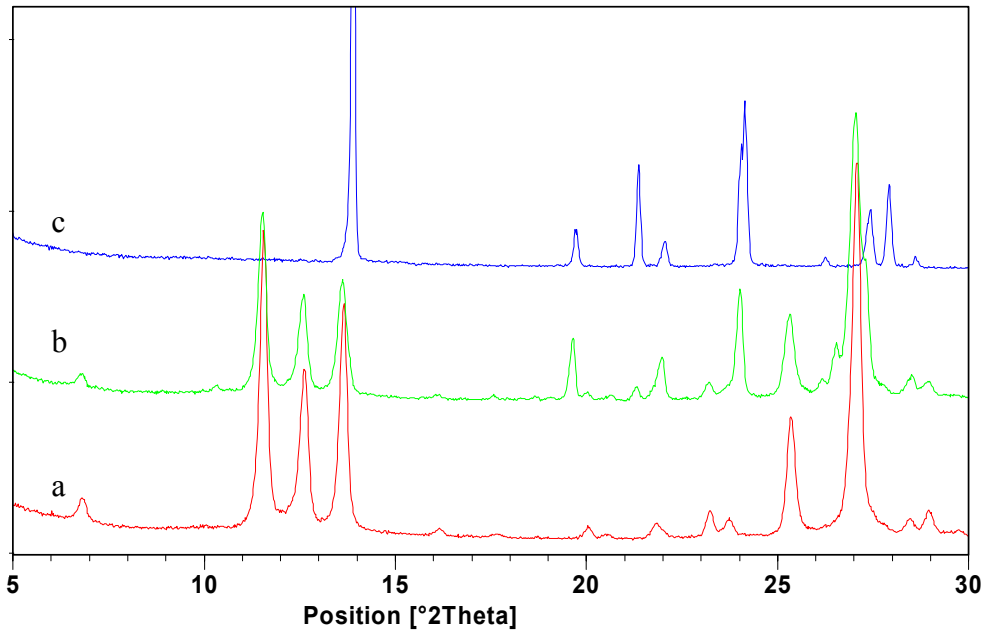

Figure 3.7 XRPD analysis of caffeine ground with theophylline and then ground again with glutaric acid. (a) Caffeine ground with theophylline. (b) The same sample after grinding with 1 equivalent of glutaric acid. (c) Reference trace of glutaric acid.

Further liquid assisted grinding experiments were performed with a 2:1 and 1:2 molar ratio of caffeine and theophylline, with analysis of the resulting samples by XRPD (Figure 3.8). Grinding at a 2:1 molar ratio gave a mixture of the new cocrystal phase (that was observed in the third competitive grinding experiment) and caffeine, whereas grinding at a 1:2 ratio gave a mixture of the new phase and theophylline. These results indicate that the new phase is a 1:1 cocrystal of caffeine and theophylline.

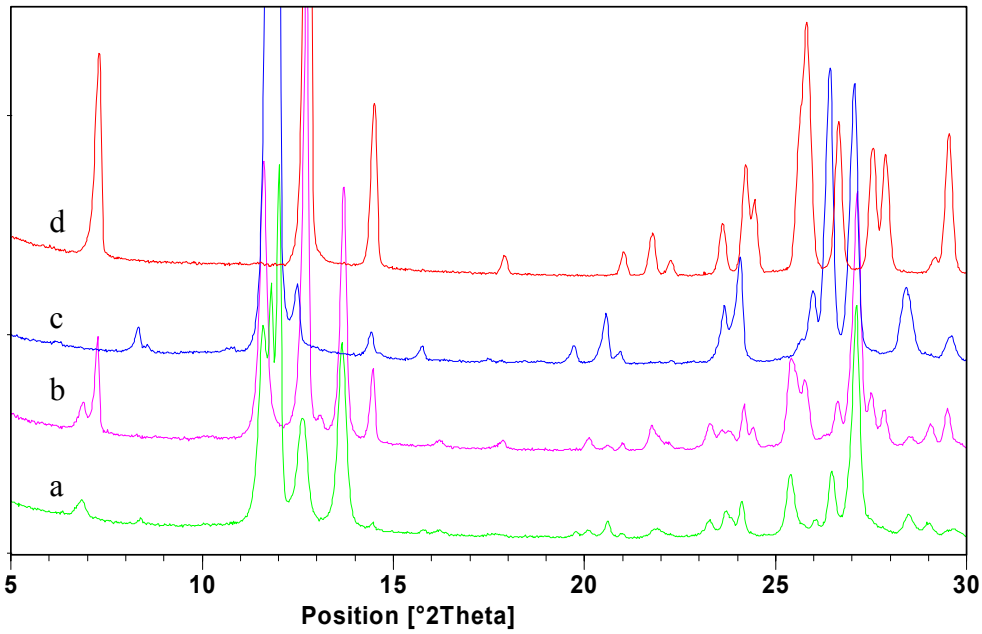

Figure 3.8 XRPD analysis of caffeine and theophylline ground at a 2:1 and 1:2 molar ratio. (a) A sample prepared by grinding caffeine and theophylline at a 2:1 ratio. (b) A sample prepared by grinding caffeine and theophylline at a 1:2 ratio. (c) Reference trace of Form II of caffeine. (d) Reference trace of Form II of theophylline.

3.3.2 Cocrystallisation by Freeze-Drying

The preparation of cocrystals by freeze-drying was investigated using the caffeine: theophylline cocrystal system. An aqueous solution of caffeine and theophylline was generated by dissolving 100 mg of caffeine and 92.8 mg of theophylline (1 mole equivalent) in 25 ml of water. The solution was freeze-dried, and the resulting solid analysed by XRPD (Figure 3.9). The XRPD trace of this sample was different to that of the 1:1 cocrystal that is generated by liquid assisted grinding (described in Section 3.3.1). The trace was also compared with those of the known polymorphs of caffeine and theophylline to determine if a mixture of cocrystal formers had been obtained rather than a cocrystal, and it was evident that the sample did not contain any of the known polymorphs of theophylline. The XRPD trace was, however, almost identical to that of Form I of caffeine (the metastable, hexagonal polymorph).[18,19] The XRPD peaks of the freeze-dried sample were shifted slightly to higher or lower 2θ

with respect to the caffeine peaks, indicating that it was a different, but related crystal form. As no peaks due to a single component phase of theophylline were observed, and there was no indication that theophylline was present as an amorphous phase (no amorphous halo in the XRPD trace and no glass transition observed by DSC) it was concluded that a new cocrystal form of caffeine and theophylline had been isolated.

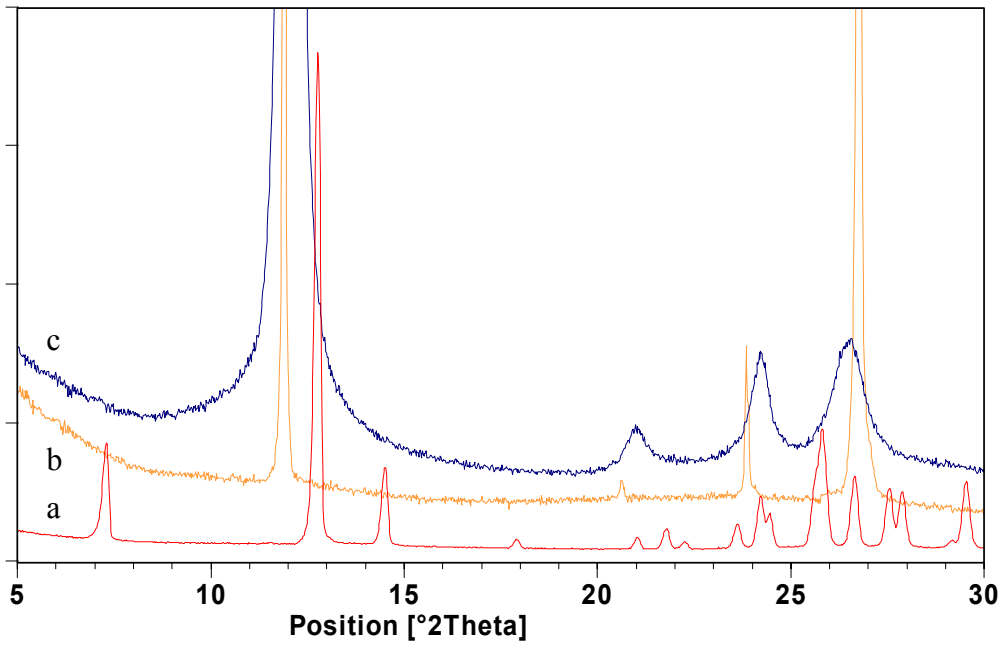

Figure 3.9 XRPD analysis of a sample prepared by freeze-drying caffeine and theophylline in a 1:1 molar ratio. (a) Reference trace of theophylline Form II. (b) Reference trace of caffeine Form I. (c) XRPD trace of a sample prepared by freeze-drying caffeine and theophylline in a 1:1 molar ratio.

More freeze-drying experiments were conducted with varying ratios of caffeine and theophylline. It was observed that as the relative theophylline content was increased, XRPD peak positions deviated progressively more from those of Form I of caffeine (though the new crystal phase was not obtained at all when theophylline was freeze-dried alone). Examples of the change in XRPD peak position with relative composition are shown in Figure 3.10. This result suggested that the new phase was a solid solution of caffeine and theophylline that was isostructural with Form I of

caffeine and where the unit cell dimensions of the solid solution vary slightly with theophylline content. Caffeine molecules can therefore be replaced by theophylline molecules in this phase without disrupting the crystal packing, which is possible as caffeine and theophylline molecules are almost identical in size and shape.

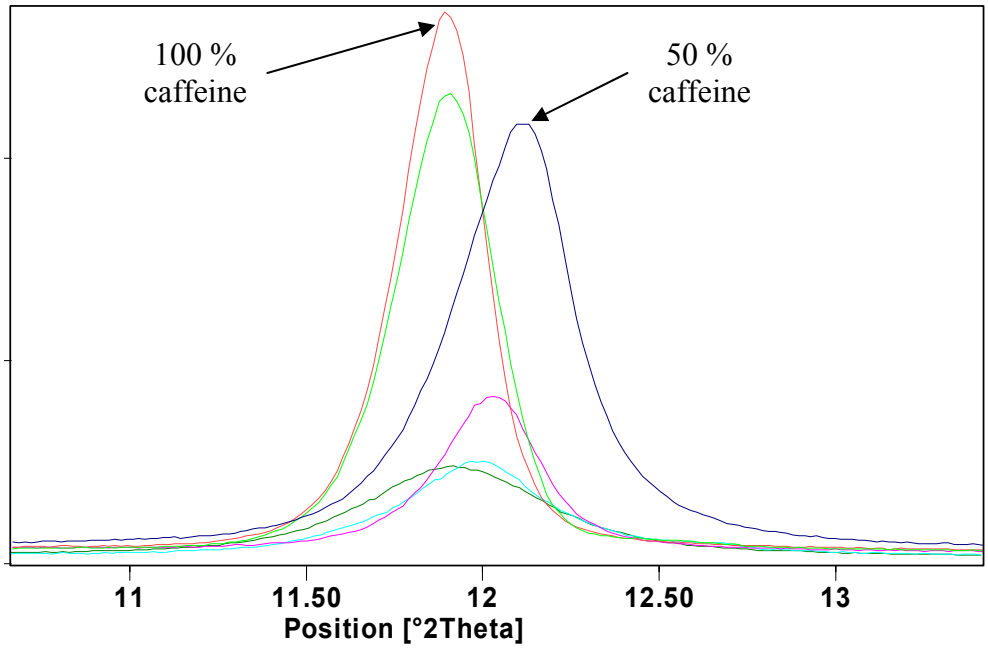

Figure 3.10 XRPD analysis of freeze-dried samples of caffeine and theophylline showing variation in peak position as caffeine contents are varied from 100 % to 50 %. Differences in peak intensity are due to variations in the amount of material used in generating the XRPD traces.

Solid solutions of metals are common, and variations in lattice parameters with composition in these systems has been found to be linear in most cases (Vegard's law).[20] In order to determine if the caffeine:theophylline solid solution followed Vegard's law, relative peak positions (calculated by dividing peak positions at each composition by the peak positions of pure caffeine Form I and multiplying by 100 %) for a range of compositions were plotted against percentage caffeine content (Figure 3.11). The resulting graph showed clear trends in peak positions with percentage caffeine content. XRPD peaks corresponding to crystal planes of the type {h00} and

{hk0} were shifted to higher 2θ values as the relative caffeine content decreased. In contrast, crystal planes of the type {10-2} were shifted to lower 2θ values. This showed that as the relative caffeine content decreases, the a and b axes of the hexagonal unit cell contract, and the unique c axis expands. The R^2 values for the data are not sufficiently high to conclude that the variation between composition and lattice parameters is linear as per Vegard's law.

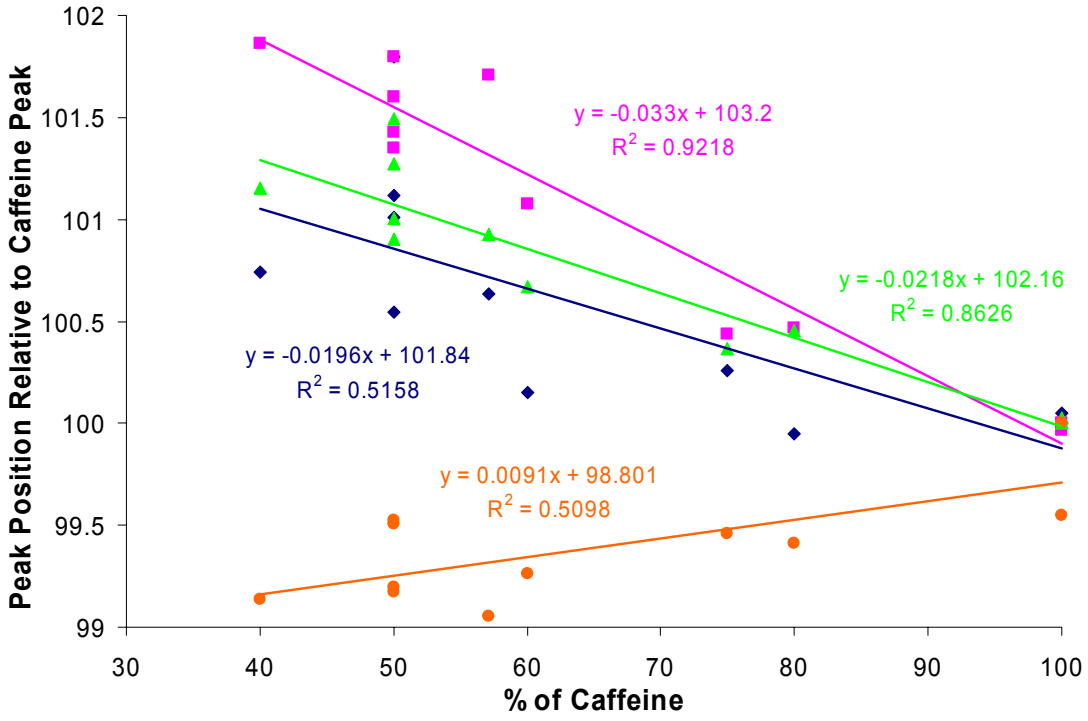

Figure 3.11 A plot showing how XRPD peak positions of freeze-dried caffeine/theophylline mixtures with a range of compositions vary with percentage caffeine content. The pink squares correspond to the peak from the {300} family of crystal planes, the green triangles to the {4-20} planes, the dark blue diamonds to the {2-10} planes and the orange circles to the {10-2} planes. Relative peak positions were calculated by dividing the peak positions at each composition by the peak positions of pure caffeine Form I and multiplying by 100 %.

Having successfully used freeze-drying to prepare a new cocrystal phase of caffeine and theophylline, the technique was applied to other systems which are known to form cocrystals.[4,5,7,12,21] The systems that were investigated, and resulting observations, are shown in Table 3.2.

Table 3.2 A table listing attempted freeze-drying cocrystal formation experiments and outcomes as determined by XRPD analysis.

Cocrystal System	Solvent	Outcome
Caffeine:Theophylline	Water	New crystal form – Solid solution of caffeine and theophylline
2:1 Caffeine:Oxalic acid	Water	The previously reported cocrystal form was obtained
2:1 Theophylline:Oxalic acid	Water	The previously reported cocrystal form was obtained
2:1 Theophylline:Oxalic acid (Freeze-dried at a 1:2 ratio)	Water	New crystal form – A 1:1 theophylline: oxalic acid cocrystal
1:1 Phenazine:Mesaconic acid	t-Butanol	The previously reported cocrystal form was obtained
2:1 RS-Ibuprofen:4,4-Bipyridyl	t-Butanol	The previously reported cocrystal form was obtained
1:1 Caffeine:Adipic acid	Water	No evidence of cocrystal formation

Cocrystal formation was achieved in all but one of the freeze-drying experiments, that with caffeine and adipic acid. This cocrystal has also been found to be difficult to obtain by other preparation methods.[21]

3.3.2.1 Insight into the Mechanism of Cocrystal Formation by Freeze-Drying

It was assumed that cocrystal formation by freeze-drying would proceed via an amorphous phase, and evidence to support this assumption was obtained from cryo-grinding experiments which are known to favour the formation of amorphous

phases.[22] It was found to be possible to prepare the solid solution of caffeine and theophylline by grinding in a planetary mill at -10 °C (Figure 3.12), suggesting that cocrystallisation of this phase proceeds via an amorphous intermediate. The amorphous phase has not been observed experimentally, however, probably because it is unstable and rapidly crystallises at ambient temperature (at which characterisation was performed).

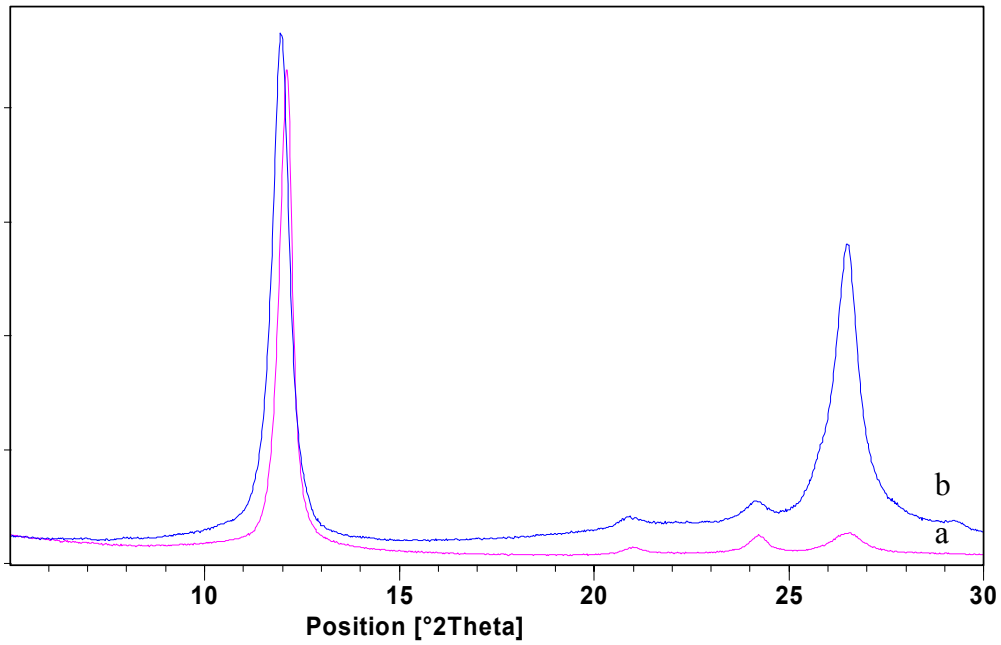

Figure 3.12 XRPD analysis of the solid solution of caffeine and theophylline prepared by different methods. (a) Solid solution of caffeine and theophylline prepared by freeze-drying. (b) Solid solution of caffeine and theophylline obtained by grinding an equimolar ratio of the two compounds in a planetary ball mill at -10 °C for 48 hours.

3.3.3 Cocrystallisation at the Interface between Two Solvent Layers

3.3.3.1 Phenazine:Mesaconic Acid Cocrystal

Saturated solutions of phenazine in xylene and mesaconic acid in water were prepared. 2 ml of the phenazine solution was layered onto 2 ml of the mesaconic acid

solution and held in a sealed vial. Precipitate formed at the solvent interface within a few seconds and was isolated on a filter paper. The XRPD trace of this solid was different to that of the reported cocrystal phase (CSD ref. WOQBAF)[7] and all known polymorphs of phenazine and mesaconic acid, indicating that a new crystal form had been isolated (Figure 3.13).

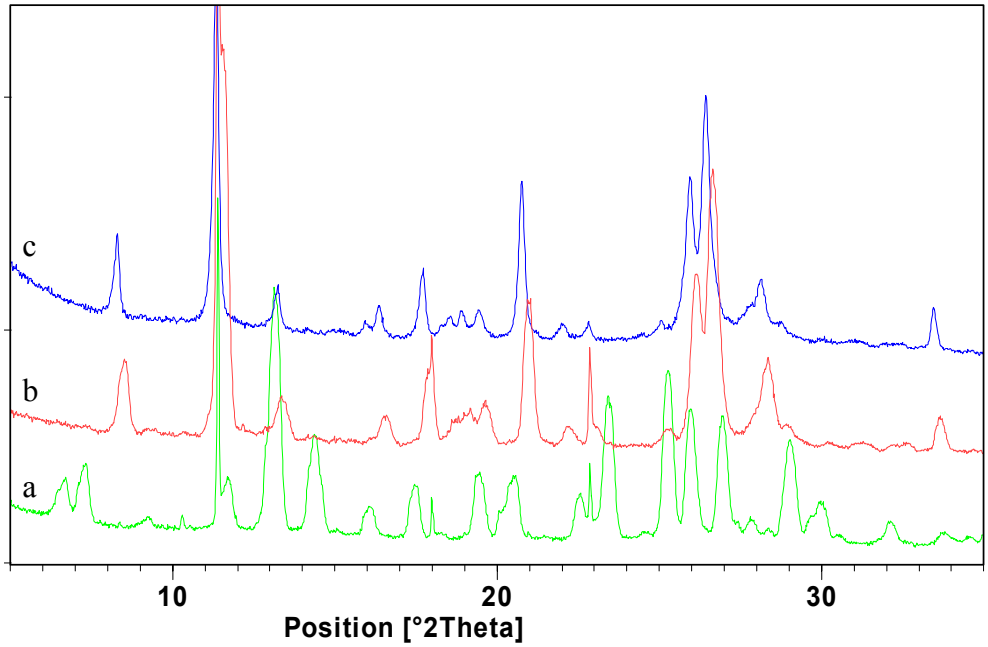

Figure 3.13 XRPD analysis of a sample obtained by cocrystallising phenazine and mesaconic acid at a water/xylene solvent interface. (a) A sample obtained by cocrystallising phenazine and mesaconic acid at a water/xylene solvent interface. (b) The same sample after 10 days of storage under ambient conditions. (c) Reference trace of the reported cocrystal of phenazine and mesaconic acid.

This new crystal phase converted to the known form of the phenazine:mesaconic acid cocrystal during 10 days of storage on a glass slide under ambient conditions. Thermal analysis of the new phase showed a broad endotherm consistent with solvent loss in the DSC trace (Figure 3.14). In addition, a 4 % weight loss was observed during TGA analysis, corresponding to 0.72 moles of water, suggesting that the new phase was a monohydrate of the cocrystal (Figure 3.15).

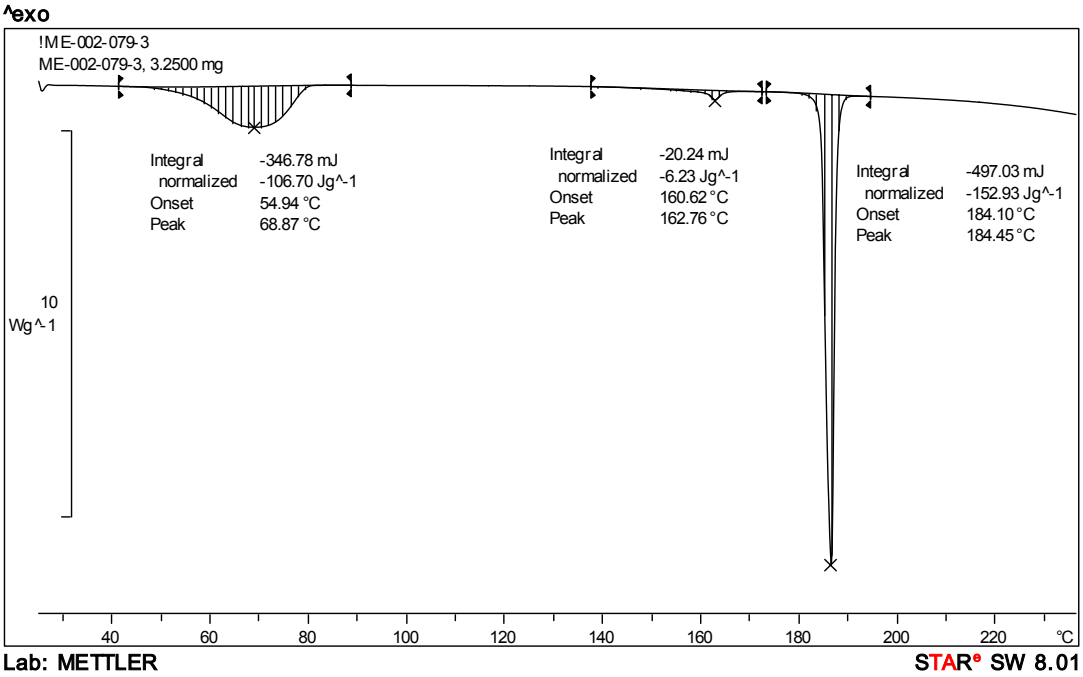

Figure 3.14 DSC thermogram of a sample obtained by cocrystallising phenazine and mesaconic acid at a water/xylene solvent interface (pinhole in lid of DSC pan).

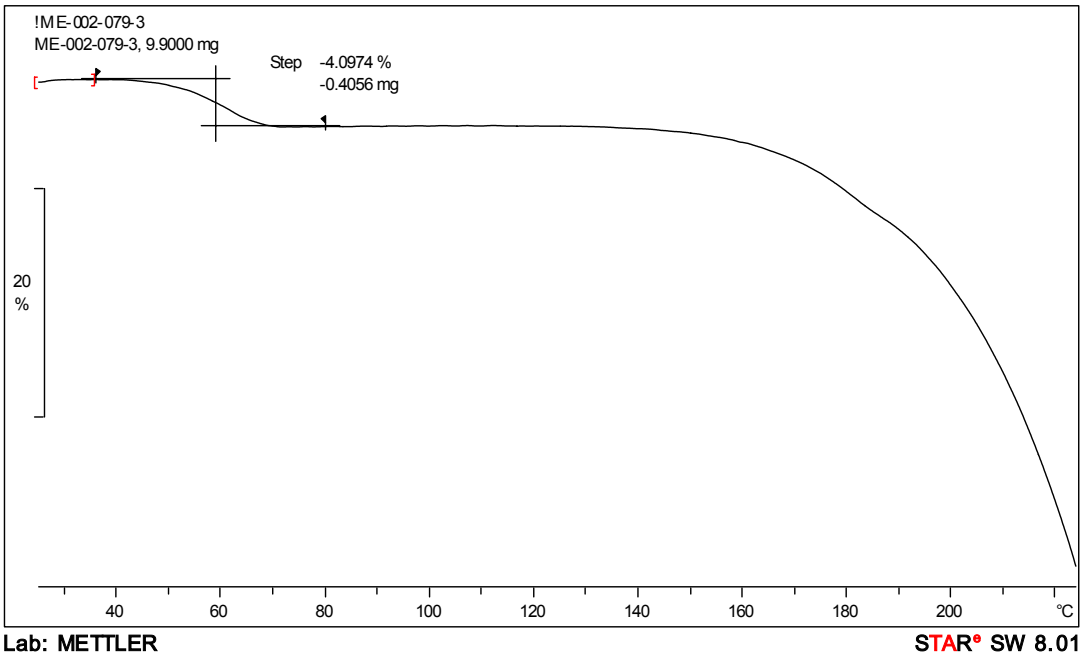

Figure 3.15 TGA thermogram of a sample obtained by cocrystallising phenazine and mesaconic acid at a water/xylene solvent interface. The 4.01 % weight loss between 45 and 74 °C corresponds to 0.72 moles of water (calculated on the basis of a 1:1 cocrystal of phenazine and mesaconic acid).

The solvent interface cocrystallisation method was modified slightly in an attempt to grow large crystals suitable for structure solution by single crystal X-ray diffraction. Instead of using saturated solutions of phenazine in xylene and mesaconic acid in water, the solutions were diluted before combining. The rate of crystallisation was slower in this experiment, yielding crystals suitable for structure solution, and the new phase was confirmed to be a monohydrate of the phenazine:mesaconic acid cocrystal (Figure 3.16). A comparison of simulated and experimental XRPD traces showed that the single crystal that was used to obtain the crystal structure was representative of the bulk of the sample (Figure 3.17).

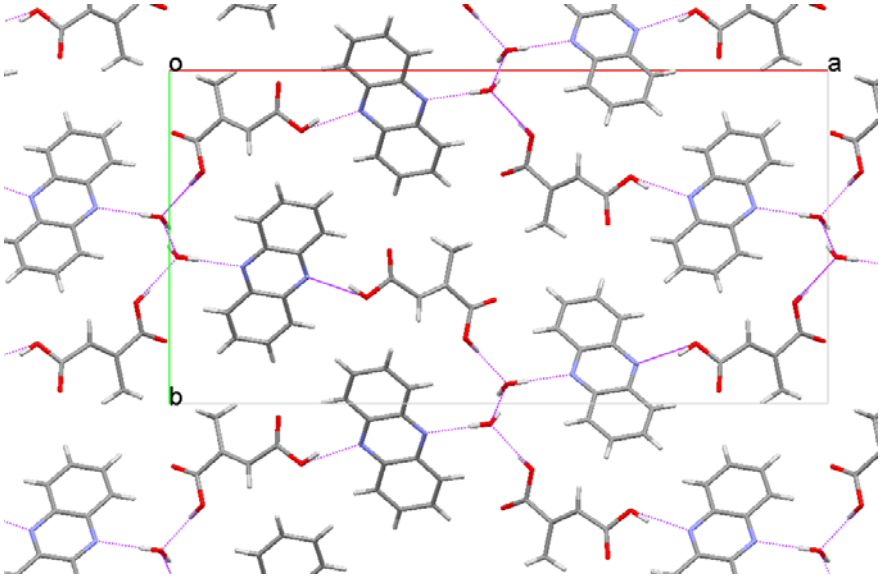

180 K

$Pna2_1$

Orthorhombic

a = 27.495 Å

b = 14.043 Å

c = 4.0898 Å

R_1 = 4.28 %

Figure 3.16 Molecular packing arrangement in the crystal structure of the monohydrate of the 1:1 phenazine:mesaconic acid cocrystal.

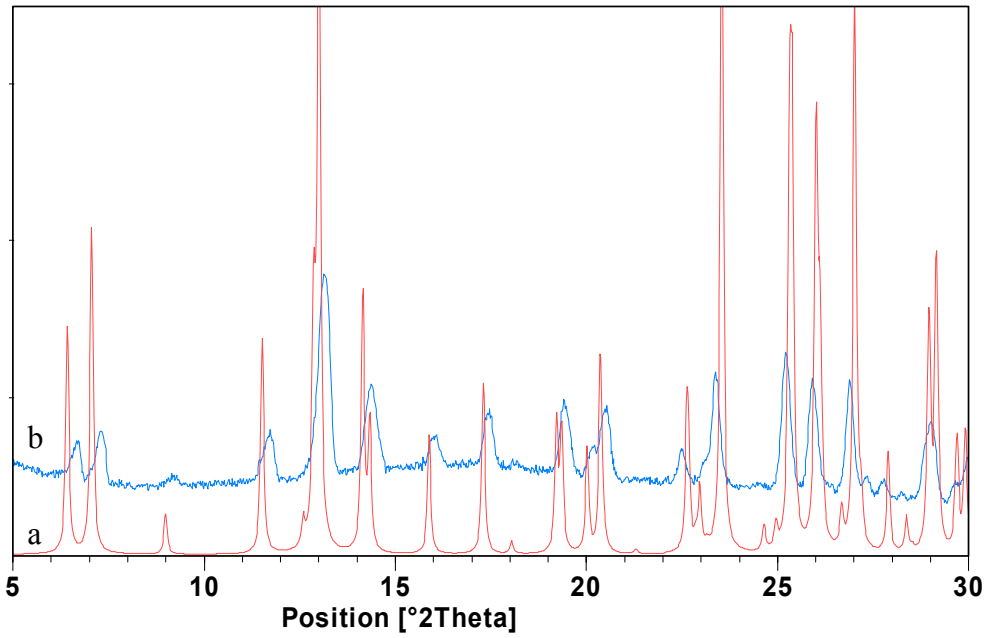

Figure 3.17 Overlay of experimental and simulated XRPD traces of the phenazine:mesaconic acid cocrystal monohydrate. (a) Simulated trace from the crystal structure of the monohydrate of the phenazine:mesaconic acid cocrystal. (b) Experimental trace of the sample obtained by cocrystallising phenazine and mesaconic acid at a water/xylene solvent interface. The slight differences in peak positions are due to thermal expansion (The crystal structure used for the simulation was collected at 180 K).

Cocrystal formation between phenazine and mesaconic acid at the interface between two immiscible solvents was successful, and a new cocrystal phase was identified. This monohydrate was not obtained from grinding experiments with phenazine, mesaconic acid and an equimolar quantity of water, nor could it be obtained from conventional solution crystallisations due to the low aqueous solubility of phenazine.

After removing the precipitated monohydrate of the phenazine:mesaconic acid cocrystal from the solvent interface, the vial was re-sealed and stored under ambient conditions. A second crop of precipitate formed slowly at the interface over several days. The size of crystals in this second batch was noticeably larger than in the previous crop. The XRPD trace of this sample was different to those of both the

monohydrate and the reported anhydrous form of the phenazine:mesaconic acid cocrystal, indicating that another new crystal form had been isolated (Figure 3.18).

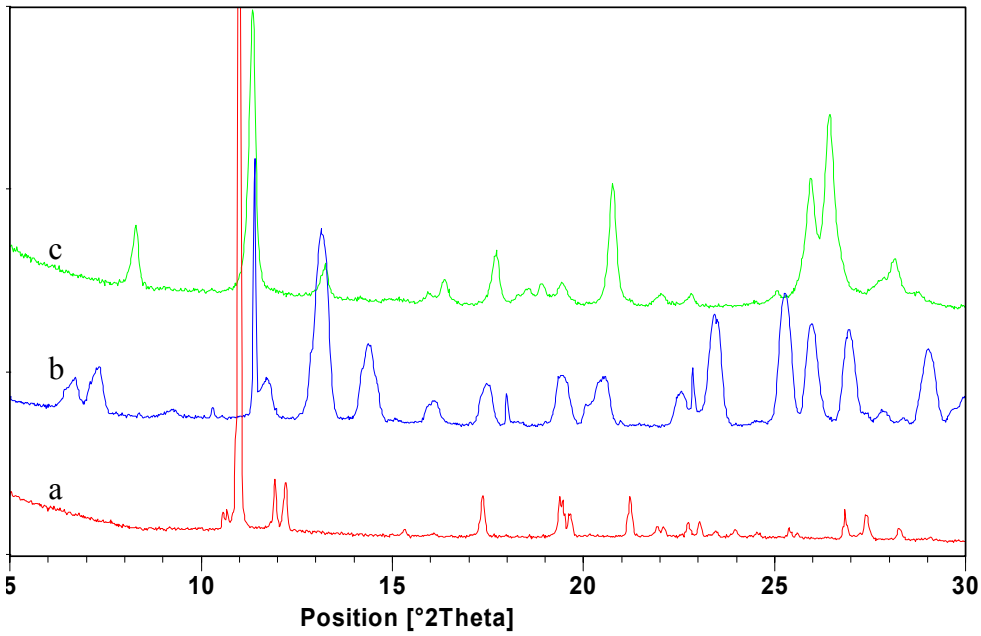

Figure 3.18 XRPD analysis of the second crop of crystals obtained from cocrystallising phenazine and mesaconic acid at a water/xylene solvent interface. (a) The second crop of crystals obtained from cocrystallising phenazine and mesaconic acid at a water/xylene solvent interface. (b) Reference trace of the monohydrate of the phenazine:mesaconic acid cocrystal. (c) Reference trace of the previously reported phenazine:mesaconic acid cocrystal.

The crystal structure of this new form was obtained by single crystal X-ray diffraction and found to be a new polymorph of the 1:1 phenazine:mesaconic acid cocrystal (this polymorph will be referred to as Form II, the previously reported phase as Form I). Phenazine and mesaconic acid molecules form hydrogen bonded chains (Figure 3.19), just as in the structure of Form I, but there is a different 3-dimensional packing arrangement of the chains. A comparison of simulated and experimental XRPD traces showed that the single crystal that was used to obtain the crystal structure was representative of the bulk of the sample (Figure 3.20).

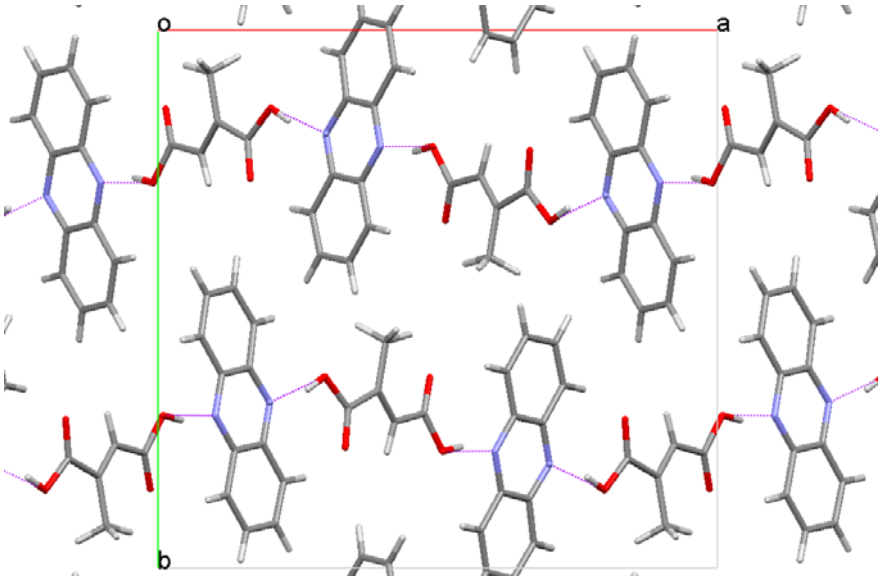

Figure 3.19 Molecular packing arrangement in the crystal structure of Form II of the 1:1 phenazine:mesaconic acid cocrystal.

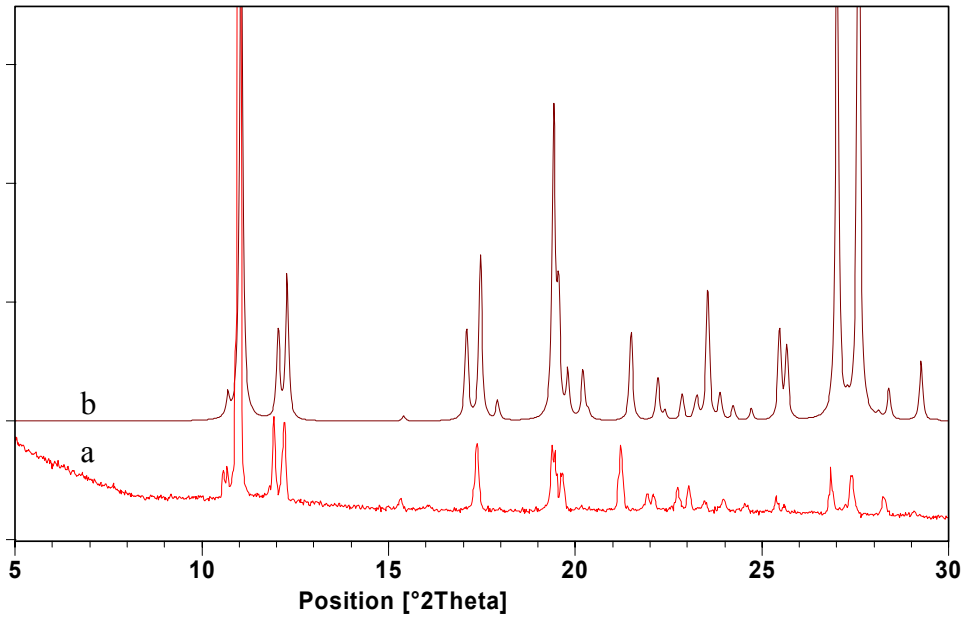

Figure 3.20 Overlay of experimental and simulated XRPD traces of Form II of the phenazine:mesaconic acid cocrystal. (a) The second crop of precipitate obtained by cocrystallising phenazine and mesaconic acid at a water/xylene solvent interface. (b) Simulated trace from the crystal structure of Form II of the phenazine:mesaconic acid cocrystal. The slight differences in peak positions are due to thermal expansion (The crystal structure was collected at 180 K).

3.3.3.2 Caffeine:1-Hydroxy-2-naphthoic Acid Cocrystal

The solvent interface cocrystallisation method was also applied to the caffeine: 1-hydroxy-2-naphthoic acid cocrystal.[10] A saturated solution of 1-hydroxy-2-naphthoic acid in diisopropyl ether (DIPE) was layered onto a saturated solution of caffeine in water. Precipitate formed at the solvent interface within a few seconds and was isolated on a filter paper. The XRPD trace of this solid was different to that of the previously reported cocrystal phase and all polymorphs of caffeine and 1-hydroxy-2-naphthoic acid, indicating that a new crystal form had been isolated (Figure 3.21).

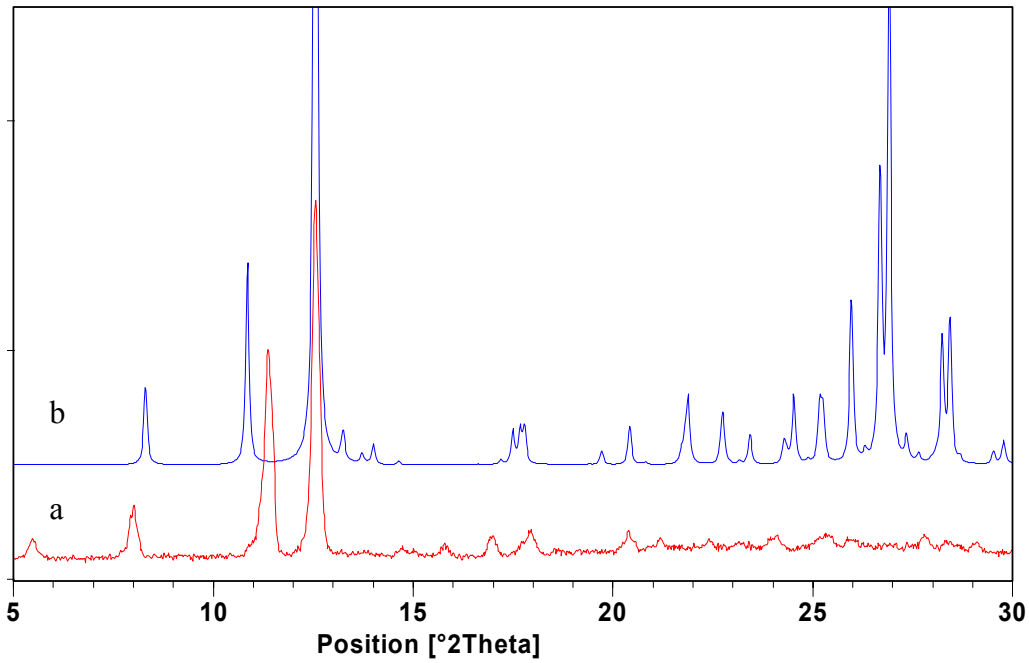

Figure 3.21 XRPD analysis of a new polymorph of the caffeine:1-hydroxy-2-naphthoic acid cocrystal. (a) A sample obtained by cocrystallising caffeine and 1-hydroxy-2-naphthoic acid at a water/DIPE solvent interface. (b) Simulated trace of the reported cocrystal of caffeine and 1-hydroxy-2-naphthoic acid (CSD ref KIGKIV).[10]

This new crystal phase was subsequently obtained in liquid assisted grinding experiments with several different solvents (see Section 4.3.9 for further details), and is believed to be a new polymorph of the 1:1 caffeine:1-hydroxy-2-naphthoic cocrystal.

Cocrystallisation at the interface between two solvent layers was also attempted with RS-ibuprofen and nicotinamide.[23] A saturated solution of nicotinamide in water was layered onto a saturated solution of RS-Ibuprofen in chloroform, but no precipitate formed at the solvent interface. The likely explanation for this negative result is that the solubility of RS-ibuprofen in water, or nicotinamide in chloroform, was not sufficiently low to prevent the compounds from diffusing across the solvent interface. This diffusion would have lead to the solutions being below the concentration limit of the cocrystal, removing the driving force for precipitation of the cocrystal.

3.3.4 Cocrystallisation by Salt Swapping

The aqueous solubility of RS-ibuprofen is less than 1 $mg.ml^{-1}$, while in contrast, the aqueous solubility of the sodium salt of RS-ibuprofen is > 200 $mg.ml^{-1}$. This difference in solubility was exploited for the cocrystallisation of RS-ibuprofen with 4,4-bipyridyl.

An aqueous solution of RS-ibuprofen sodium salt (46.1 mg in 200 µl) was mixed with an aqueous solution of 4,4-bipyridyl dihydrochloride (20 mg in 200 µl, 0.5 mole equivalents). A precipitate formed instantaneously and was isolated on a filter paper. XRPD analysis confirmed that the known cocrystal phase of RS-ibuprofen and 4,4-bipyridyl had been obtained (Figure 3.22).

As predicted, on combining the two salt forms, RS-ibuprofen and 4,4-bipyridyl neutralised and co-precipitated. Sodium and chloride ions remained in solution.

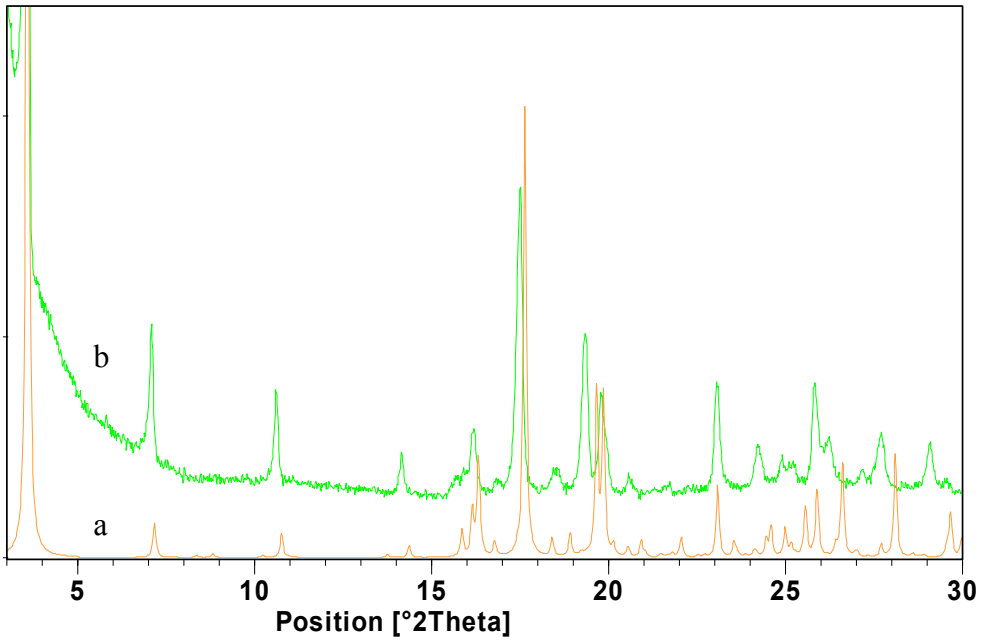

Figure 3.22 XRPD analysis of a sample obtained by cocrystallising RS-ibuprofen and 4,4-bipyridyl by salt swapping. (a) Simulated trace of the 2:1 RS-ibuprofen:4,4-bipyridyl cocrystal (calculated from CSD crystal structure SODDIZ).[12] (b) A sample obtained by mixing aqueous solutions of RS-ibuprofen sodium salt and 4,4-bipyridyl dihydrochloride. The slight differences in peak positions are due to thermal expansion (CSD structure SODDIZ was collected at 200 K).

3.4 Other Significant Results

3.4.1 Thermal Dissociation of the Caffeine:Theophylline Cocrystal

The 1:1 cocrystal of caffeine and theophylline that was prepared by liquid assisted grinding (described in Section 3.1.1) was analysed by DSC. There was a small endothermic event at 147 °C, followed by a sharp endotherm at 201 °C consistent with a melting event (Figure 3.23).

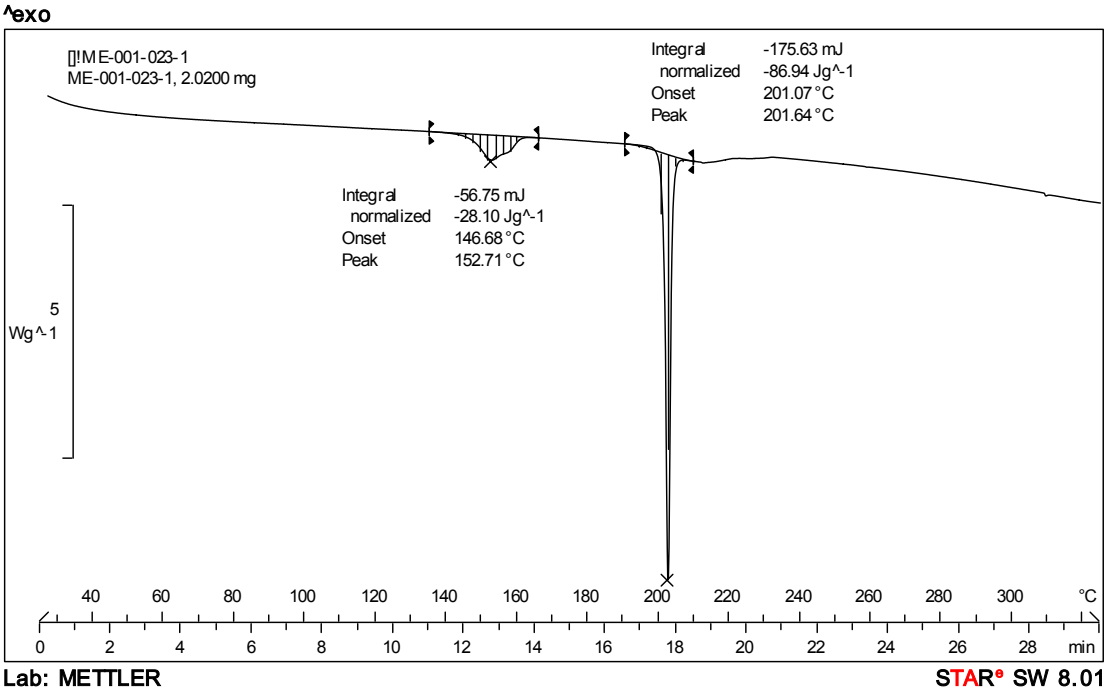

Figure 3.23 DSC thermogram of the 1:1 cocrystal of caffeine and theophylline prepared by liquid assisted grinding.

In order to determine the nature of the small endothermic event, the sample was heated to 170 °C in a sealed DSC pan and cooled to ambient temperature. The sample was then removed from the DSC pan and analysed by XRPD. The XRPD trace was made up of peaks corresponding to Form I of caffeine and Form II of theophylline, showing that the cocrystal had dissociated (Figure 3.24).

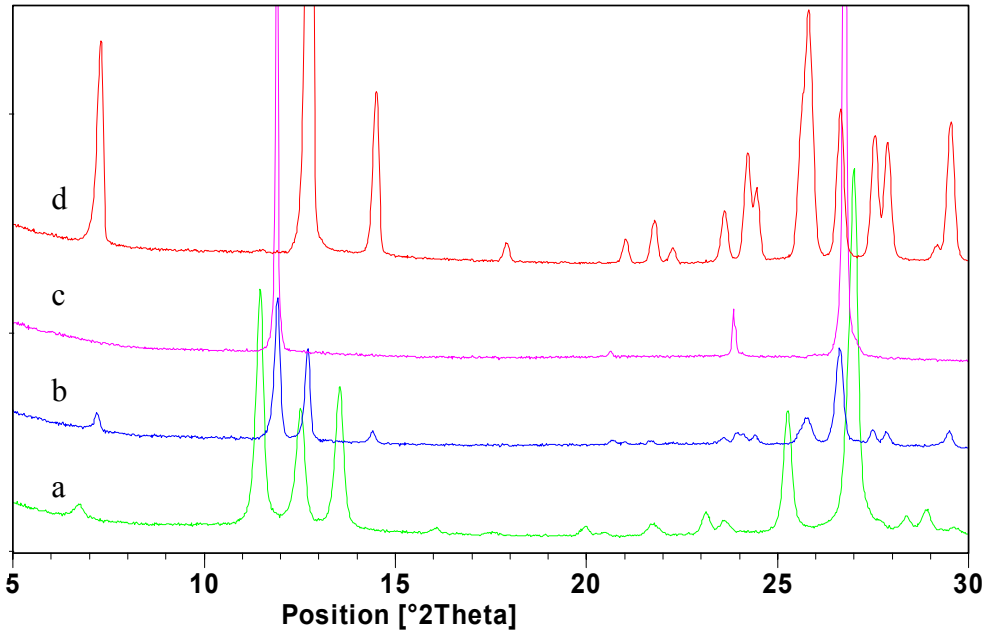

Figure 3.24 XRPD analysis of thermal dissociation of a 1:1 cocrystal of caffeine and theophylline. (a) The 1:1 caffeine:theophylline cocrystal prepared by liquid assisted grinding (b) The same sample after heating to 170 °C. (c) Reference trace of Form I of caffeine. (d) Reference trace of Form II of theophylline.

It is interesting that this cocrystal dissociation event is endothermic, indicating an increase in enthalpy. A spontaneous form change is always accompanied by a decrease in the free energy of the system, meaning that the dissociation must be associated with an increase in entropy. Recent work on the crystal structure of Form I of caffeine has given an explanation for this increase in entropy.[24] Descamps et al found that the caffeine molecules in this crystal form freely rotate at temperatures above 260 K, an entropically favourable phenomenon. If molecules of caffeine were not able to rotate in the cocrystal phase, as would be the case if there were hydrogen bonding interactions between the caffeine and theophylline molecules, then an increase in entropy would be expected on dissociation of the cocrystal.

The caffeine/theophylline mixture which results from the dissociation of the 1:1 caffeine:theophylline cocrystal melts at 201 °C, a temperature significantly lower than the melting points of caffeine and theophylline (which were found to be 236 °C and 270 °C, respectively), indicating that the two compounds have formed a eutectic mixture.

3.4.2 Insights into the Mechanism of Cocrystal Formation by Grinding Resulting from Study of the Caffeine:Theophylline Cocrystal

As described in Section 1.2.3.2, there is debate in the literature as to the mechanism by which cocrystallisation occurs during grinding experiments.

Two different forms of the caffeine:theophylline cocrystal have been obtained by grinding; a solid solution from dry grinding at -10°C, and a 1:1 cocrystal from liquid assisted grinding at ambient temperature with nitromethane. It is believed that the solid solution crystallised from an amorphous intermediate that was generated during grinding, and that the 1:1 cocrystal phase must have crystallised by a different mechanism. Cocrystallisation from a liquid intermediate (formed due to localised melting at hot spots caused by impacts of the metal balls in the grinding vial) does not provide an adequate explanation in this case as the cocrystal has been shown to dissociate below its melting temperature. Another possibility is cocrystallisation via a solution phase. Although grinding is usually thought to be a solid state process as the amount of solvent added during liquid assisted grinding is small (~20 μl), this amount is enough to cover all of the solid particles that are present in the grinding vial with several layers of solvent molecules (this is described in more detail in Chapter 8), and so a solution mediated cocrystallisation mechanism is not unlikely.

This 1:1 form of the caffeine:theophylline cocrystal has subsequently been prepared by crystallisation from solution (from a 3:2 mixture of DMF and dioxane), which supports the solution mediated cocrystallisation theory.

3.5 Conclusions

It has been demonstrated that cocrystallisation grinding experiments do not always yield the most thermodynamically favourable solid forms. This suggests that grinding should not be used alone as a tool for screening for cocrystal formation. In some cases a negative result may be obtained even though cocrystal formation between two coformers is possible.

Three alternative cocrystallisation methods have been successfully applied to the preparation of pharmaceutical cocrystals. These methods are a useful addition to the set of cocrystallisation tools that are available to solid form and process chemists working in the pharmaceutical industry as they have potential applications in cocrystal screening, cocrystal polymorph screening and the large scale manufacture of cocrystals.

A solid solution of caffeine and theophylline has been prepared. To the knowledge of the author this is the first example of a solid solution formed between two active pharmaceutical compounds. This crystal phase is isostructural with Form I of caffeine, and so has hexagonal symmetry. This means that the molecules of caffeine and theophylline must either be rotating, or orientationally disordered in the crystal structure.

3.6 Further Work

An investigation into the rotation of caffeine and theophylline molecules in the solid solution of caffeine and theophylline could be conducted. The rotation of caffeine molecules in Form I of caffeine has been studied using dielectric measurements,[24] and this technique should be applied to characterising the solid solution.

To date, it has not been possible to grow crystals of the caffeine:theophylline cocrystals, or of the new polymorph of the caffeine:1-hydroxy-2-naphthoic acid

cocrystal, that are suitable for crystal structure determination. Further work should be performed in order to obtain these crystal structures.

Cocrystallisation at an interface between two solvents could be studied in more detail to determine why this technique gave new polymorphic forms of two cocrystals, and whether it could be a widely applicable tool for investigating cocrystal polymorphism.

The three alternative cocrystallisation techniques described in this chapter should be applied to a wider range of systems to systematically assess advantages and limitations relative to conventional cocrystallisation techniques.

The applicability of the three alternative cocrystallisation techniques to the manufacture of cocrystals on a large scale should be investigated.

3.7 References

1. Yu L. Amorphous pharmaceutical solids: preparation, characterization and stabilization. *Adv. Drug Deliv. Rev.*, 2001, 48(1), 27-42.

2. Kauzmann W. The nature of the glassy state and the behavior of liquids at low temperatures. *Chem. Rev.*, 1948, 43, 219-256.

3. Sane S. V., Hsu C. C. Strategies for Successful Lyophilization Process Scale-Up. *Am. Pharm. Rev.*, 2007, 10(1), 132-136.

4. Trask A. V., Motherwell W. D. S., Jones W. Pharmaceutical cocrystallization: Engineering a remedy for caffeine hydration. *Cryst. Growth Des.*, 2005, 5(3), 1013-1021.

5. Trask A. V., Motherwell W. D. S., Jones W. Physical stability enhancement of theophylline via cocrystallization. *Int. J. Pharm.*, 2006, 320(1-2), 114-123.

6. Friscic T., Childs S. L., Rizvi S. A. A., Jones W. The role of solvent in mechanochemical and sonochemical cocrystal formation: a solubility-based approach for predicting cocrystallisation outcome. *CrystEngComm*, 2009, 11(3), 418-426.

7. Batchelor E., Klinowski J., Jones W. Crystal engineering using co-crystallisation of phenazine with dicarboxylic acids. *J. Mater. Chem.*, 2000, 10(4), 839-848.

8. Nguyen K. L., Friscic T., Day G. M., Gladden L. F., Jones W. Terahertz time-domain spectroscopy and the quantitative monitoring of mechanochemical cocrystal formation. *Nat. Mater.*, 2007, 6(3), 206-209.

9. Yalkowsky S. H., He Y. Handbook of Aqueous Solubility Data. Boca Raton, Fla.: CRC Press LLC, 2003, 1-1512

10. Bucar D.-K., Henry R. F., Lou X., Duerst R. W., Borchardt T. B., MacGillivray L. R., Zhang G. G. Z. Co-Crystals of Caffeine and Hydroxy-2-naphthoic Acids: Unusual Formation of the Carboxylic Acid Dimer in the Presence of a Heterosynthon. *Mol. Pharmaceutics*, 2007, 4(3), 339-346.

11. Childs S. 2007. Cocrystallization methods for active agents and guest molecules. Application: WO: (SSCI, Inc., USA). p 130pp.

12. Bailey Walsh R. D., Bradner M. W., Fleischman S., Morales L. A., Moulton B., Rodriguez-Hornedo N., Zaworotko M. J. Crystal engineering of the composition of pharmaceutical phases. *Chem. Commun.*, 2003, (2), 186-187.

13. Zhang Y., Grant D. J. W. Similarity in structures of racemic and enantiomeric ibuprofen sodium dihydrates. *Acta Crystallogr., Sect. C: Cryst. Struct. Commun.*, 2005, C61(9), m435-m438.

14. Dolling B., Gillon A. L., Orpen A. G., Starbuck J., Wang X.-M. Homologous families of chloride-rich 4,4'-bipyridinium salt structures. *Chem. Commun.*, 2001, (6), 567-568.

15. Trask A. V., Motherwell W. D. S., Jones W. Solvent-drop grinding: green polymorph control of cocrystallisation. *Chem. Commun.*, 2004, (7), 890-891.

16. Ebisuzaki Y., Boyle P. D., Smith J. A. Methylxanthines. I. Anhydrous theophylline. *Acta Crystallogr., Sect. C: Cryst. Struct. Commun.*, 1997, C53(6), 777-779.

17. Caira M. R., Nassimbeni L. R., Wildervanck A. F. Selective formation of hydrogen bonded cocrystals between a sulfonamide and aromatic carboxylic acids in the solid state. *J. Chem. Soc., Perkin Trans. 2*, 1995, (12), 2213-2216.

18. Cesaro A., Starec G. Thermodynamic properties of caffeine crystal forms. *J. Phys. Chem.*, 1980, 84(11), 1345-1346.

19. Enright G. D., Terskikh V. V., Brouwer D. H., Ripmeester J. A. The Structure of Two Anhydrous Polymorphs of Caffeine from Single-Crystal Diffraction and Ultrahigh-Field Solid-State 13C NMR Spectroscopy. *Cryst. Growth Des.*, 2007, 7(8), 1406-1410.

20. Jacob K. T., Raj S., Rannesh L. Vegard's law: a fundamental relation or an approximation? *Int. J. Mater. Res.*, 2007, 98(9), 776-779.

21. Bucar D. K., Henry R. F., Lou X. C., Borchardt T. B., Zhang G. G. Z. A "hidden" co-crystal of caffeine and adipic acid. 2007, (5), 525-527.

22. Descamps M., Willart J. F., Dudognon E., Caron V. Transformation of pharmaceutical compounds upon milling and comilling: The role of T-g. *J. Pharm. Sci.*, 2007, 96(5), 1398-1407.

23. Berry D. J., Seaton C. C., Clegg W., Harrington R. W., Coles S. J., Horton P. N., Hursthouse M. B., Storey R., Jones W., Friscic T., Blagden N. Applying Hot-Stage Microscopy to Co-Crystal Screening: A Study of Nicotinamide with Seven Active Pharmaceutical Ingredients. *Cryst. Growth Des.*, 2008, 8(5), 1697-1712.

24. Descamps M., Correia N. T., Derollez P., Danede F., Capet F. Plastic and Glassy Crystal States of Caffeine. *J. Phys. Chem. B*, 2005, 109(33), 16092-16098.

4 Cocrystal Polymorphism

4.1 Introduction

As described in Chapter 1, polymorphism is a key issue in the pharmaceutical industry. In order for cocrystal forms of APIs to be used in future pharmaceutical drug products it will be necessary to understand the polymorphic behaviour of cocrystals.

Polymorphism in pharmaceutical cocrystals has not been extensively studied.[1] Early work led to suggestions that cocrystals are less prone to polymorphism than free forms and salt forms of API's,[2-4] but there is no clear scientific rationale for why this should be the case. A study of the CSD in 2008, not limited to pharmaceutical systems, identified 33 sets of polymorphic cocrystals,[5] and there are now also several reported examples of polymorphism in pharmaceutical cocrystals,[6-8] including three different polymorphs of the ethenzamide:gentisic acid cocrystal.[9] Porter et al have speculated that the lack of extensive polymorphism observed in cocrystal systems to date is due to difficulties with methods for screening for cocrystals rather than a decreased tendency for cocrystals to be polymorphic.[6] Whereas solution based crystallisation screens are widely used for investigating the polymorphism of APIs, this approach is not so applicable to cocrystals as solution crystallisation often generates mixtures of coformers rather than cocrystal phases (as described in Section 1.2.3.2). To date, no systematic approaches to investigating cocrystal polymorphism have been reported. The methods that have been used to prepare different polymorphs of individual systems are liquid assisted grinding,[10] solution crystallisation,[9,10] slurrying,[11] and polymer nucleated crystallisation.[6]

The work in this chapter is not a systematic study of cocrystal polymorphism, but rather a collection of examples that have been identified during work for this thesis. Not all of the examples described are pharmaceutical systems.

4.2 Experimental

Variable temperature X-ray powder diffraction (VT-XRPD) experiments were performed by Florence Danede of the Unite Materiaux et Transformation, Universite Lille 1.

4.3 Results

4.3.1 Caffeine:Theophylline Cocrystal

Three multicomponent crystal forms of caffeine and theophylline have been isolated. The XRPD traces of these forms are shown in Figure 4.1.

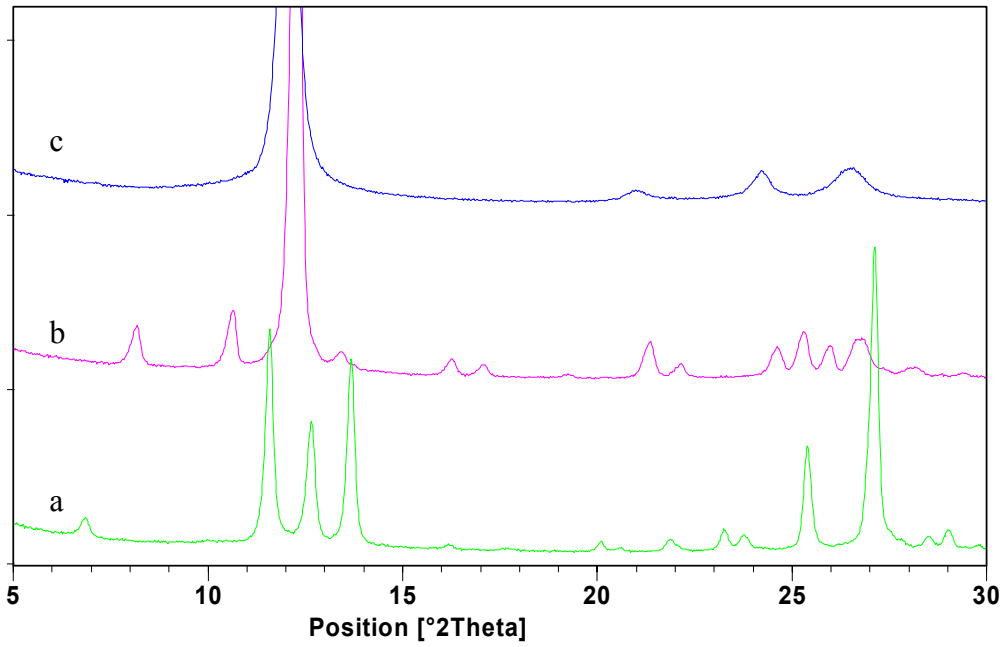

Figure 4.1 Overlay of XRPD traces of three multicomponent crystal forms of caffeine and theophylline. (a) Form III. (b) Form II. (c) Form I.

Form I is a solid solution of caffeine and theophylline that was prepared by freeze-drying (see Section 3.3.2 for further details). A PLM image of crystals of Form I is shown in Figure 4.2a. The crystals have lath or needle-like habits and lengths of up to 20 μm. On re-analysing this sample after 6 days of storage under ambient conditions, a decrease in crystal size was observed (Figure 4.2b), suggesting that a change in crystal form may have occurred. This was confirmed by XRPD analysis (Figure 4.3). The new crystal form will be referred to as Form II of the caffeine:theophylline system.

a b

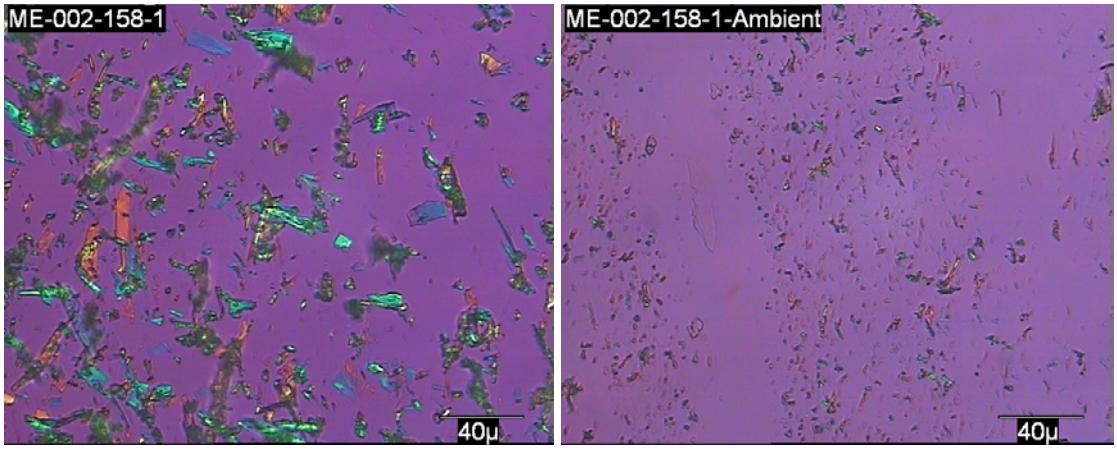

Figure 4.2 Polarised light microscopy images of caffeine:theophylline forms. (a) The solid solution of caffeine and theophylline after preparation by freeze-drying. (b) The same sample after storage under ambient conditions for 6 days (Form II, a caffeine:theophylline cocrystal).

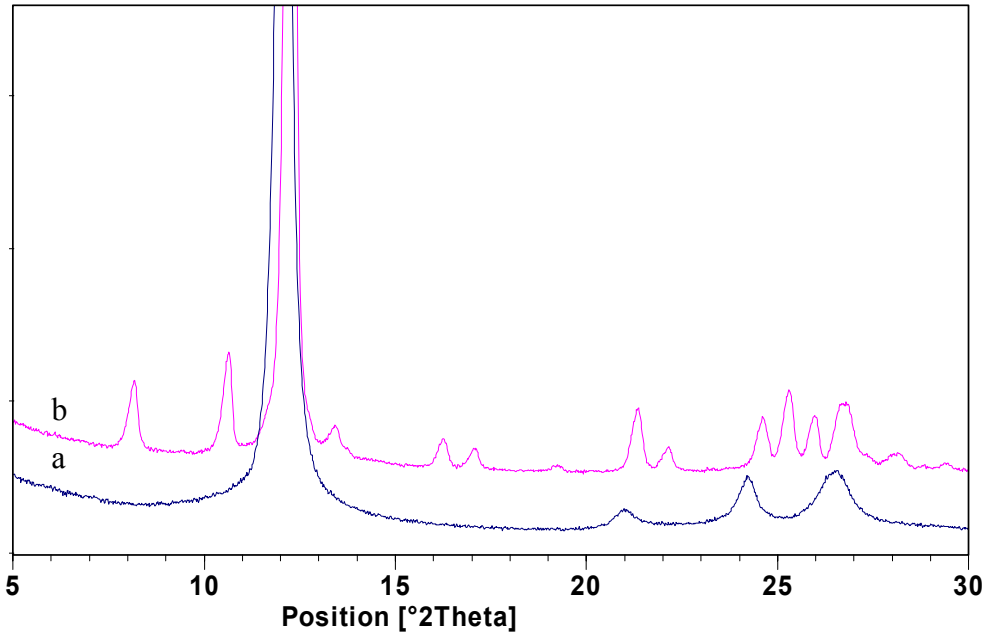

Figure 4.3 XRPD analysis of the solid solution of caffeine and theophylline before and after storage under ambient conditions. (a) The solid solution of caffeine and theophylline immediately after preparation by freeze-drying. (b) The same sample after storage under ambient conditions (Form II, a caffeine:theophylline cocrystal).

In Form I, the solid solution, the ratio of caffeine and theophylline can be varied. If the solid solution is prepared with more caffeine than theophylline, after storing the sample under ambient conditions, a mixture of Form II and caffeine is obtained. Similarly, if Form I is prepared with an excess of theophylline, a mixture of Form II and theophylline is generated after ambient storage (Figure 4.4). This indicates that the ratio of caffeine to theophylline in Form II is 1:1.

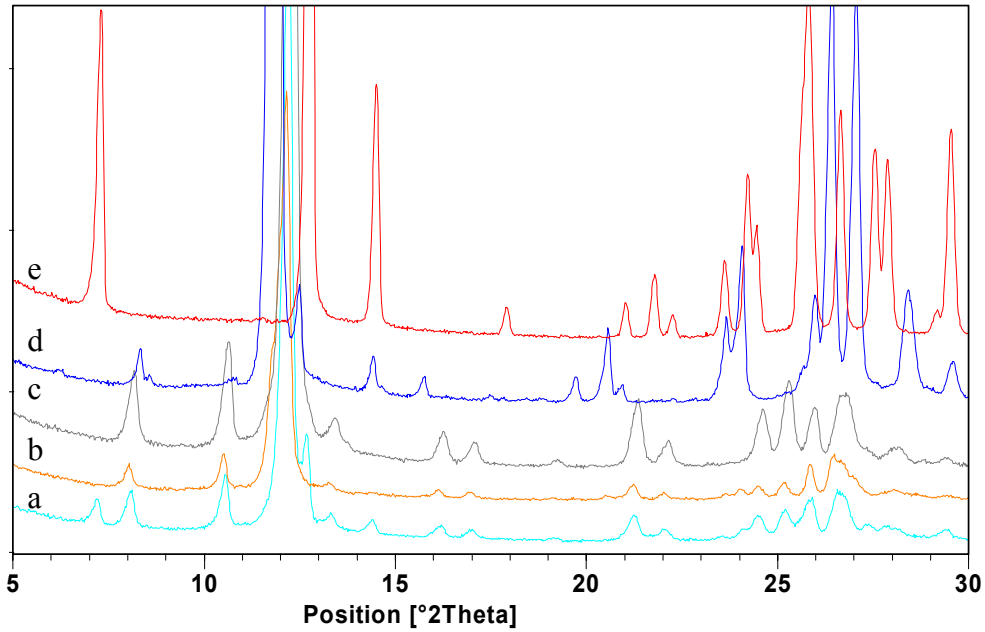

Figure 4.4 XRPD analysis of the conversion of Form I, the solid solution of caffeine and theophylline, to Form II. (a) A sample of Form I prepared at a 2:3 ratio of caffeine to theophylline after storage under ambient conditions. (b) A sample of Form I prepared at a 3:2 ratio of caffeine to theophylline after storage under ambient conditions. (c) Reference trace of Form II of the cocrystal. (d) Reference trace of Form II of caffeine.[12] (e) Reference trace of Form II of theophylline.[13]

A series of potential crystal structures for the 1:1 cocrystal of caffeine and theophylline was generated by crystal structure prediction. More information about crystal structure prediction is given in Chapter 7. The simulated XRPD traces of these forms were compared with the experimental trace of cocrystal Form II. A match was found with the 10th lowest energy structure (monoclinic $P2_1/c$, a = 7.009, b = 14.563, c = 21.655 and β = 49.99) from the predictions (Figure 4.5). There are slight differences between peak positions of the simulated and experimental XRPD traces of this crystal form, especially at high angles. This suggests that there are small differences between the unit cell dimensions of Form II of the cocrystal and the theoretical crystal structure that corresponds to Form II.

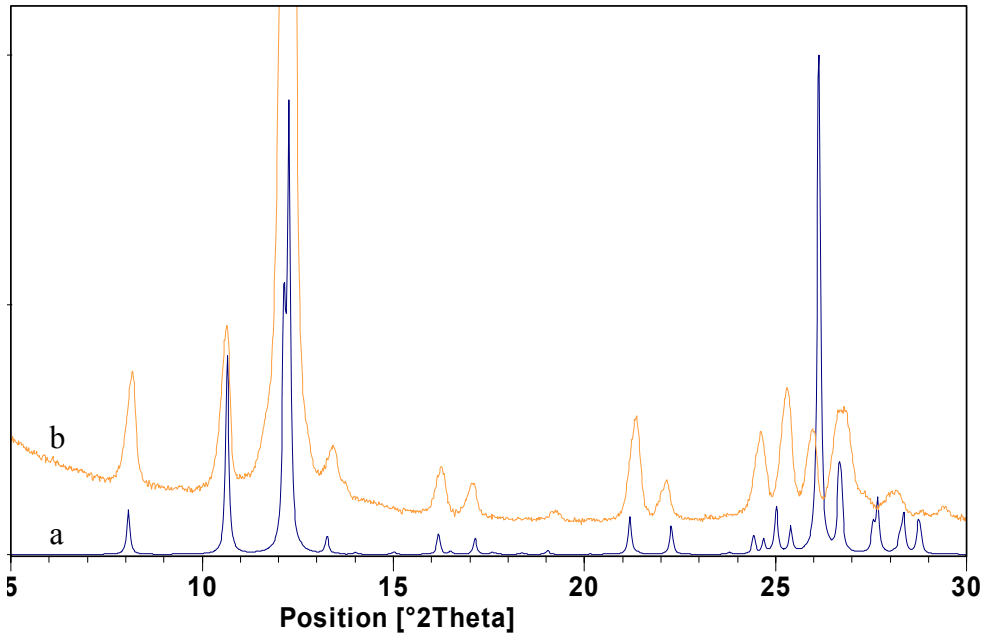

Figure 4.5 Overlay of experimental and simulated XRPD traces of Form II of the caffeine:theophylline cocrystal. (a) Simulated trace from the 10th lowest energy predicted cocrystal structure of 1:1 caffeine:theophylline. (b) Experimental trace of Form II of the caffeine:theophylline cocrystal. The slight differences in peak positions are due to imperfect prediction of the unit cell lengths and angles of the CSP structure.

A Pawley refinement[14] was performed on the experimental XRPD trace of Form II of the caffeine:theophylline cocrystal using the unit cell parameters from the 10th lowest energy predicted crystal structure as a starting point. The unit cell parameters were refined to a = 7.122, b = 14.481, c = 22.413 and β = 48.73 respectively, and the overall fit was good with a χ^2 value of 3.18 (Figure 4.6). It was not possible to perform a Rietveld refinement[15] as peak intensities in the experimental XRPD trace were strongly affected by preferred orientation.

The molecular packing arrangement of the 10th lowest energy predicted crystal structure of the 1:1 caffeine:theophylline cocrystal is shown in Figure 4.7. Caffeine and theophylline molecules form pair-wise hydrogen bonding interactions, and pairs align to form 1-dimensional stacks.

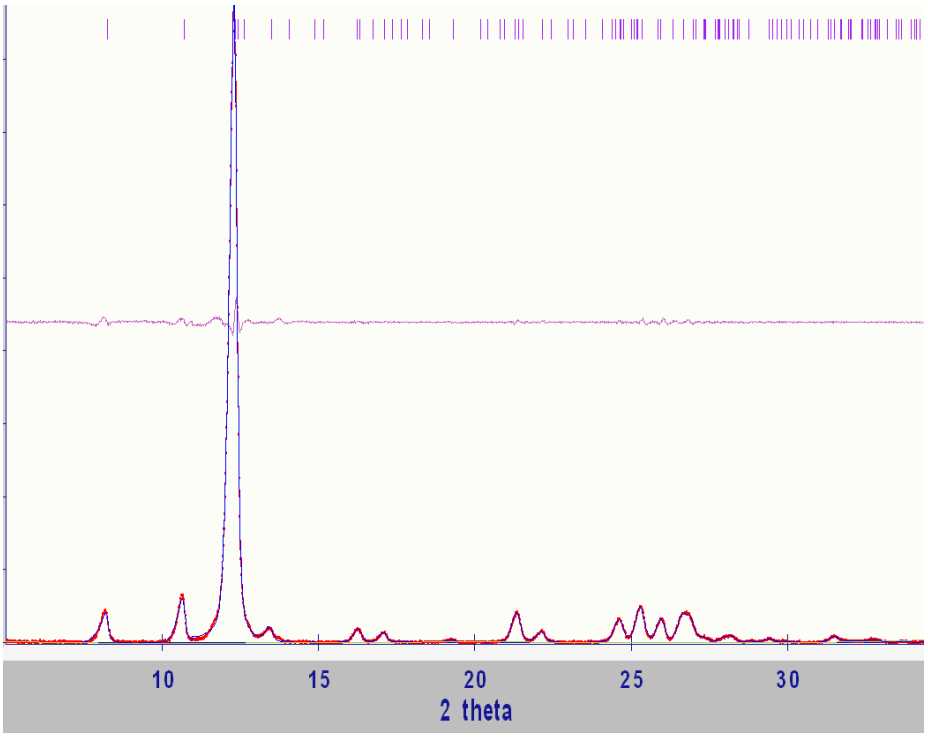

Figure 4.6 Results of Pawley refinement for Form II of the caffeine:theophylline cocrystal. The experimental XRPD trace is shown in red, the Pawley fit is overlaid in blue and the difference trace for these two patterns is shown in pink.

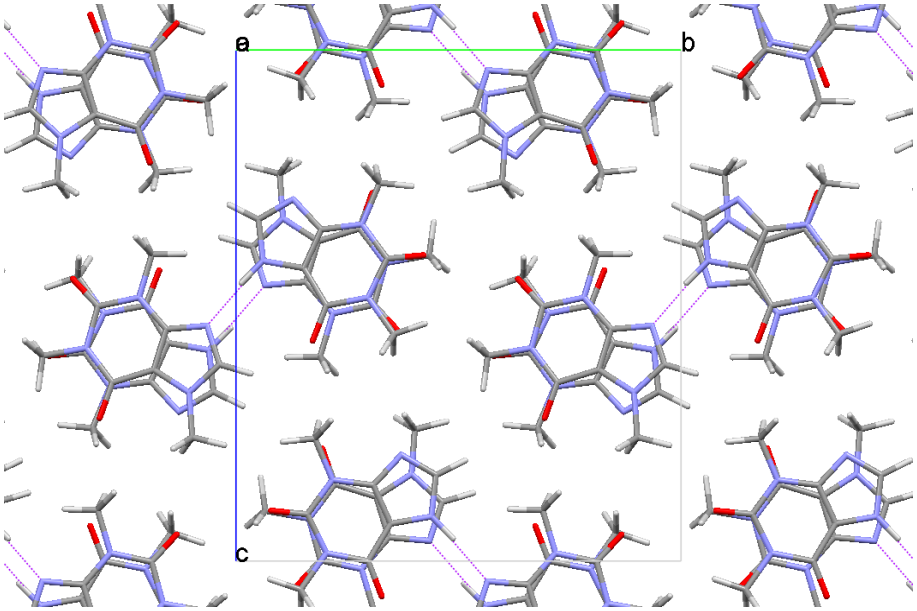

Figure 4.7 Molecular packing arrangement in the calculated crystal structure of Form II of the caffeine:theophylline cocrystal.

Form III is a 1:1 cocrystal of caffeine and theophylline that was prepared by liquid assisted grinding (see Section 3.3.1 for further details).

No matches for Forms I and III were found in the set of molecules generated by crystal structure prediction.

The relative thermodynamic stability of the three multicomponent forms of caffeine and theophylline is Form III > Form II > Form I. As shown above, under ambient conditions Form I converts to Form II. This conversion takes between 24 and 48 hours. A much slower conversion of Form II to Form III has also been observed under ambient conditions (a sample of Form II partially converted to Form III during a three year period (Figure 4.8)).

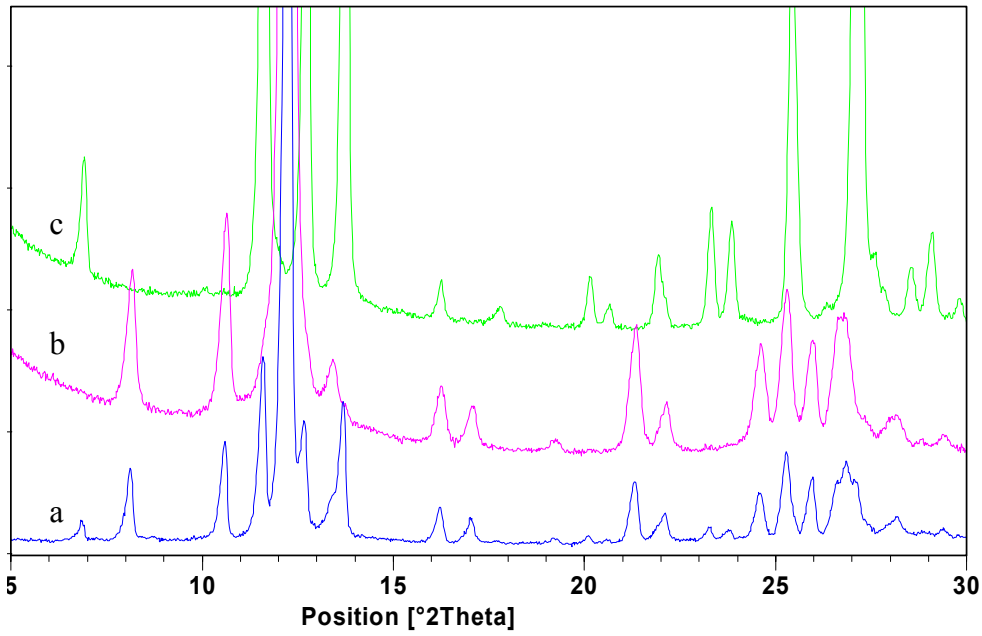

Figure 4.8 XRPD analysis of Form II of the caffeine:theophylline cocrystal after storage under ambient conditions for 3 years. (a) Form II of the caffeine:theophylline cocrystal after storage under ambient conditions for 3 years. (b) Reference trace of Form II of the caffeine:theophylline cocrystal. (c) Reference trace of Form III of the caffeine:theophylline cocrystal.

4.3.2 1:1 Caffeine:1-Hydroxy-2-naphthoic Acid Cocrystal

Form I of this cocrystal was reported by Bucar et al,[16] and a new polymorph, Form II, was prepared by cocrystallisation at the interface between two solvent layers (see Section 3.3.3 for XRPD traces and further details).

Cocrystal formation was also investigated by liquid assisted grinding with a selection of solvents (this work was conducted with Saranja Sivachelvam, a summer student at the Department of Chemistry, University of Cambridge). 103.2 mg of caffeine and 100 mg of 1-hydroxy-2-naphthoic acid (1 mole equivalent) were ground with 20 µl of solvent. Both Form I and Form II of the cocrystal were isolated from this cocrystallisation screen. Grinding with polar solvents (high dielectric constant) favoured generation of Form I, whereas non-polar solvents tended to give Form II. The results are summarised in Table 4.1.

Table 4.1 A table showing the outcome of grinding a 1:1 molar ratio of caffeine and 1-hydroxy-2-naphthoic acid with different solvents.

Solvent	Dielectric Constant	Outcome
Water	80.4	Form I
DMSO	46.5	Form I
Acetonitrile	37.5	Form I
DMF	36.7	Form I
Methanol	32.6	Form I
Acetone	20.7	Form I
Butanol	17.8	Form I
Chlorobenzene	5.7	Form II
Diisopropyl ether	3.9	Form I
Dichloroethane	3.4	Form II
t-Butylmethyl ether	3.1	Form I + Form II
Cyclohexane	2.0	Form I + Form II

4.3.3 1:1 Theophylline:Formamide Cocrystal

A new crystal form was obtained by slow evaporation of a solution of theophylline in formamide. The crystals were suitable for single crystal X-ray structure determination. The sample was found to be a 1:1 cocrystal of theophylline and formamide (Figure 4.9). Theophylline and formamide form hydrogen bonded chains with one amide-extended amide interaction and one N-H···N hydrogen bond.

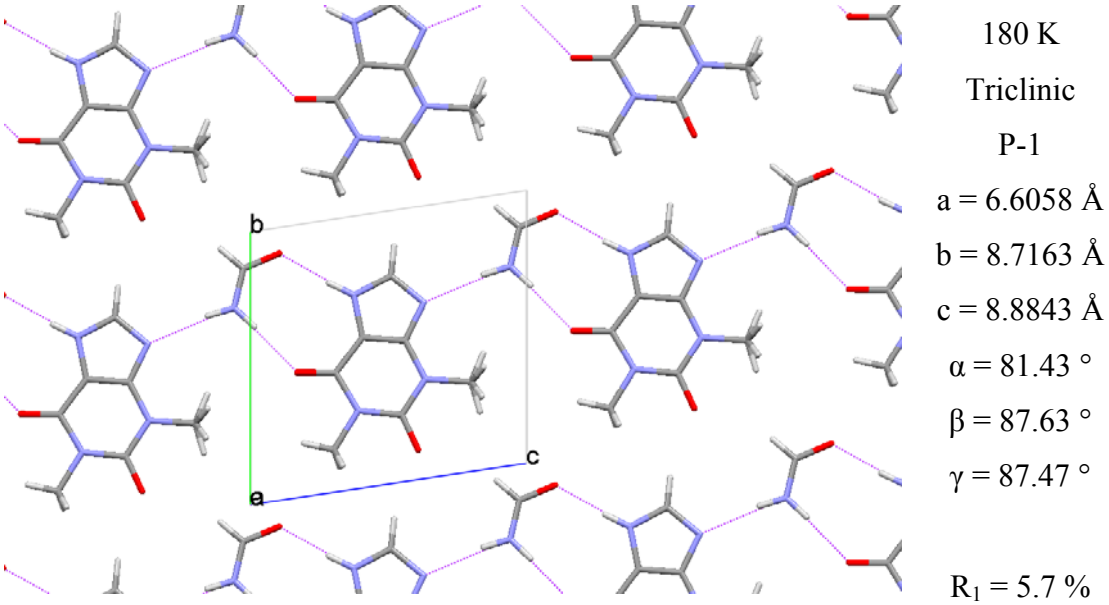

Figure 4.9 Molecular packing arrangement in the crystal structure of a 1:1 cocrystal of theophylline and formamide at 180 K.

Small differences were observed between the XRPD trace simulated from the single crystal structure and that of the experimental sample (Figure 4.10). Peaks at 18.9 and 25.3 °2θ in the experimental trace were absent from the simulated trace. Also, peaks at 18.3, 19.4, 24.7 and 25.9 °2θ in the simulated trace were absent from the experimental trace.

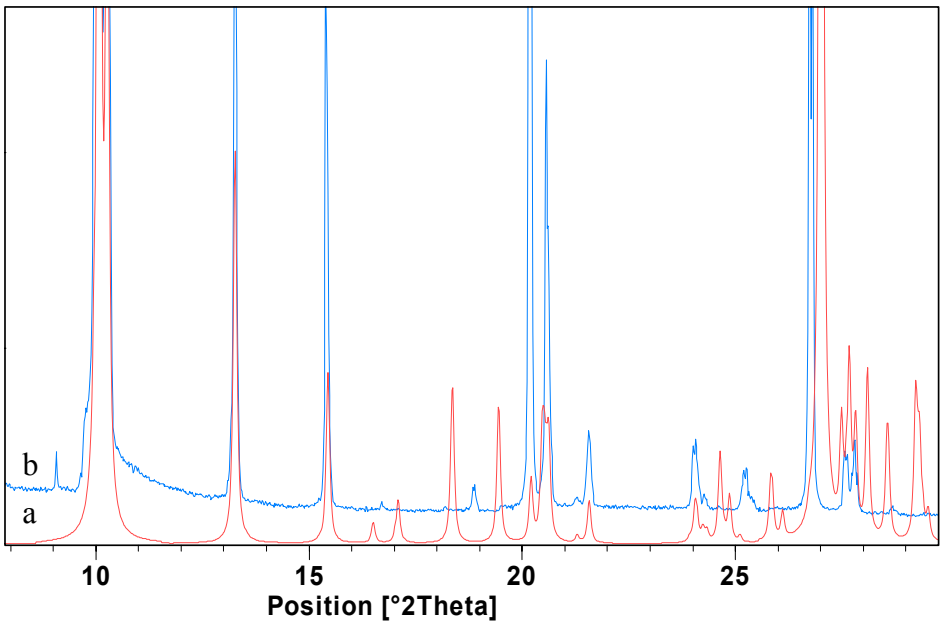

Figure 4.10 Overlay of room temperature experimental and low temperature simulated XRPD traces of the 1:1 theophylline:formamide cocrystal. (a) Simulated trace from the crystal structure of the 1:1 theophylline:formamide cocrystal (180 K). (b) Experimental trace of the sample obtained by slow evaporation of a solution of theophylline in formamide. Some differences in the traces are too large to be caused by thermal expansion, e.g. between 16 and 20 °2θ there are two peaks in the experimental trace, but no corresponding peaks in the simulated trace. There are also a greater number of peaks in the simulated trace in this region.

Single crystal X-ray structure determination was repeated, with the temperature of data collection increased from 180 K to 270 K (Figure 4.11). The 270 K crystal structure had a different space group to the 180 K structure, showing that a polymorphic conversion occurs between these two temperatures (the polymorph that is stable at 180 K will be referred to as Form I, the polymorph that is stable under ambient conditions as Form II). The two single crystal structures are very similar, the main difference being a mirror plane in the Form II structure which is not present at low temperature. The simulated XRPD trace of the 270 K structure matched the trace of the experimental sample of the formamide solvate (Figure 4.12).

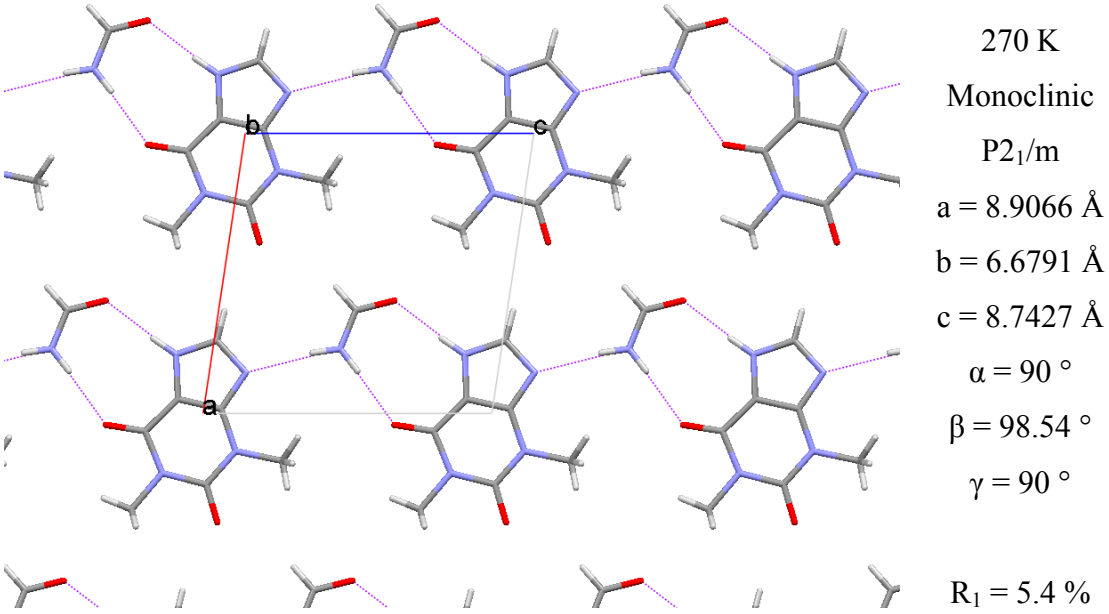

Figure 4.11 Molecular packing arrangement in the crystal structure of Form II of the 1:1 cocrystal of theophylline and formamide at 270 K.

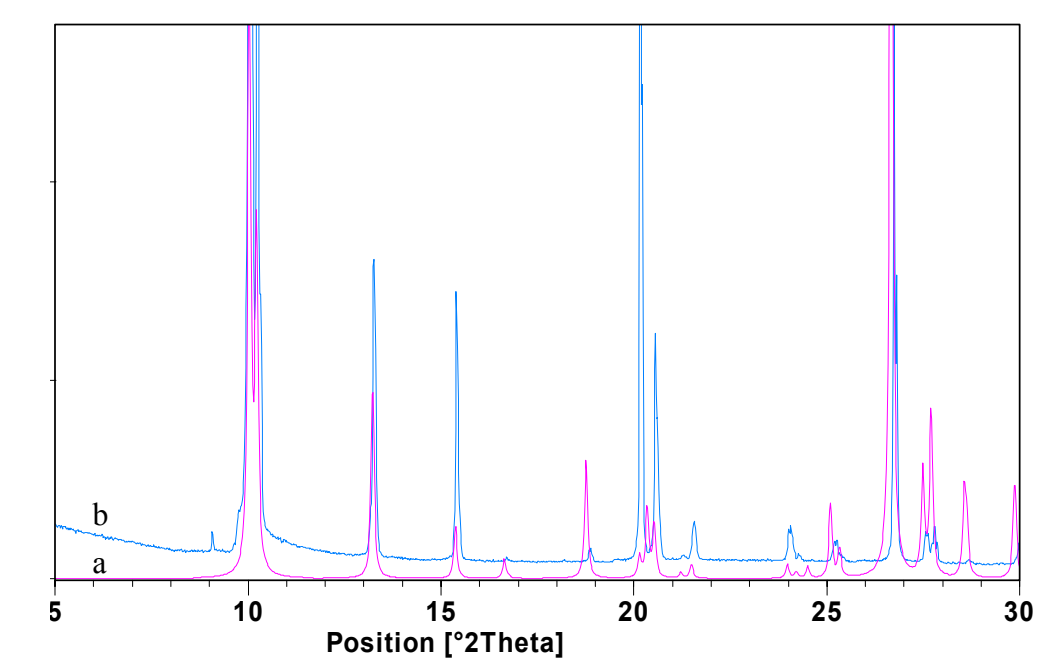

Figure 4.12 Overlay of experimental and simulated XRPD traces of Form II of the 1:1 theophylline:formamide cocrystal. (a) Simulated trace from the crystal structure of Form II of the 1:1 theophylline:formamide cocrystal (270 K). (b) Experimental trace of the sample obtained by slow evaporation of a solution of theophylline in formamide.

4.3.4 1:1 Theophylline:Pyrazinamide Cocrystal

Form I of the 1:1 theophylline:pyrazinamide cocrystal was obtained by evaporation of an equimolar solution of theophylline and pyrazinamide in tetrahydrofuran. The crystal structure of this form is shown in Figure 4.13. Theophylline molecules form dimers through extended amide-extended amide hydrogen bonding interactions, and pyrazinamide molecules form dimers through amide-amide arrangements. The dimers of theophylline and pyrazinamide link to form 1-dimensional hydrogen bonded chains.

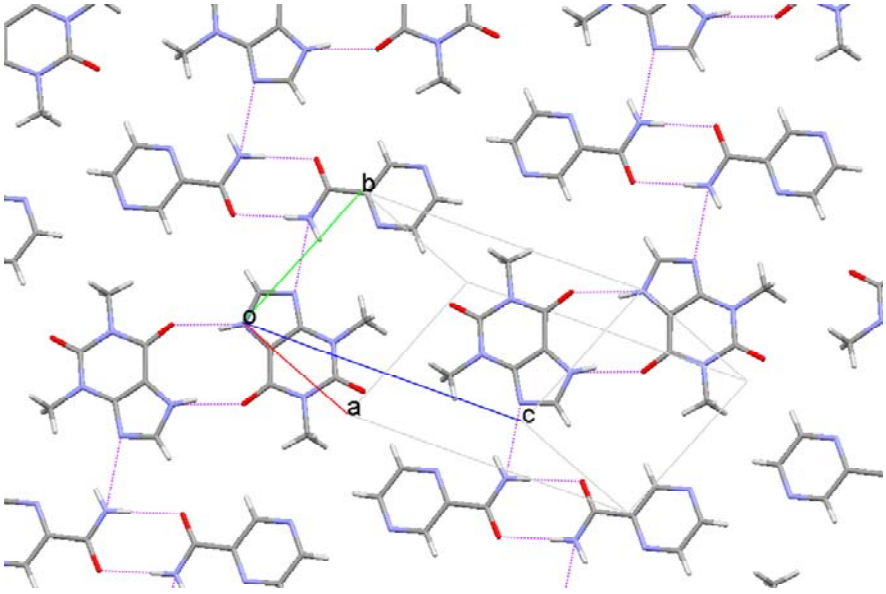

180 K
P-1
Triclinic
a = 7.4800 Å
b = 7.6959 Å
c = 12.7028 Å
α = 86.113 °
β = 75.930 °
γ = 68.995 °
R_1 = 5.48 %

Figure 4.13 Molecular packing arrangement in the crystal structure of Form I of the 1:1 cocrystal of theophylline and pyrazinamide.

Grinding theophylline and pyrazinamide in an equimolar ratio, with toluene or with DMF, gave a sample with an XRPD trace that did not match that of Form I of the cocrystal, or any of the known forms of theophylline and pyrazinamide (Figure 4.14).

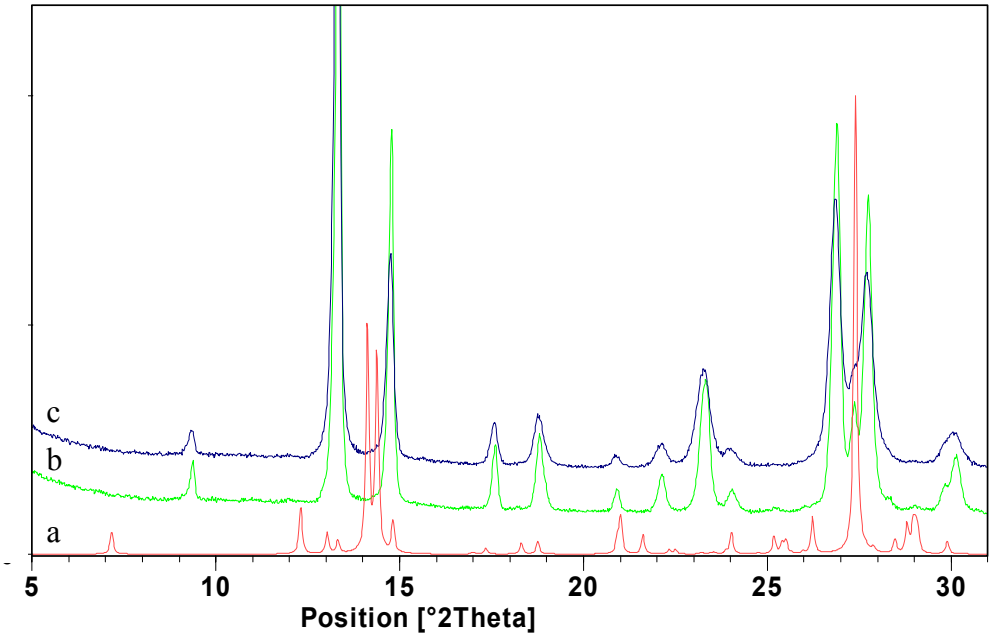

Figure 4.14 XRPD analysis of samples prepared by liquid assisted grinding of an equimolar amount of theophylline and pyrazinamide. (a) Simulated trace from the crystal structure of Form I of the 1:1 theophylline:pyrazinamide cocrystal. (b) A sample obtained by grinding an equimolar amount of theophylline and pyrazinamide with DMF. (c) A sample obtained by grinding an equimolar amount of theophylline and pyrazinamide with toluene.

Because grinding at a 1:1 molar ratio appears to have given a pure phase by XRPD, the new crystal form obtained by grinding is believed to be a 1:1 cocrystal of theophylline and pyrazinamide (there is no evidence of XRPD peaks corresponding to excess theophylline or pyrazinamide). This polymorph will be called Form II.

With this system, the cocrystallisation method that is used to prepare the cocrystal of theophylline and pyrazinamide influences the polymorphic form that is obtained. Cocrystallisation from solution, using both polar and non-polar solvents, gave Form I of the cocrystal, whereas cocrystallisation by liquid assisted grinding, with both polar and non-polar solvents, gave Form II of the cocrystal.

4.3.5 1:1 Theophylline:Benzamide Cocrystal

On grinding 150 mg of theophylline and 107.3 mg of benzamide (1 mole equivalent) with 30 µl of nitromethane, a new crystal form was obtained. The XRPD trace of this form did not match any of the known polymorphs of theophylline or benzamide suggesting that this new form was a 1:1 cocrystal (Figure 4.15).

A second grinding experiment was conducted using the same amounts of theophylline and benzamide. The two compounds were initially ground together dry, and the resulting sample was analysed by XRPD. The XRPD trace contained peaks corresponding to theophylline Form II and benzamide Form I, and there was no evidence of cocrystal formation. Nitromethane was then added, and the solid was re-ground. XRPD analysis after this liquid assisted grinding step showed not only that theophylline and benzamide were no longer present, suggesting that cocrystallisation had occurred, but also that this was a different crystal phase to that obtained from the first experiment (Figure 4.15). This phase is believed to be a second polymorph of the 1:1 theophylline:benzamide cocrystal.

The key difference between the preparation methods for these two polymorphs is the initial dry grinding step in the second experiment. It is possible that dry grinding generated seeds of the second form of the cocrystal, and that these subsequently directed crystallisation during the liquid assisted grinding stage of the experiment.

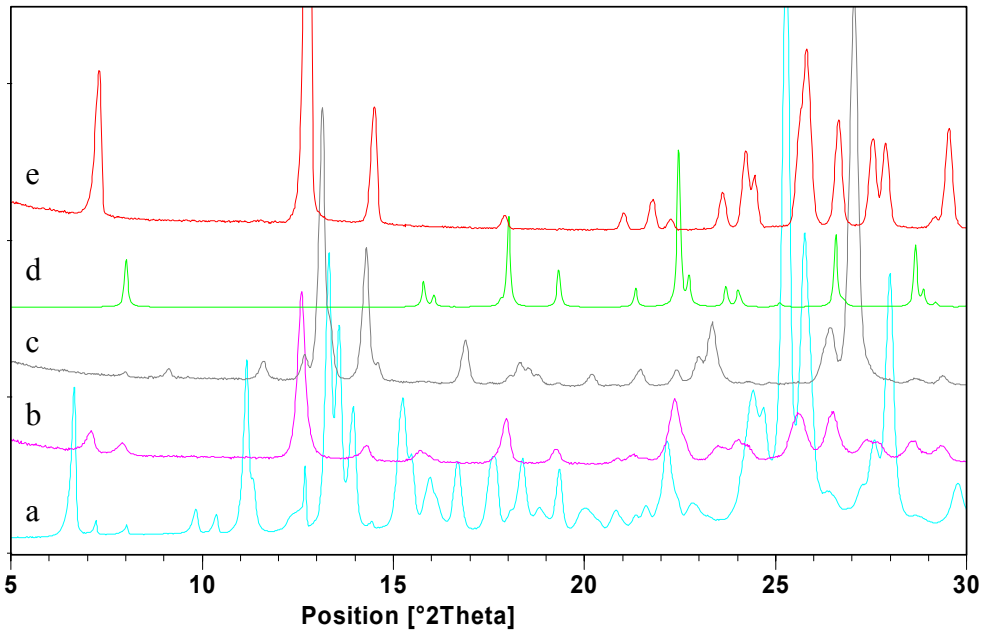

Figure 4.15 XRPD analysis of two polymorphs of a theophylline:benzamide cocrystal prepared by grinding an equimolar ratio of theophylline and benzamide. (a) A sample obtained by grinding an equimolar ratio of theophylline and benzamide with nitromethane. (b) A sample obtained by dry grinding an equimolar ratio of theophylline and benzamide. (c) The same sample after a second grinding period with nitromethane. (d) Simulated trace of Form I of benzamide (CSD ref BZAMID01). (e) Reference trace of Form II of theophylline.

4.3.6 Theophylline Monohydrate

There is only one reported polymorph of theophylline monohydrate, and a crystal structure of this form has been obtained by Sun et al.[17]

Slow evaporation of an aqueous solution of theophylline gave a sample which by XRPD appeared to be a mixture of Form I of theophylline monohydrate and a new crystal phase (Figure 4.16). In the DSC thermogram of the sample there were two peaks in the water loss endotherm (onset 74 °C), again suggesting that the sample was a mixture of forms, and also indicating that the new form was hydrated (Figure 4.17).

By TGA, there was a weight loss corresponding to 0.88 moles of water between 60 and 110 °C. Given that some water loss could have occurred before the TGA experiment was performed, this result is consistent with water loss from a mixture of two polymorphs of theophylline monohydrate.

The new polymorph of the monohydrate is less thermodynamically stable than Form I: gentle crushing of crystals of Form II was found to be enough to cause conversion to Form I (Figure 4.16b).

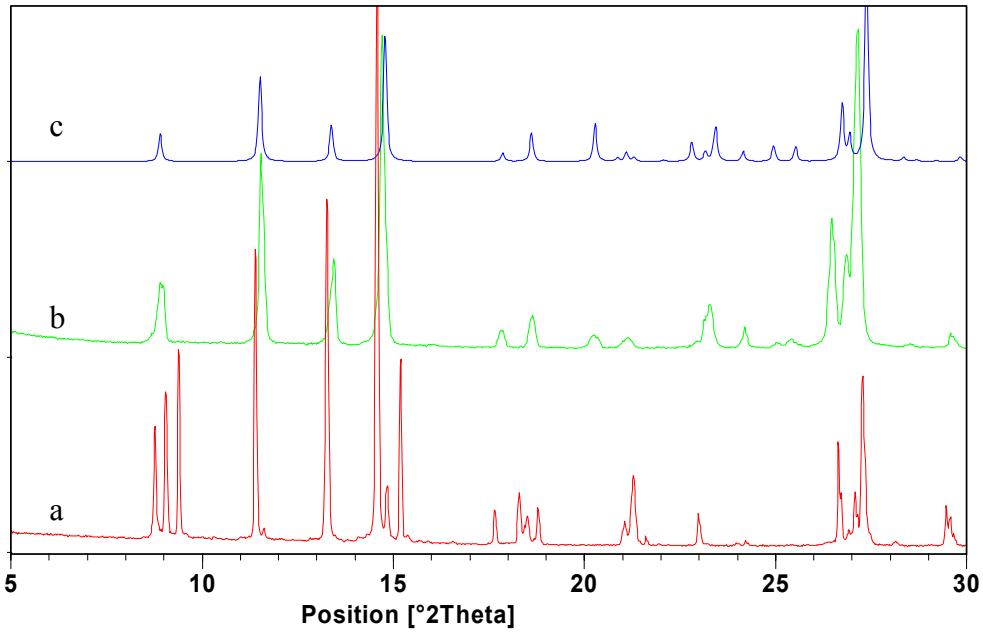

Figure 4.16 XRPD analysis of a sample prepared by slow evaporation of an aqueous solution of theophylline. (a) A sample prepared by slow evaporation of an aqueous solution of theophylline. (b) The same sample after gentle crushing on a glass slide with a spatula. (c) Simulated trace of Form I of theophylline monohydrate (CSD ref THEOPH01).[17]

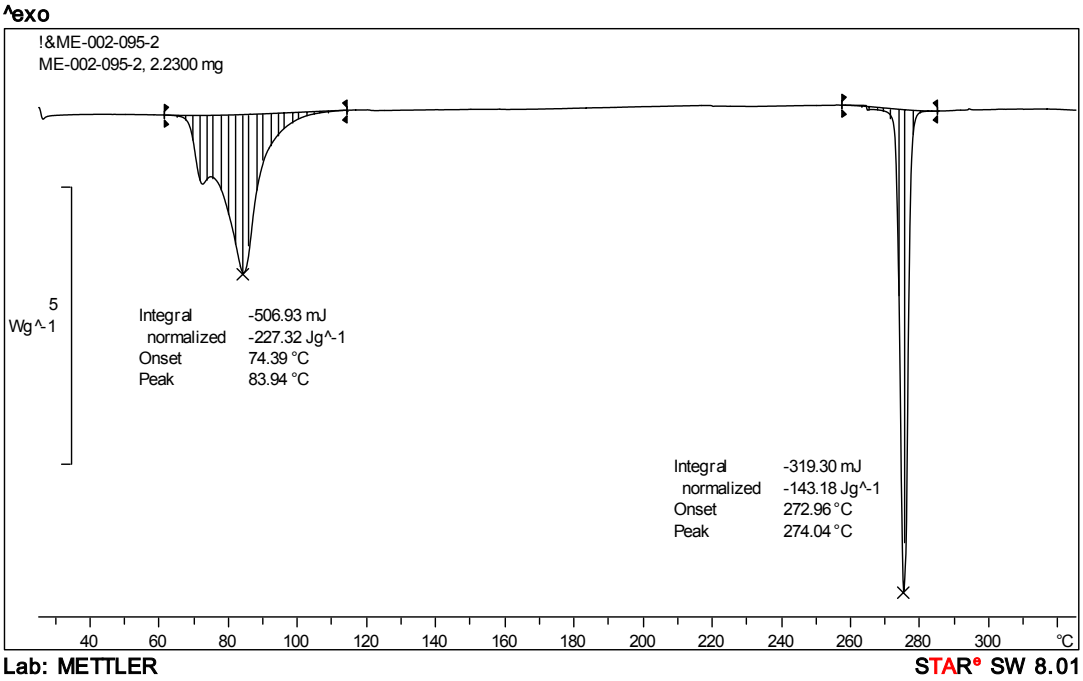

Figure 4.17 DSC thermogram of a sample obtained by slow evaporation of an aqueous solution of theophylline (pinhole in lid of DSC pan).

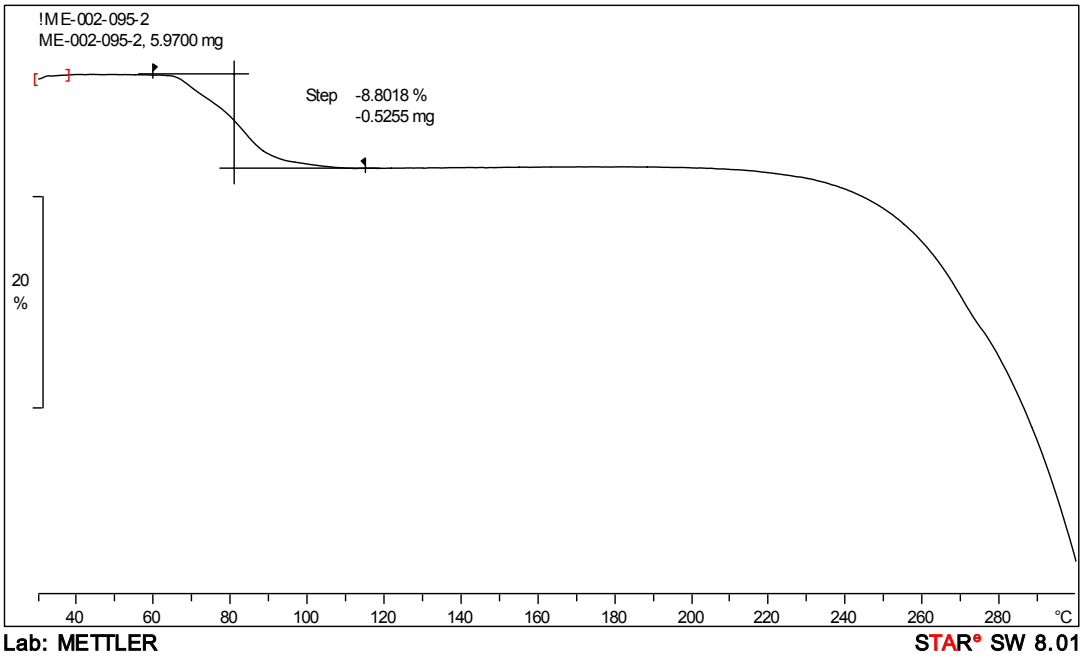

Figure 4.18 TGA thermogram of a sample obtained by slow evaporation of an aqueous solution of theophylline. The 8.8 % weight loss between 60 and 110 °C corresponds to 0.88 moles of water.

4.3.7 1:1 Theophylline:Acetic Acid Cocrystal

Form I of the 1:1 theophylline:acetic acid cocrystal was first isolated by Shyam Karki of the Department of Chemistry, University of Cambridge, and can be prepared by evaporation of a solution of theophylline in acetic acid.

A sample of Form II of theophylline was stored on a glass slide in an atmosphere of acetic acid for 48 hours. The sample was then analysed by XRPD and found to have changed form. The XRPD trace did not match Form I of the acetic acid cocrystal or any of the known forms of theophylline suggesting that a new form of the acetic acid cocrystal of theophylline had been obtained (Figure 4.19). Both forms of the acetic acid cocrystal are highly unstable, and within 24 hours under ambient conditions they lose acetic acid and convert to Form II of theophylline.

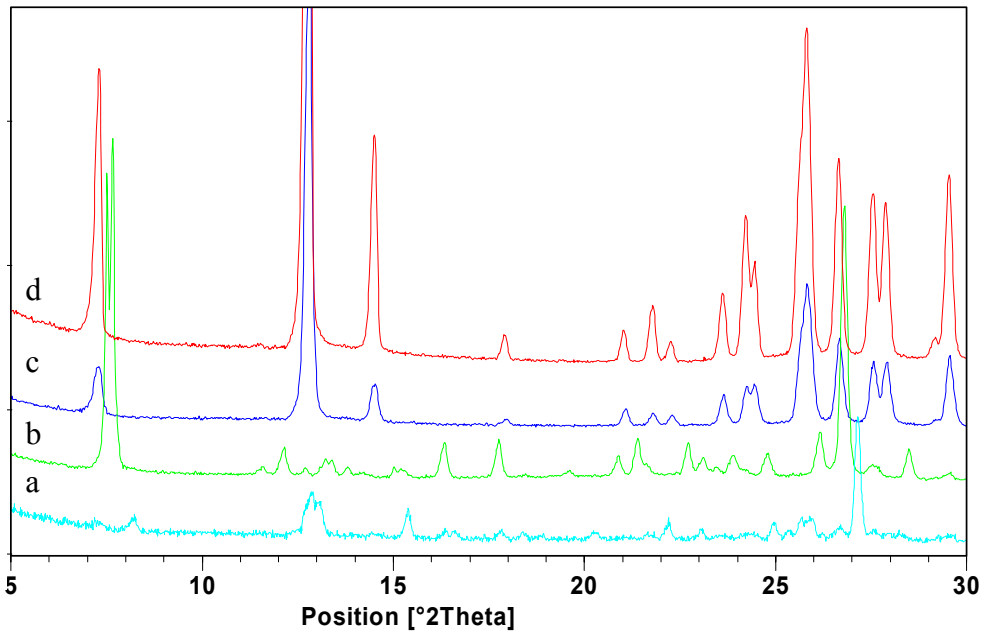

Figure 4.19 XRPD analysis of a sample prepared by storing theophylline in an atmosphere of acetic acid. (a) A sample obtained after storing Form II of theophylline in an acetic acid atmosphere. (b) A sample of Form I of the 1:1 theophylline:acetic acid cocrystal. (c) Form II of the theophylline:acetic acid cocrystal after storage under ambient conditions for 24 hours. (d) Reference trace of Form II of theophylline.

4.3.8 2:1 5-Fluorouracil:Phenazine Cocrystal

Form I of the 2:1 5-fluorouracil:phenazine cocrystal was first isolated by Amit Delori of the Department of Chemistry, University of Cambridge, and can be prepared by slow evaporation of a 2:1 molar ratio solution of 5-fluorouracil and phenazine in methanol. 5-Fluorouracil is a well known chemotherapy drug.

Crystals of Form I of the cocrystal, prepared by slow evaporation from a methanol solution, have a block-like habit and are up to 50 μm in length (Figure 4.20a). In contrast, if the same solution is pipetted onto a glass slide and allowed to evaporate rapidly, crystallites less than 5 μm in size are obtained (Figure 4.20c). Transmission electron microscopy analysis of this sample showed that there was also a difference in crystal habit (Figure 4.20d), with crystallites having a rectangular, thin-plate morphology and lengths of between 0.5 and 2 μm. In contrast, the fragment of a crystal of Form I shown in Figure 4.20b appears to be more block-like than plate-like and does not have a rectangular habit (this sample was gently crushed between two glass slides prior to TEM analysis). This observation suggested that evaporation on a glass slide may have given a different crystal form.

Selected area electron diffraction patterns from the sample prepared by evaporation on a glass slide were also recorded (Figure 4.21). These diffraction patterns were not consistent with Form I of the 5-fluorouracil:phenazine cocrystal, nor with any of the known polymorphs of 5-fluorouracil and phenazine, suggesting that a new cocrystal phase of 5-fluorouracil and phenazine had been obtained.

Background information on interpreting TEM images and diffraction patterns is given in Chapter 5.

A discussion on the defects that are present in the crystals of Form II of the cocrystal can be found in Chapter 9.

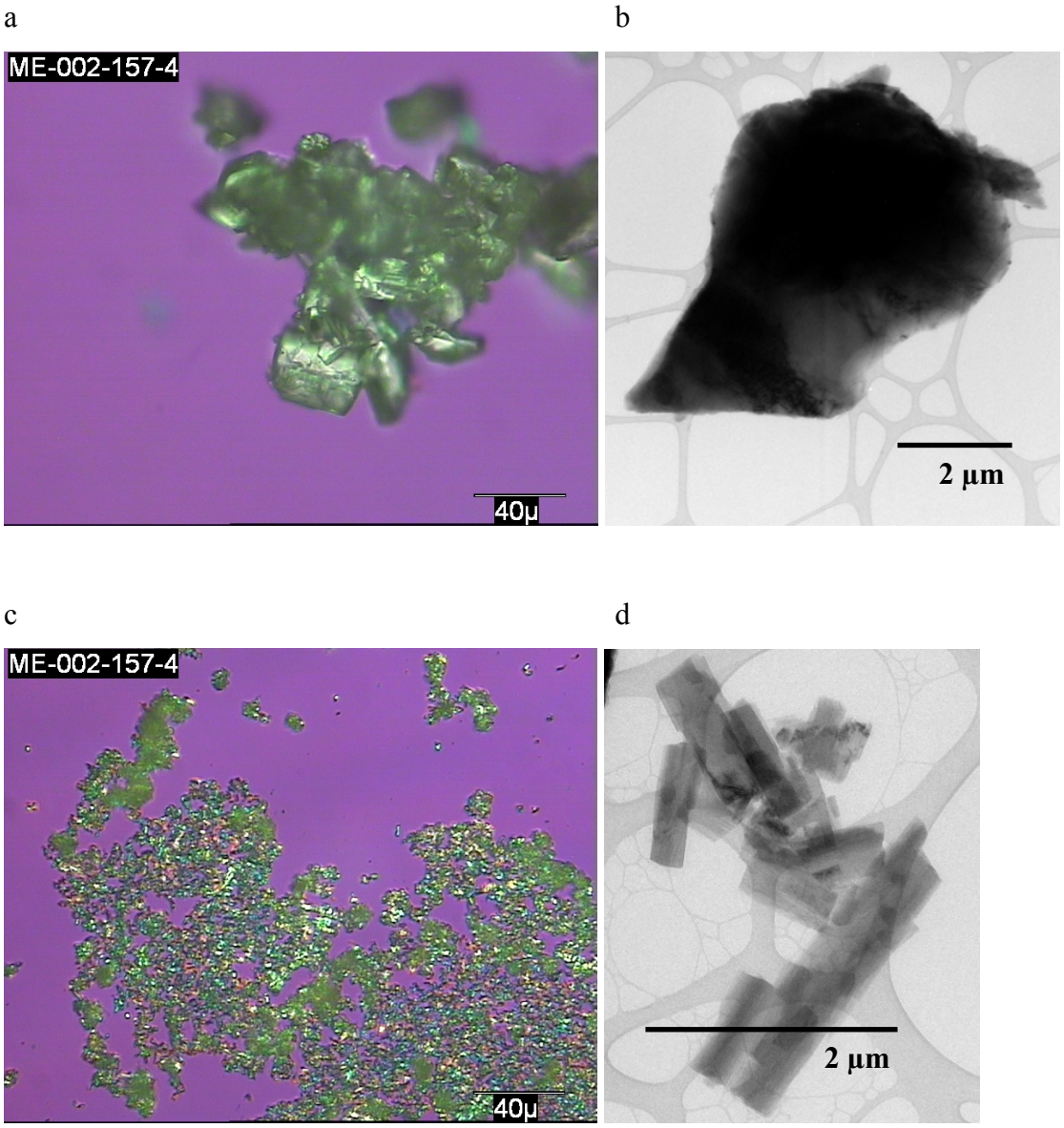

Figure 4.20 PLM and TEM images of samples obtained by slow and fast evaporation of a 2:1 molar ratio solution of 5-fluorouracil and phenazine in methanol. (a) PLM image of crystals of Form I of the 5-fluorouracil:phenazine cocrystal obtained by slow evaporation. (b) TEM image of a fragment of a crystal of Form I. (c) PLM image of crystals obtained by fast evaporation on a glass slide. (d) TEM image of crystals obtained by fast evaporation onto a TEM sample grid on a glass slide.

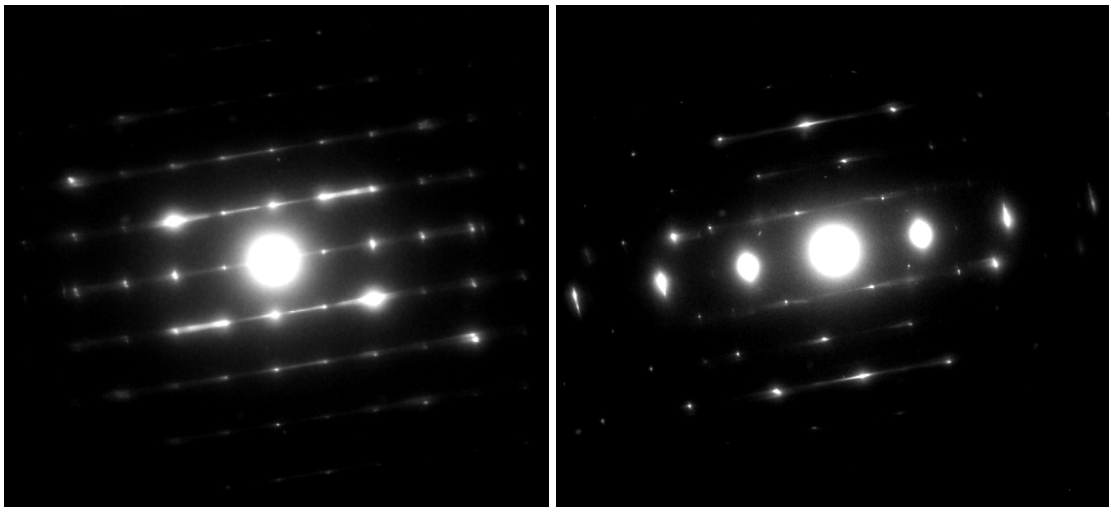

Figure 4.21 Selected area electron diffraction patterns from crystallites obtained by evaporation of a 2:1 molar ratio solution of 5-fluorouracil and phenazine in methanol on a TEM grid on a glass slide.

4.3.9 1:1 Phenazine:Mesaconic Acid Cocrystal

Form I of this cocrystal was reported by Batchelor et al.[18] A monohydrate of the cocrystal and a new polymorph, Form II, were prepared by cocrystallisation at the interface between two solvent layers (see Section 3.3.3 for further details).

Cocrystal formation was also investigated by liquid assisted grinding with a selection of solvents (this work was conducted with Saranja Sivachelvam, a summer student at the Department of Chemistry, University of Cambridge). 138.5 mg of phenazine and 100 mg of mesaconic acid (1 mole equivalent) were ground with 20 μl of solvent. Both Form I and Form II of the cocrystal were isolated from this cocrystallisation screen, and grinding with polar solvents (high dielectric constant) tended to favour generation of Form II, whereas non-polar solvents gave Form I. The main exception to this trend was in grinding with water, but the cocrystal is known to form a monohydrate and this may have influenced the result. Observations are summarised in Table 4.2.

Table 4.2 A table showing the outcome of grinding a 1:1 molar ratio of phenazine and mesaconic acid with different solvents.

Solvent	Dielectric Constant	Outcome
Water	80.4	Form I
DMSO*	46.5	New crystal form
Acetonitrile	37.5	Form II
DMF	36.7	Form II
Methanol	32.6	Form I
Acetone	20.7	Form I
Butanol	17.8	Form I
Dichloromethane	9.1	Form I
Chlorobenzene	5.7	Form I
Diisopropyl ether	3.9	Form I
t-Butylmethyl ether	3.1	Form I
Cyclohexane	2.0	Form I

* 100 µl of solvent was used in this experiment.

A new crystal form was obtained from the liquid assisted grinding experiment with DMSO. An XRPD trace of this phase is shown in Figure 4.22. This form converted to Form II of the cocrystal during heating at 90 °C for three hours, suggesting that it was a DMSO solvate of the phenazine:mesaconic acid cocrystal (i.e. a three component cocrystal). During TGA analysis there was a weight loss of 17.0 %, corresponding to 0.68 moles of DMSO, before sublimation occurred above 170 °C (Figure 4.23). It is believed that a 1:1:1 cocrystal was isolated from the grinding experiment, and that partial de-solvation occurred prior to TGA analysis being performed.

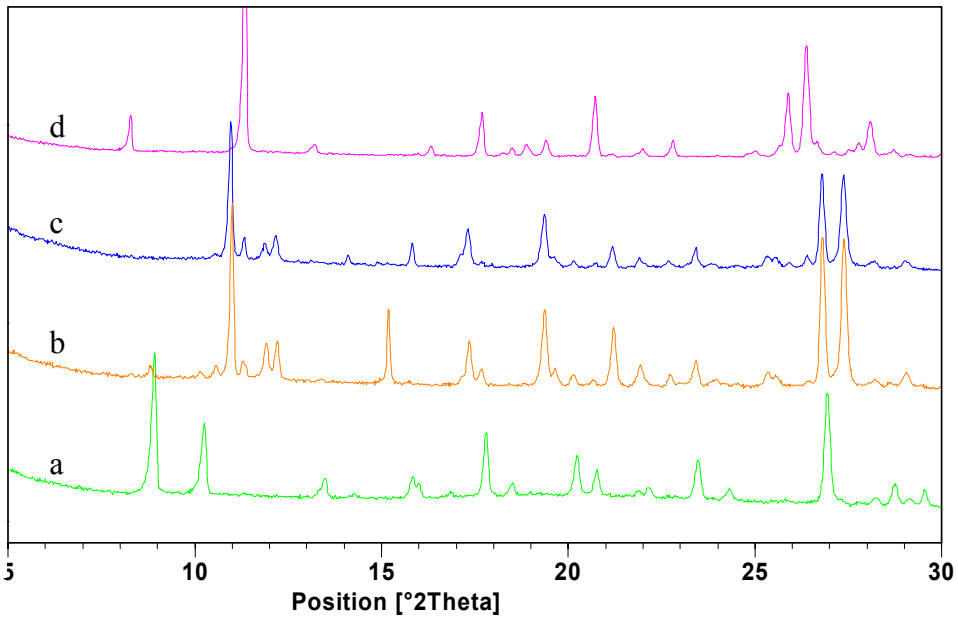

Figure 4.22 XRPD analysis of a sample prepared by grinding phenazine and mesaconic acid with DMSO. (a) A sample prepared by grinding phenazine and mesaconic acid with DMSO. (b) The same sample after heating at 90 °C for 3 hours. (c) Reference trace of Form II of the 1:1 phenazine:mesaconic acid cocrystal. (d) Reference trace of Form I of the phenazine:mesaconic acid cocrystal.

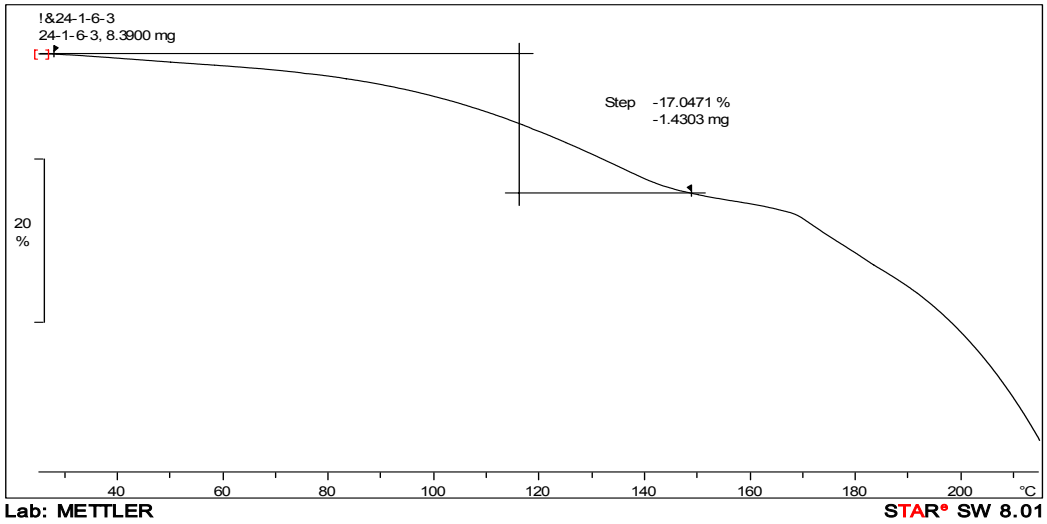

Figure 4.23 TGA thermogram of a sample obtained by grinding phenazine and mesaconic acid in an equimolar ratio with DMSO. The 17.0 % weight loss between 25 and 150 °C corresponds to 0.68 moles of DMSO (calculated on the basis of a 1:1 phenazine:mesaconic acid cocrystal).

Evidence for the existence of a third anhydrous polymorph of the 1:1 phenazine: mesaconic acid cocrystal was obtained from analysing Form I by DSC (Figure 4.24). A small endotherm at 161 °C was observed, followed by an endotherm at 183 °C consistent with a melting event. The small endotherm at 161 °C was an indication that a change in crystal form had occurred before the cocrystal melted.

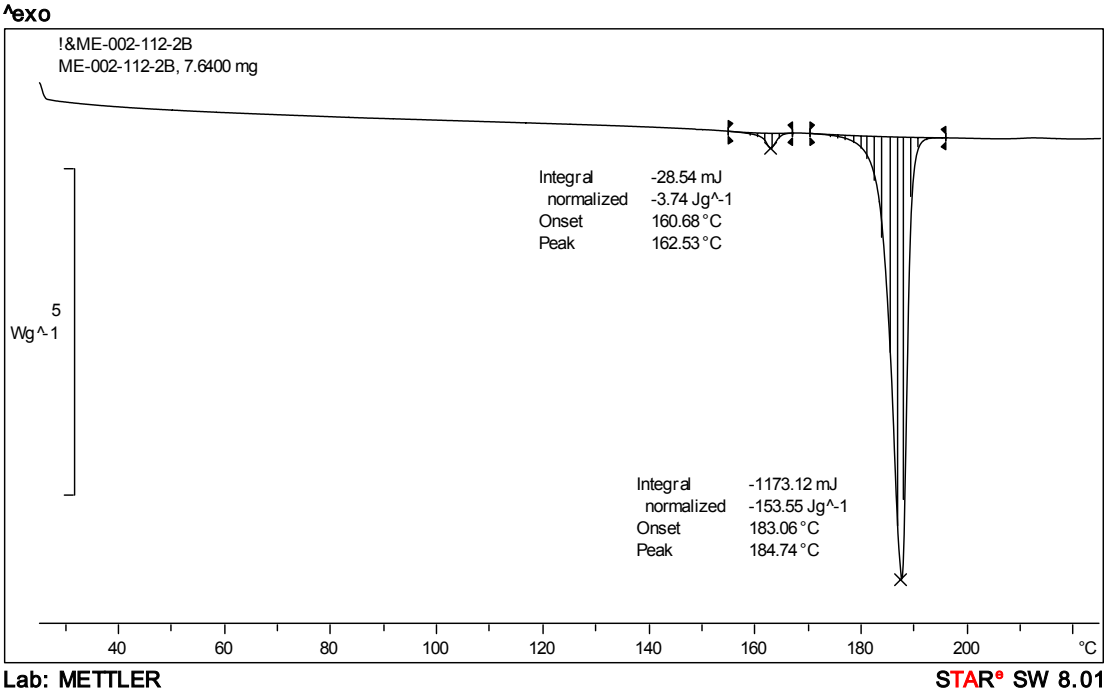

Figure 4.24 DSC thermogram of Form I of the 1:1 phenazine:mesaconic acid cocrystal.

VT-XRPD analysis was performed on Form I of the cocrystal to investigate this potential form change. XRPD traces were recorded at 140 °C and 170 °C, temperatures below and above the endothermic event seen by DSC (Figure 4.25). There were small, but significant differences in these XRPD traces, demonstrating that a change in crystal form (solid-solid transition) had occurred, and that a third polymorph of the 1:1 phenazine:mesaconic acid cocrystal had been generated. A further XRPD trace was recorded after cooling the sample back to ambient temperature (Figure 4.26). This trace matched that of Form I of the cocrystal, demonstrating that Form III is a metastable polymorph under ambient conditions and that Form I and Form III have an enantiotropic relationship.

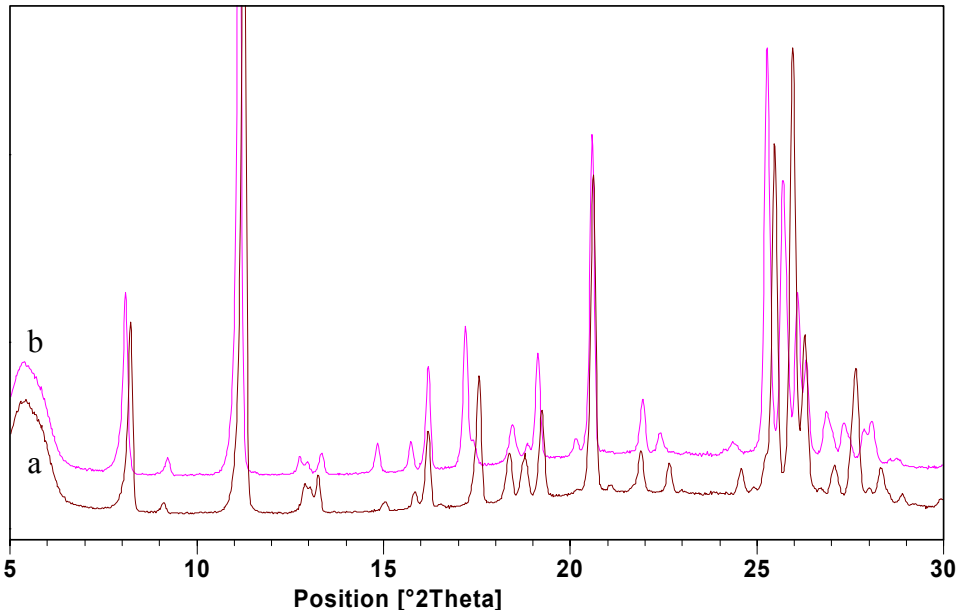

Figure 4.25 VT-XRPD analysis of a sample of Form I of the phenazine:mesaconic acid cocrystal. (a) The sample at 140 °C. (b) The sample at 170 °C.

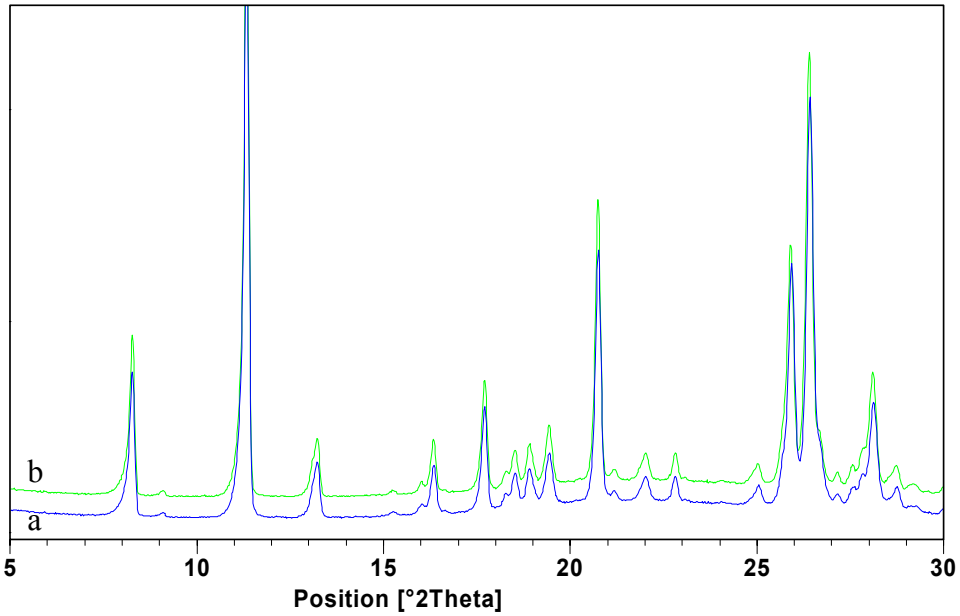

Figure 4.26 XRPD analysis of a sample of Form I of the phenazine:mesaconic acid cocrystal before and after heating to 170 °C as part of a VT-XRPD experiment. (a) A sample of Form I of the phenazine:mesaconic acid cocrystal. (b) The same sample after heating to 170 °C.

4.3.10 1:2 Mesaconic acid:Urea Cocrystal

Work on the mesaconic acid:urea cocrystal system was conducted with Saranja Sivachelvam, a summer student at the Department of Chemistry, University of Cambridge.

Form I of the 1:2 mesaconic acid:urea cocrystal was obtained by evaporation of a 1:2 molar ratio solution of mesaconic acid and urea in nitromethane. The single crystal X-ray structure of this form was determined, and the molecular packing arrangement is shown in Figure 4.27. Each urea molecule forms an amide-carboxylic acid hydrogen bonding interaction with a molecule of mesaconic acid, an amide-amide hydrogen bonding interaction with a second molecule of urea, and also an interaction between its two NH_2 groups and one of the carbonyl groups of a second mesaconic acid molecule.

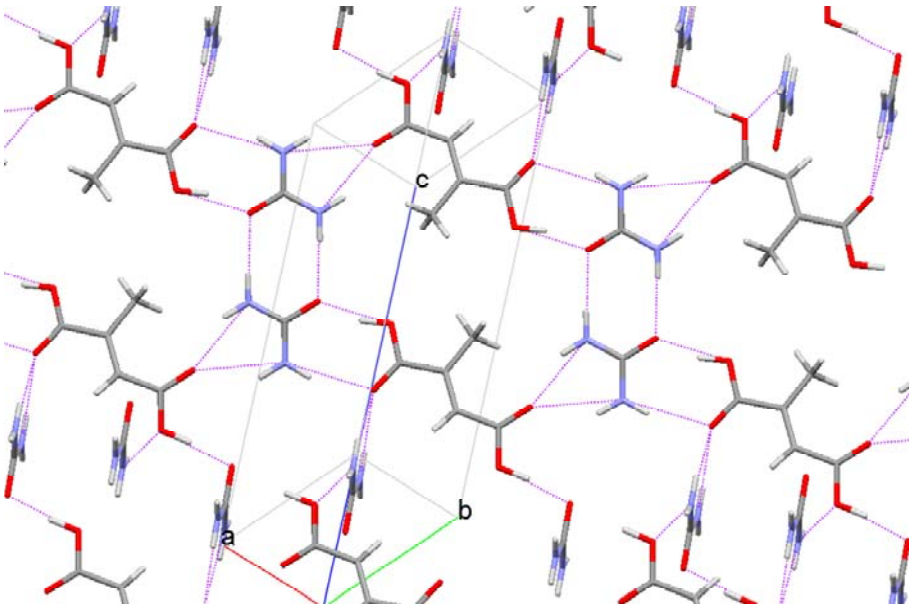

180 K

P-1

Triclinic

a = 5.0674 Å

b = 8.2900 Å

c = 8.2900 Å

α = 78.061 °

β = 86.751 °

γ = 72.861 °

R_1 = 4.12 %

Figure 4.27 Molecular packing arrangement in the crystal structure of Form I of the 1:2 cocrystal of mesaconic acid and urea.

Crystallisation of a 1:2 molar ratio solution of mesaconic acid and urea in methanol by evaporation gave a sample with an XRPD trace that did not match that of Form I of the cocrystal, or any of the known forms of mesaconic acid and urea (Figure 4.28). It is believed that this is a second polymorph of the 1:2 cocrystal.

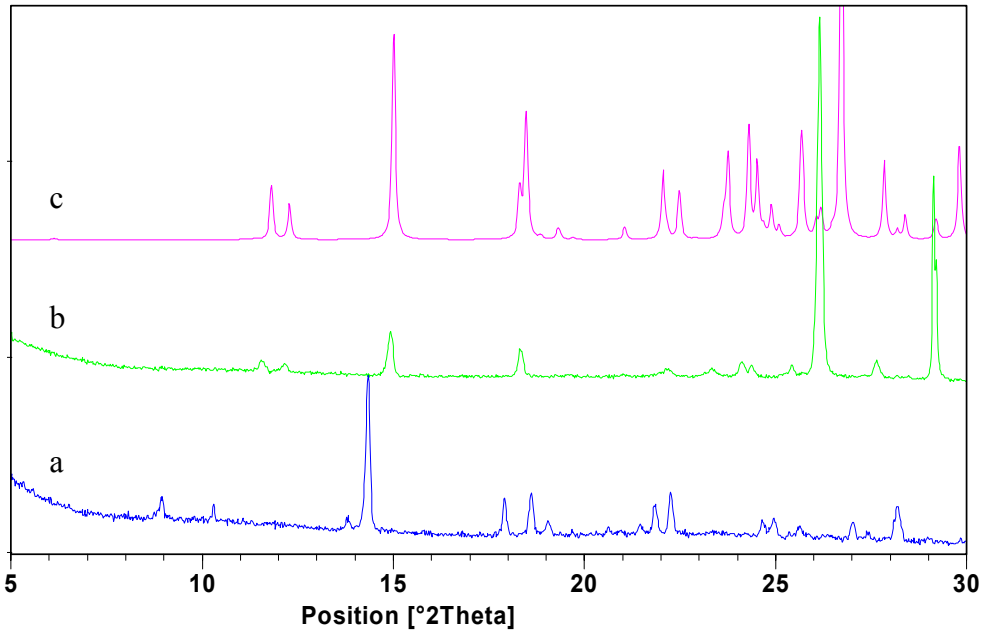

Figure 4.28 XRPD analysis of the mesaconic acid:urea cocrystal. (a) A sample prepared by evaporation of a 1:2 molar ration solution of mesaconic acid and urea in methanol. (b) A sample prepared by evaporation of a 1:2 molar ration solution of mesaconic acid and urea in nitromethane. (c) Simulated trace from the crystal structure of the 1:2 mesaconic acid:urea cocrystal. The slight differences in peak positions between b and c are due to thermal expansion (The crystal structure was collected at 180 K).

4.3.11 1:1 L-malic acid:L-tartaric acid Cocrystal

Form I of the 1:1 L-malic acid:L-tartaric acid cocrystal was reported by Aakeroy et al (CSD structure NIVYOG).[19]

Grinding L-malic and L-tartaric acid in equimolar amounts without solvent gave a sample which had an XRPD trace that was different to that of Form I of the cocrystal and the known polymorphs of L-malic acid and L-tartaric acid. It is believed that this new crystal form is a second polymorph of the 1:1 L-malic acid:L-tartaric acid cocrystal (Form II). Form II was also obtained by liquid assisted grinding with non-polar solvents such as cyclohexane and chloroform (Figure 4.29), whereas polar solvents such as water and DMSO gave Form I during grinding experiments.

Form II of the cocrystal was found to convert to Form I during storage under ambient conditions indicating that Form I is the more thermodynamically stable polymorph (Figure 4.29).

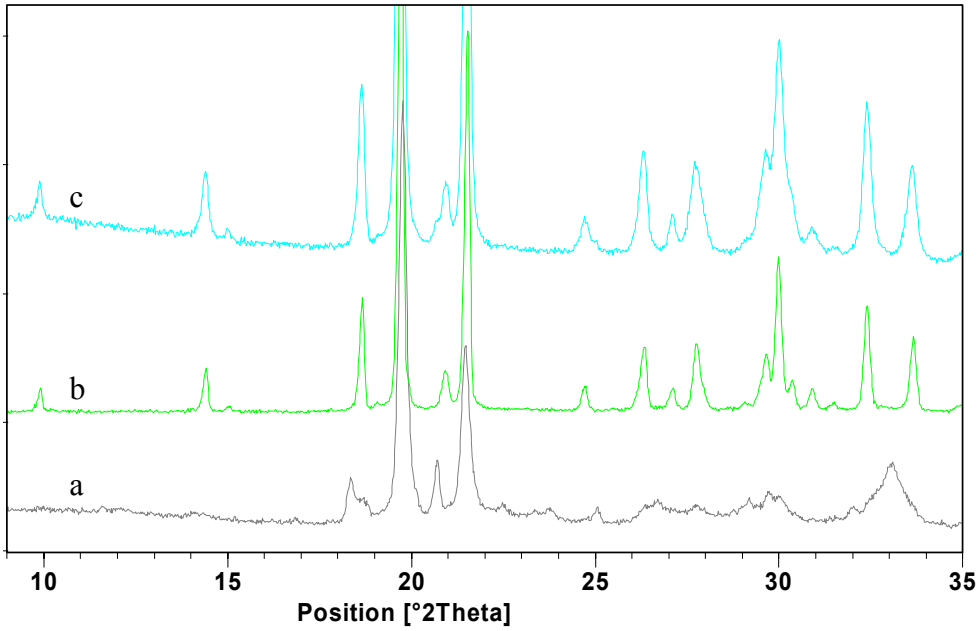

Figure 4.29 XRPD analysis of Form II of the L-malic acid:L-tartaric acid cocrystal. (a) A sample prepared by an equimolar amount of L-malic acid and L-tartaric acid with chloroform. (b) The same sample after storage under ambient conditions for two months. (c) Reference trace of Form I of the L-malic acid:L-tartaric acid cocrystal.

4.4 Discussion

4.4.1 Propensity of Cocrystal Polymorphism

Several cocrystal systems, with a variety of APIs, were studied during this PhD project. Though cocrystal polymorphism was not investigated directly, well over half of these systems were found to have more than one polymorphic form. This is strong evidence against claims that cocrystals are inherently less prone to polymorphism than single component forms.

4.4.2 Methods of Screening for Cocrystal Polymorphs

An overview of the new polymorphic cocrystal forms that were described in Section 4.3, and the cocrystallisation methods used to prepare these different polymorphs, is given in Table 4.3.

Many different techniques and conditions were used in generating these cocrystal polymorphs including solution crystallisation, liquid assisted grinding, thermal methods, storage under ambient conditions, storage in a solvent atmosphere, crystallisation at the interface between two solvents and freeze-drying. It would not have been possible to obtain all of these crystal forms if just one approach had been used. For example, one of the polymorphs of the theophylline:pyrazinamide cocrystal was obtained from solution cocrystallisations, but not from liquid assisted grinding experiments. For the second polymorph the opposite was true.

These observations indicate that cocrystal screening strategies should include a selection of different cocrystallisation methods.

Table 4.3 An overview of the cocrystallisation methods that were used to prepare the polymorphic cocrystals that are described in Section 4.3 of this Chapter.

Cocrystal System	Number of Forms Identified	Cocrystallisation Methods Used to Prepare the Polymorphs
Caffeine:Theophylline	3 (including one solid solution)	Form I – Freeze-drying Form II – Spontaneous conversion Form III – LAG / solution
1:1 Caffeine:1-Hydroxy-2-naphthoic acid	2 (one previously reported, one new)	Form II – Grown between two solvent layers Both forms obtained by LAG
1:1 Theophylline:Formamide	2	Form change on cooling
1:1 Theophylline:Pyrazinamide	2	Form I – Solution Form II – LAG
1:1 Theophylline:Benzamide	2	Both forms obtained by grinding
Theophylline monohydrate	2 (one previously reported, one new)	Form II was obtained by slow evaporation
1:1 Theophylline:Acetic acid	2 (one previously identified, one new)	Form I – Solution Form II – Atmosphere of acetic acid
2:1 5-fluorouracil:Phenazine	2 (one previously identified, one new)	Both forms were obtained from a methanol solution (Form II by fast evaporation)
1:1 Phenazine:Mesaconic acid	5 (3 polymorphs + monohydrate + DMSO solvate)	Monohydrate grown between solvent layers Form III – Form change on heating All other forms obtained by LAG
1:2 Mesaconic acid:Urea	2	Form I – Grinding / solution (nitromethane) Form II – Solution (methanol)
1:1 L-Malic acid:L-Tartaric acid	2 (one previously reported, one new)	Both forms were obtained by LAG

4.5 Other Significant Results

4.5.1 The Amide-Extended Amide Synthon in Theophylline Cocrystals

The amide-extended amide synthon is present in two of the theophylline cocrystals published in the CSD, a 1:1 cocrystal of theophylline and urea, and a 2:1 cocrystal monohydrate of theophylline and 5-fluorouracil (Figure 4.30).

a b

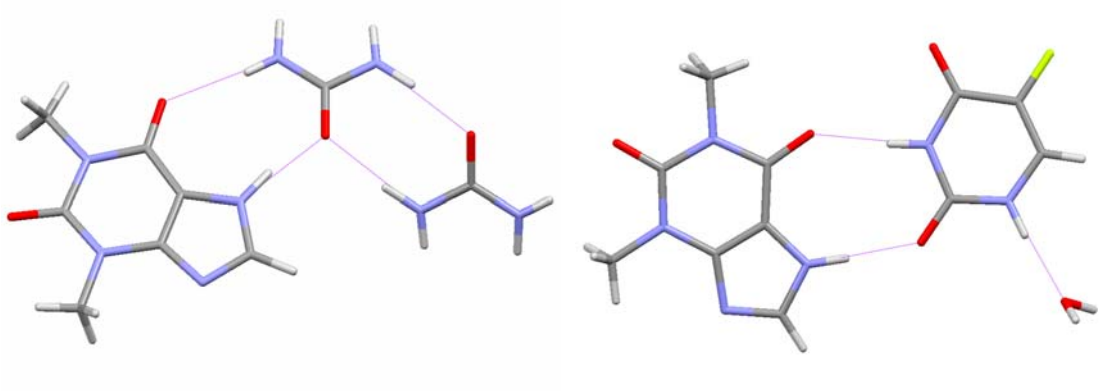

Figure 4.30 Amide-extended amide synthons in the crystal structures of (a) a 1:1 theophylline:urea cocrystal (CSD ref DUXZAX[20]), (b) the monohydrate of a 2:1 theophylline:5-fluorouracil cocrystal (CSD ref ZAYLOA[21]).

The reliability of this supramolecular synthon was investigated by attempting to cocrystallise theophylline with a set of simple amides. As described in Section 4.3.3, the amide-extended amide synthon was found to be present in the formamide cocrystal of theophylline. Cocrystallisation was also attempted with the related compounds DMF and N-methylformamide.

DMF does not have an amide proton and so cannot act as a hydrogen bond donor. A cocrystal of theophylline and DMF was prepared, and the crystal structure was solved by single crystal X-ray diffraction. As expected, there was no amide-extended amide interaction (Figure 4.31). Theophylline and DMF instead form dimers through an N-H···O=C hydrogen bond.

With N-methylformamide, there was the potential to form an amide-extended amide interaction with theophylline. The single crystal X-ray structure of a 1:1 theophylline: N-methylformamide cocrystal was obtained, but this interaction was absent. Instead, there were hydrogen bonds between the imidazole nitrogens of theophylline and the amide carbonyl and amide proton of N-methylformamide, giving a 1D hydrogen bonded network (Figure 4.32).

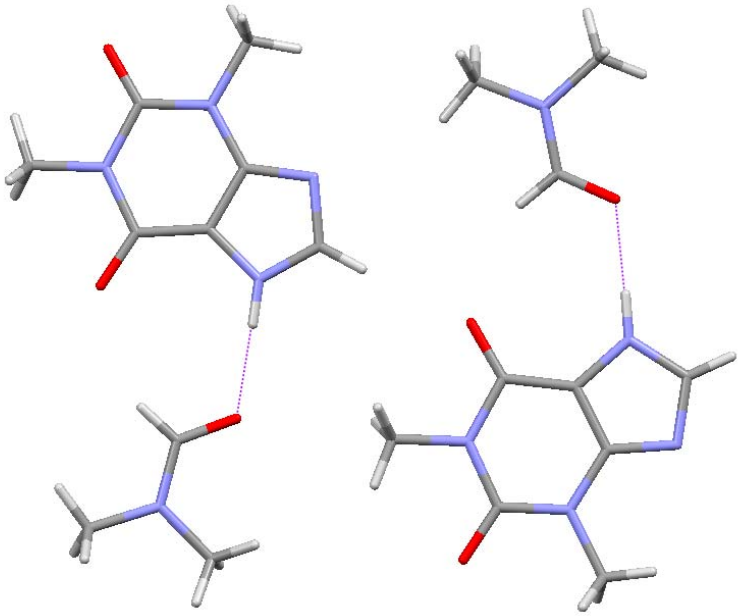

250 K
Monoclinic
$P2_1/c$
a = 4.4183 Å
b = 14.3872 Å
c = 19.3622 Å
β = 93.41 °

R_1 = 5.5 %

Figure 4.31 Intermolecular interactions in the crystal structure of a 1:1 cocrystal of theophylline and DMF.

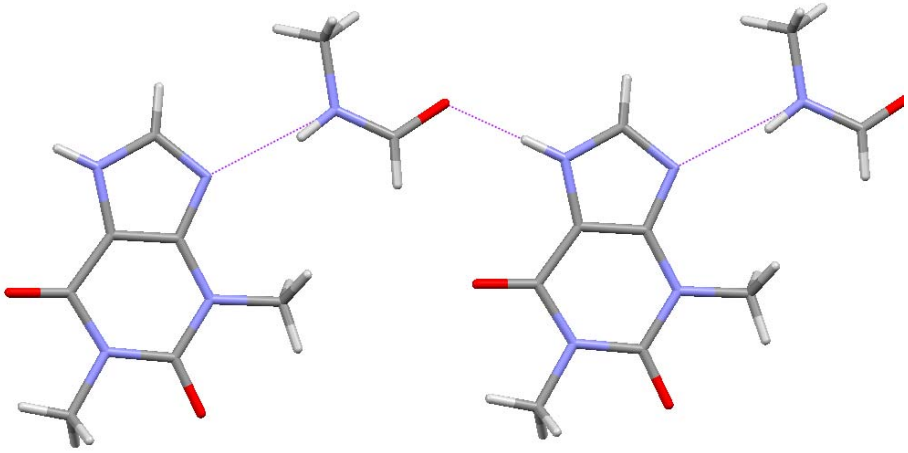

180 K
P-1
Triclinic
a = 6.6316 Å
b = 8.7905 Å
c = 9.5955 Å
α = 92.441 °
β = 92.929 °
γ = 90.609 °
R_1 = 11.7 %

Figure 4.32 Intermolecular interactions in the crystal structure of a 1:1 cocrystal of theophylline and N-methylformamide.

Cocrystals of theophylline with acetamide and benzamide were also prepared, but it has not been possible to obtain crystal structures to determine if there is an amide-extended amide interaction.

The crystal structure of a 1:1 theophylline:pyrazinamide cocrystal is shown in Figure 4.13. There is no amide-extended amide interaction, although it is possible that this synthon could be present in the second polymorph of the cocrystal.

Although the amide-extended amide synthon with theophylline has been observed in a cocrystal with formamide, it is clearly not a robust synthon that could be relied upon to be present in cocrystals of theophylline with other amides.

4.5.2 De-solvation of Theophylline Solvates

As described above, cocrystals of theophylline with formamide, N-methyl formamide and DMF were prepared. Under ambient conditions, these cocrystals were found to de-solvate. The relative rate of de-solvation was DMF > N-methylformamide > formamide, reflecting the strength of hydrogen bonding interactions in the crystal structures.

The de-solvated samples were analysed by XRPD and found to be mixtures of Form II of theophylline and a second crystal phase (Figure 4.33). The XRPD peak positions of this other phase (6.8, 13.0, 13.8, 20.7 and 27.3 °2θ) match those reported for a polymorphic form of theophylline that has recently been obtained by Roy et al from supercritical CO_2 crystallisations.[22]

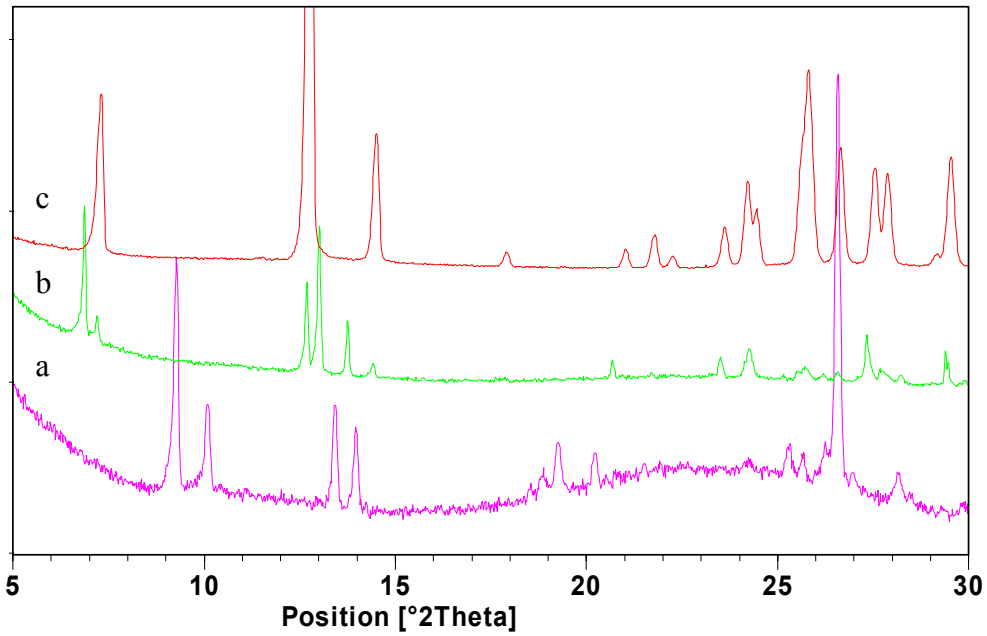

Figure 4.33 XRPD analysis of de-solvation of the 1:1 theophylline:N-methyl-formamide cocrystal. (a) XRPD trace of a sample of the 1:1 theophylline: N-methylformamide cocrystal. (b) XRPD trace of the same sample after storage under ambient conditions for two weeks. (c) Reference trace of Form II of theophylline.

4.6 Conclusions

11 cocrystal systems were identified as being polymorphic in this study, 5 of which were completely new cocrystal systems, significantly increasing the number of known polymorphic cocrystal systems. The caffeine:theophylline and phenazine:mesaconic acid cocrystals were found to have multiple forms with three polymorphs of each system being identified as well as a monohydrate and DMSO solvate of phenazine:mesaconic acid.

In three of these systems, caffeine:1-hydroxy-2-naphthoic acid, phenazine:mesaconic acid and L-malic acid:L-tartaric acid, it was found that the polymorphic outcome of liquid assisted grinding cocrystallisations could be controlled through choice of solvent (polarity). These observations mirror a previous finding reported by Trask et al for polymorphs of a caffeine:glutaric acid cocrystal.[10]

It was demonstrated that a multi-method approach to cocrystal polymorph screening is necessary in order to identify all possible crystal forms.

Also, cocrystals have been shown to be a route to the preparation of an unusual polymorph of theophylline.

4.7 Further Work

To date, it has not been possible to grow crystals of several of the new cocrystal phases described here that are suitable for crystal structure determination. Further work should be performed in order to obtain these crystal structures.

There is also a need for a systematic comparative study of methods of screening for polymorphs of cocrystals.

4.8 References

1. Aitipamula S., Chow P. S., Tan R. B. H. Polymorphs and Solvates of a Cocrystal Involving an Analgesic Drug, Ethenzamide, and 3,5-Dinitrobenzoic Acid. *Cryst. Growth Des.*, 2010, 10(5), 2229-2238.

2. Almarsson O., Zaworotko M. J. Crystal engineering of the composition of pharmaceutical phases. Do pharmaceutical co-crystals represent a new path to improved medicines? *Chem. Commun.*, 2004, (17), 1889-1896.

3. Vishweshwar P., McMahon Jennifer A., Peterson Matthew L., Hickey Magali B., Shattock Tanise R., Zaworotko Michael J. Crystal engineering of pharmaceutical co-crystals from polymorphic active pharmaceutical ingredients. *Chem. Commun.*, 2005, (36), 4601-4603.

4. Hickey M. B., Peterson M. L., Scoppettuolo L. A., Morrisette S. L., Vetter A., Guzman H., Remenar J. F., Zhang Z., Tawa M. D., Haley S., Zaworotko M. J., Almarsson O. Performance comparison of a co-crystal of carbamazepine with marketed product. *Eur. J. Pharm. Biopharm.*, 2007, 67(1), 112-119.

5. Babu N. J., Reddy L. S., Aitipamula S., Nangia A. Polymorphs and polymorphic cocrystals of temozolomide. *Chem.--Asian J.*, 2008, 3(7), 1122-1133.

6. Porter W. W., III, Elie S. C., Matzger A. J. Polymorphism in Carbamazepine Cocrystals. *Cryst. Growth Des.*, 2008, 8(1), 14-16.

7. ter Horst J. H., Cains P. W. Co-Crystal Polymorphs from a Solvent-Mediated Transformation. *Cryst. Growth Des.*, 2008, 8(7), 2537-2542.

8. Schultheiss N., Newman A. Pharmaceutical Cocrystals and Their Physicochemical Properties. *Cryst. Growth Des.*, 2009, 9(6), 2950-2967.

9. Aitipamula S., Chow P. S., Tan R. B. H. Trimorphs of a pharmaceutical cocrystal involving two active pharmaceutical ingredients: potential relevance to combination drugs. *CrystEngComm*, 2009, 11(9), 1823-1827.

10. Trask A. V., Motherwell W. D. S., Jones W. Solvent-drop grinding: green polymorph control of cocrystallisation. *Chem. Commun.*, 2004, (7), 890-891.

11. Zhang G. G. Z., Henry R. F., Borchardt T. B., Lou X. Efficient co-crystal screening using solution-mediated phase transformation. *J. Pharm. Sci.*, 2007, 96(5), 990-995.

12. Enright G. D., Terskikh V. V., Brouwer D. H., Ripmeester J. A. The Structure of Two Anhydrous Polymorphs of Caffeine from Single-Crystal Diffraction and Ultrahigh-Field Solid-State 13C NMR Spectroscopy. *Cryst. Growth Des.*, 2007, 7(8), 1406-1410.

13. Ebisuzaki Y., Boyle P. D., Smith J. A. Methylxanthines. I. Anhydrous theophylline. *Acta Crystallogr., Sect. C: Cryst. Struct. Commun.*, 1997, C53(6), 777-779.

14. Pawley G. S. Unit-cell refinement from powder diffraction scans. *J. Appl. Crystallogr.*, 1981, 14(6), 357-361.

15. Rietveld H. M. Profile refinement method for nuclear and magnetic structures. *J. Appl. Crystallogr.*, 1969, 2(Pt. 2), 65-71.

16. Bucar D.-K., Henry R. F., Lou X., Duerst R. W., Borchardt T. B., MacGillivray L. R., Zhang G. G. Z. Co-Crystals of Caffeine and Hydroxy-2-naphthoic Acids: Unusual Formation of the Carboxylic Acid Dimer in the Presence of a Heterosynthon. *Mol. Pharmaceutics*, 2007, 4(3), 339-346.

17. Sun C., Zhou D., Grant D. J. W., Young V. G., Jr. Theophylline monohydrate. *Acta Crystallogr., Sect. E: Struct. Rep. Online*, 2002, E58(4), o368-o370.

18. Batchelor E., Klinowski J., Jones W. Crystal engineering using co-crystallisation of phenazine with dicarboxylic acids. *J. Mater. Chem.*, 2000, 10(4), 839-848.

19. Aakeroy C. B., Cooke T. I., Nieuwenhuyzen M. The crystal structure of the molecular cocrystal L-malic acid L-tartaric acid (1/1). *Supramol. Chem.*, 1996, 7(2), 153-156.

20. Wiedenfeld H., Knoch F. The crystal structure of the theophylline-urea complex. *Arch. Pharm. (Weinheim, Ger.)*, 1986, 319(7), 654-659.

21. Zaitu S., Miwa Y., Taga T. A 2:1 molecular complex of theophylline and 5-fluorouracil as the monohydrate. *Acta Crystallogr., Sect. C: Cryst. Struct. Commun.*, 1995, C51(9), 1857-1859.

22. Roy C., Vega-Gonzalez A., Subra-Paternault P. Theophylline formulation by supercritical antisolvents. *Int. J. Pharm.*, 2007, 343(1-2), 79-89.

5 Exploring the Potential Applications of TEM in Pharmaceutical Materials Analysis

5.1 Introduction

The aims of this work were to first assess the suitability of TEM for pharmaceutical analysis, by investigating the potential difficulties with sample preparation and electron beam damage, and then to explore the different types of information that can be obtained with TEM. Although the methodologies that are described in this Chapter are widely used, their application to characterising the solid form of organic pharmaceutical compounds is a relatively new area of research (see Section 1.4.1 for further details).

There have been several reported TEM studies of organic compounds, mainly of simple hydrocarbons.[1-5] As part of this previous work, strategies were developed for preparing thin samples suitable for TEM analysis, and for reducing beam damage. For example, crystal growth on a water surface, by evaporation of a solution of the compound of interest in a hydrophobic solvent such as xylene, was found to be a good way of preparing large plate-like crystals that were thin enough for TEM.[6] Electron beam damage was reduced by increasing accelerating voltages, analysing samples at low temperatures and by controlling the flux of electrons through samples.[1,5,7,8] These strategies were applied to the pharmaceutical systems studied in this Chapter.

The diagram shown in Figure 5.1 is a schematic of a TEM instrument. The electron beam coming from the electron source is shown in green at the top of the image (for the work described in this thesis a parallel (non-convergent) beam of electrons was used). The paths of electrons that pass straight through the sample are shown in green. Diffracted electrons are coloured pink and lilac. Following the paths of electron beams below the sample it can be seen that they are focussed with a lens to form an image on the viewing screen at the bottom of the instrument (most TEM instruments actually use several lenses for focussing). Both non-diffracted and diffracted beams from the same part of the sample meet at the same point on the viewing screen.

Diffraction patterns are obtained by changing the strength of the lenses so that the back focal plane is brought into focus. This plane is the level on the diagram where crossing of beams diffracted at the same angle from different regions of the sample occurs. It is in this region of the microscope that an objective aperture can be inserted (this aperture is actually a diaphragm containing holes of different size). An appropriately sized aperture is selected and aligned with the centre of the instrument, and its purpose is to stop some diffracted beams from passing down the column and contributing to the image, as shown with the lilac beams in Figure 5.1. In this manner, diffraction contrast can be produced in images, which is how bend contours are formed (see below). A condenser aperture is located above the sample and can be used to restrict the number of electrons reaching the sample. There is also a selected area aperture, which is located close to the objective aperture, and is used in diffraction mode to obtain diffraction information from a specific region of the sample.

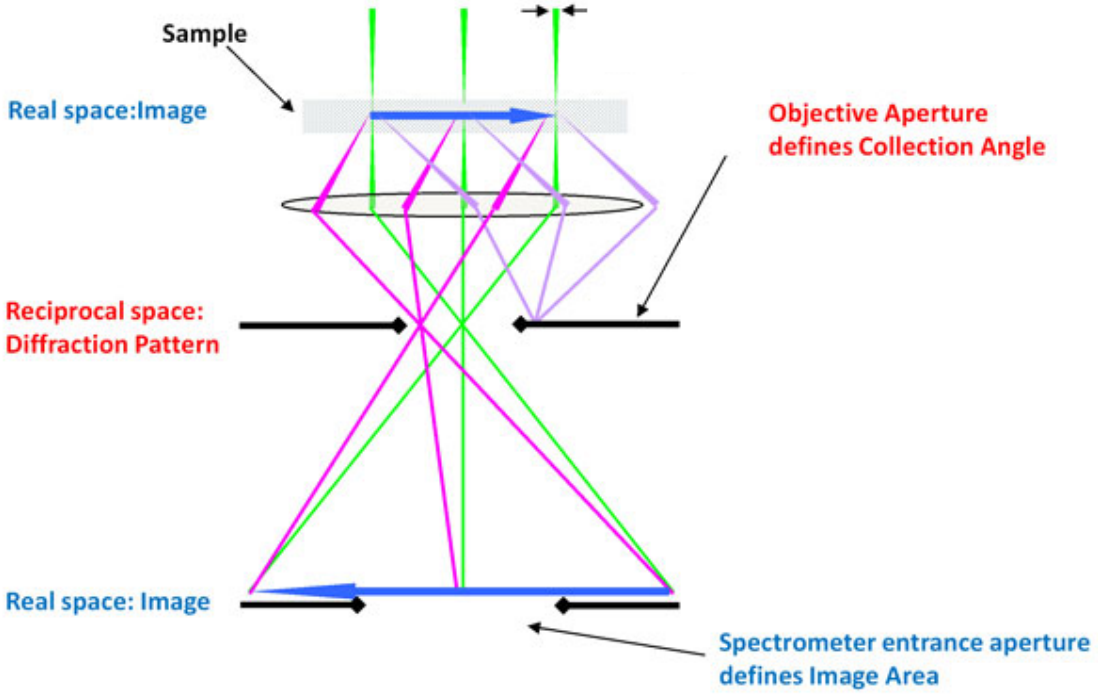

Figure 5.1 A schematic of a TEM instrument (Gatan, 2007).[9] Beams of electrons corresponding to un-scattered electrons are shown in green. Diffracted beams of electrons are shown in pink and lilac.

The TEM image of a crystal of p-terphenyl in Figure 5.2, recorded by Jones et al,[6] is given as an example to show the types of information that have been previously obtained from TEM analysis. Many of the features that are typical of TEM images can be seen in the image.

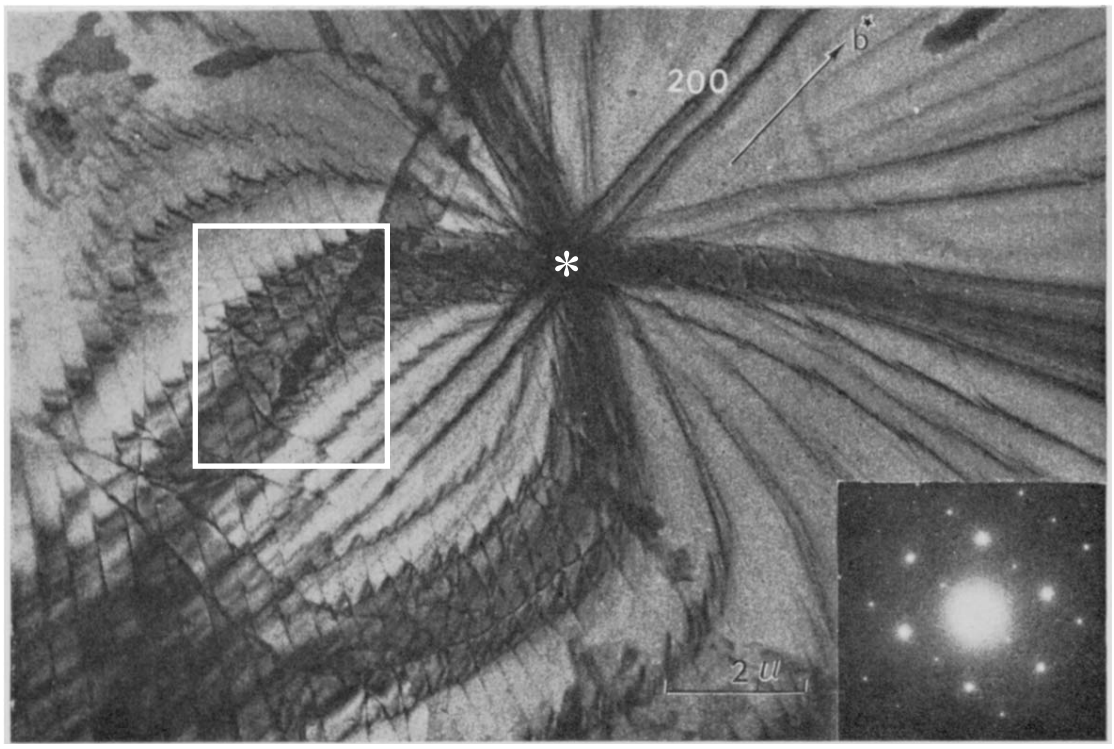

Figure 5.2 TEM image of a crystal of p-terphenyl. The corresponding electron diffraction pattern is shown as an inset. Image recorded by Jones et al.[6]

The morphology of the crystal of p-terphenyl shown in Figure 5.2 is plate-like. The crystal is at least 14 μm x 10 μm in size, but thin enough for electrons to pass through (< 500 nm), and appears lighter on the left hand side of the image than the right hand side, indicating that there is a change in crystal thickness (thicker areas appear darker). There are also regions in the top left corner of the image that appear much darker than the surrounding sample. This contrast is again due to increased sample thickness, and indicates the presence of small crystallites on the surface of the main plate-like crystal. The dark lines which cross at the top middle of the image are bend contours.[8] These bend contours show areas of the crystal where Bragg scattering

conditions are met, so at every point along a bend contour the orientation between the crystal and electron beam is constant, and each corresponds to diffraction from one set of crystal planes. In the region marked with an asterisk the crystal is bent into a dome shape, which results in several bend contours crossing at a single point, and forming a bend contour pole. The presence of crystal defects can also be seen,[6] as in the region highlighted with a white box. The defects are revealed by the discontinuous nature of bend contours in the image, which results from distortion of crystal planes in the vicinity of the defects.

The corresponding TEM diffraction pattern is shown as an inset at the bottom right of the image. The large central spot is from electrons that have passed through the sample without interacting. The other spots each correspond to diffraction from one set of crystal planes, and were indexed by Jones et al, allowing crystallographic directions to be applied to the image.

The examples presented in this Chapter demonstrate that similar information can be obtained about pharmaceutical crystals.

5.2 Experimental

5.2.1 Growth of Plates of Organic Compounds on a Water Surface

The method that was used to prepare plate-like crystals of p-terphenyl is given as an example. A 2.7 x 10^{-3} molar solution of p-terphenyl in p-xylene was prepared by dissolving 6.25 mg of p-terphenyl in 10 ml of p-xylene. 5 drops of this solution were pipetted carefully onto a water surface in a crystallization dish half-filled with distilled water. The p-xylene solution was allowed to evaporate yielding thin-plate crystals of p-terphenyl on the water surface.

The area and thickness of plates of p-terphenyl was increased by covering the crystallization dish with parafilm to control the rate of evaporation of the p-xylene solution, and by adding 10 % of ethanol to the water to reduce the surface tension at the site of crystallisation.

5.3 Results and Discussion

5.3.1 Sample Preparation for TEM

The importance of preparing thin specimens for TEM analysis can be seen by comparing the bright field image of a thin crystal of p-terphenyl in Figure 5.2 with that of much thicker crystals of paracetamol grown from solution in methanol in Figure 5.3a. The crystals of paracetamol appear dark as they are too thick for many electrons to penetrate, and though the crystal habit could be determined from the image, no other useful information was yielded. It was, however, possible to obtain electron diffraction patterns from the paracetamol crystals by focussing on the edges and corners where they are thinner (Figure 5.3b).

a b

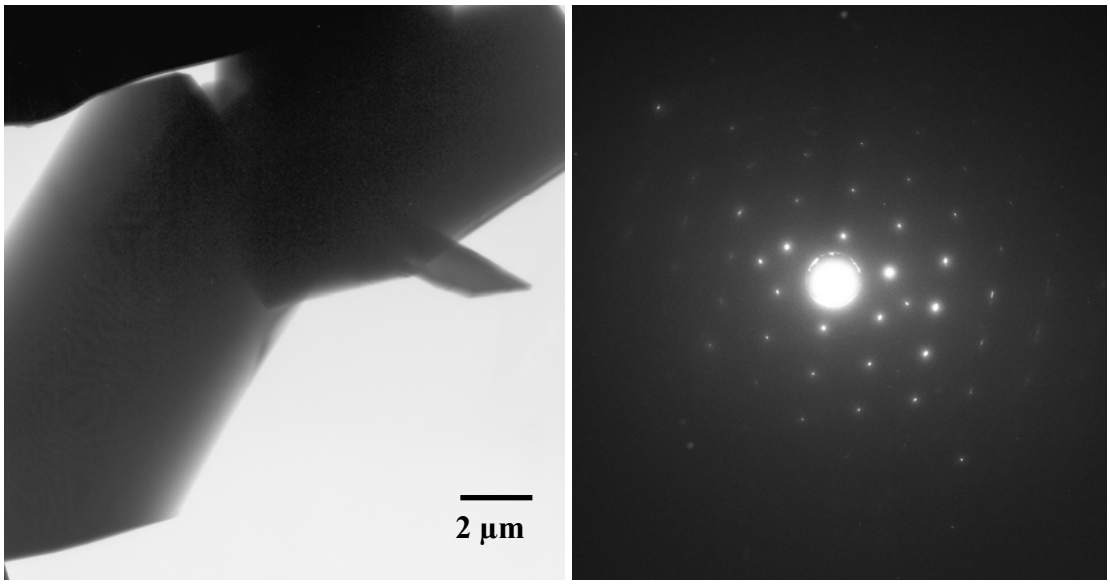

Figure 5.3 TEM analysis of paracetamol Form I prepared from a methanol solution. (a) TEM image showing hexagonal block shaped crystals. (b) Selected area electron diffraction pattern recorded from the edge of one of these crystals.

As described above, crystallisation on a water surface has previously been used to grow large, thin crystals of organic compounds for TEM analysis.[6] Thin foil crystals

of p-terphenyl up to 1 mm in length were prepared by this method. PLM and SEM analysis revealed that these thin foils had a range of thicknesses and a parallelepiped morphology (Figure 5.4).

a b

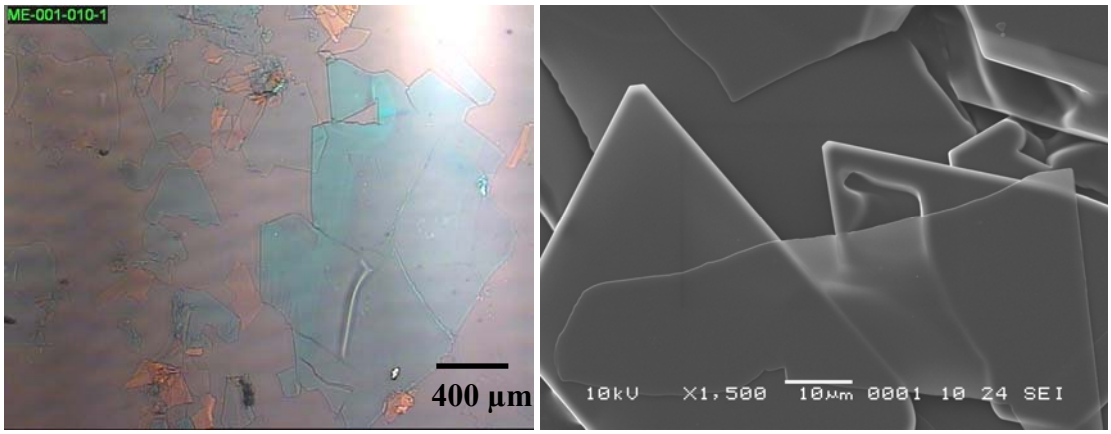

Figure 5.4 (a) PLM image of p-terphenyl crystallized on a water surface. (b) SEM image of p-terphenyl crystallized on a water surface.

This technique was applied to the crystallisation of several pharmaceutical compounds selected on the basis of low aqueous solubility (the compounds are listed in Table 5.1). It was not, however, possible to prepare large plate-like crystals of these materials. Microcrystalline powders were instead obtained.

It was speculated that the high surface tension of the water surface could be inhibiting crystal growth. The water surface crystallisation technique was modified by the addition of between 1 and 10 % of ethanol to lower the surface tension. Crystals of p-terphenyl grown by this method were larger, and thicker, than those obtained by crystallisation on pure water. Again, no plate-like crystals of the pharmaceutical compounds were obtained (Observations are summarised in Table 5.1). A possible reason for the difficulty in obtaining large plates of the pharmaceuticals could be that, in contrast to p-terphenyl, the usual morphology of the crystals of these compounds is not plate-like (with the exception of cholesterol, where needles grew instead of the usual plates) and so large crystals are not able to grow in a very thin film of solution on a water surface. This crystal growth technique could be limited to compounds which both naturally crystallise as plates and have low aqueous solubility.

Table 5.1 Observations from the crystallisation of pharmaceutical compounds on a water or water/ethanol surface.

Compound (Predicted crystal habit)	Crystallisation solvent	Percentage of ethanol in solution providing crystallisation surface*	Observations of resulting crystals
p-Terphenyl (Plate)	p-Xylene	0	Thin plates
	p-Xylene	10	Larger thin plates
Carbamazepine Form III (Prism)	p-Xylene	0	Dissolved in the water
Indomethacin (Block)	p-Xylene	0	Needle shaped crystals
	di-n-Butyl ether	0	Agglomerations of small needle shaped crystals
	di-n-Butyl ether	5	Agglomerations of small needle shaped crystals
Griseofulvin (Block)	p-Xylene	0	Microcrystalline powder
	p-Xylene	5	Microcrystalline powder
Flurbiprofen (Prism)	p-Xylene	0	Microcrystalline powder
	p-Xylene	5	Microcrystalline powder
Ketoprofen (Prism)	p-Xylene	0	Microcrystalline powder
	p-Xylene	5	Microcrystalline powder
Cholesterol (Plate)	p-Xylene	0	Needle shaped crystals
	p-Xylene	5	Needle shaped crystals

* Note that the concentration of ethanol at the surface of the solution will be greater than that in the bulk of the solution

Several other strategies for preparing thin crystals were investigated including rapid evaporative crystallisation, rapid solution cooling, crystallisation from the melt and grinding in a ball mill.

Crystals of aspirin and nifedipine, a calcium channel blocker, suitably thin for TEM analysis were prepared by evaporative crystallisation from a drop of solution pipetted directly onto a TEM grid on a glass slide. TEM images of these samples are shown in Figure 5.5. The crystal of aspirin has a thin, plate-like morphology and is at least 10 μm x 10 μm in size. Bend contours are clearly visible in the image, and the white line running from bottom left to middle right is a crack in the crystal. The two dark lines running from top left to bottom right are from part of the carbon film that is used to support the samples. The nifedipine crystals are smaller, up to 4 μm in length, with a rectangular plate morphology, and again, bend contours can be seen. Some crystals are overlapping, or are orientated towards the electron beam, and so appear darker. The faint lacy network that can be seen in the image, marked with an asterisk, is the amorphous carbon support film.

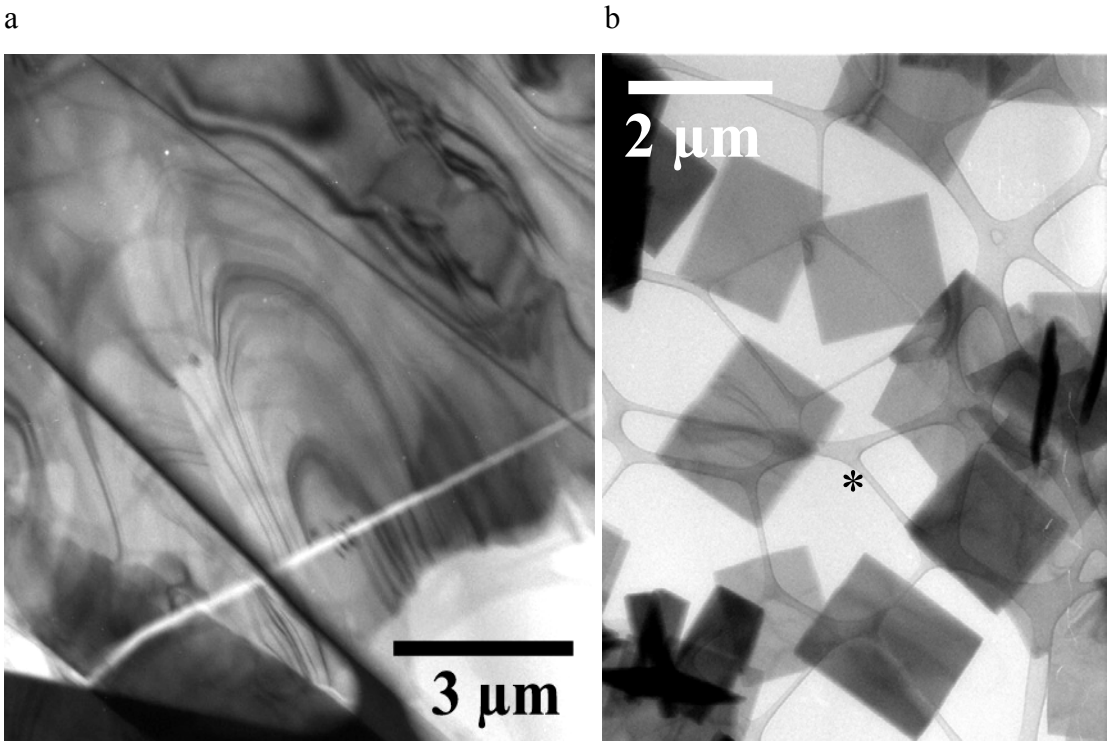

Figure 5.5 TEM images of (a) aspirin Form I crystallised by evaporation from acetonitrile (sample analysed at -178 °C) and (b) nifedipine Form I crystallised by evaporation from ethanol.

This method of sample preparation was found to be only applicable to compounds that have plate, lath or needle habits. Crystals with other morphologies were too thick for imaging.

Crystallisation from the melt was investigated with paracetamol. Molten paracetamol was thinly spread across a TEM grid and allowed to cool and crystallise, and the resulting crystals were thin enough for imaging (Figure 5.6). The way that bend contours on the image abruptly stop in some regions indicates the presence of domain boundaries in the crystals. This sample preparation technique is only suitable for the small percentage of pharmaceutical compounds that do not thermally degrade on melting.

a b

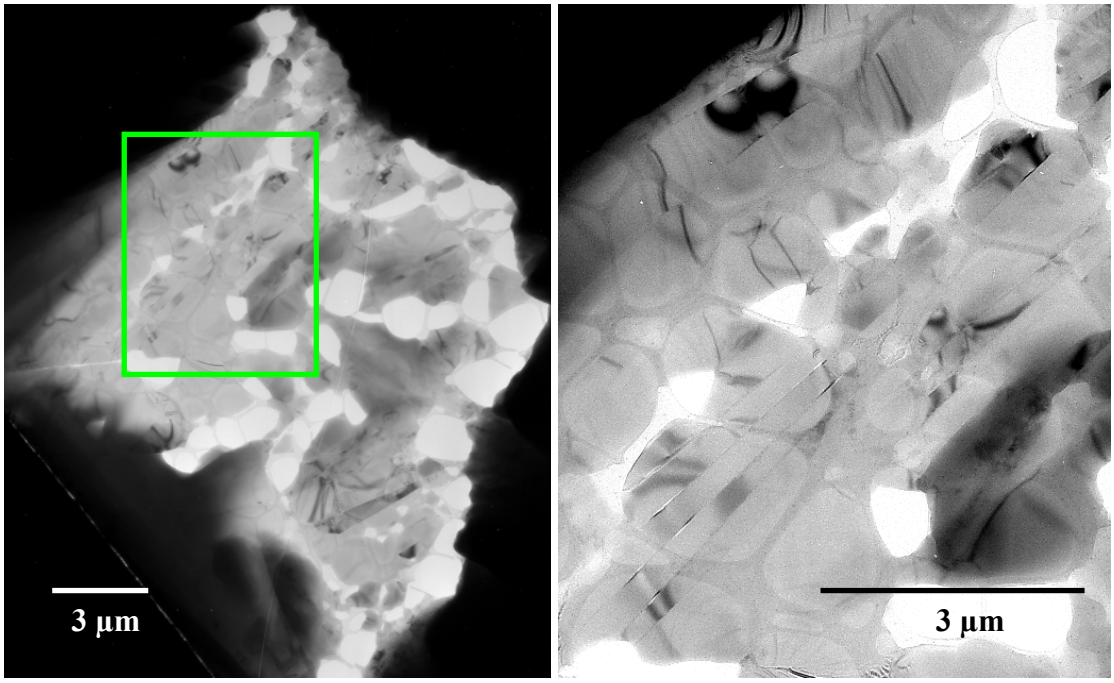

Figure 5.6 (a) TEM image of paracetamol Form I crystallised from the melt. (b) A magnification of the highlighted region.

Grinding in a ball mill was found to be a reliable method of generating crystals that are sufficiently thin for imaging by TEM. The crystals of Form III of the 1:1 caffeine:theophylline cocrystal shown in Figure 5.7 were prepared by grinding an

equimolar amount of caffeine and theophylline in the presence of nitromethane. These crystals have a lath habit and lengths of between 50 and 500 nm. It is evident from the image that TEM is a good technique for analysing pharmaceutical nanomaterials (this is explored further in Chapter 8).

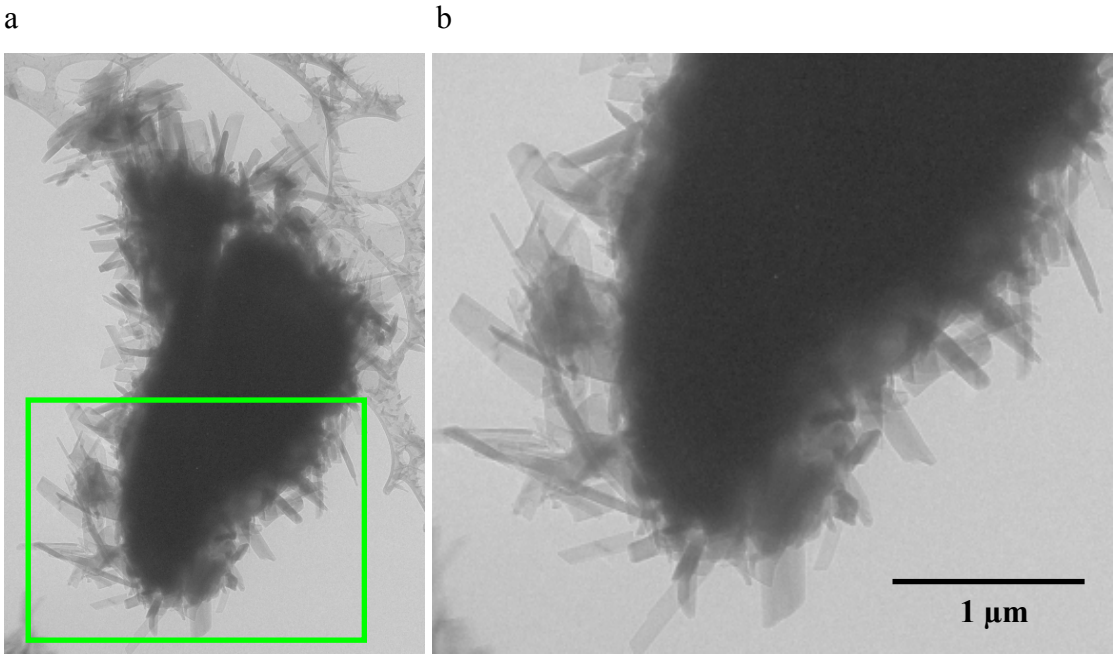

Figure 5.7 (a) Sub-micron sized crystallites of Form III of the 1:1 caffeine: theophylline cocrystal prepared by grinding in a ball mill. (b) A magnification of the highlighted region.

With pharmaceutical analysis, it is often important to ensure that any sample preparation that is performed prior to characterisation does not cause a change in crystal form. In these cases, if crystals were initially too large for TEM analysis, an appropriate approach to sample preparation was found to be gentle crushing between two glass slides. The resulting crystal fragments usually remain too thick for imaging, but are suitable for diffraction studies, enabling identification of the crystal phase. Data from TEM analysis of crystals of ranitidine hydrochloride, a compound used for treatment of heartburn, that were prepared in this manner are shown in Figure 5.8. The TEM image shows a crystal fragment of ranitidine hydrochloride with a rectangular

shape that is too thick for any detail to be seen, but the selected area electron diffraction pattern obtained from this crystal could be used to determine the polymorphic form of this crystal. The pattern was indexed to the <10-1> zone axis of Form II of ranitidine hydrochloride. Further details about the indexing process, and the use of TEM for phase identification, are given in Section 5.3.4 and Chapter 6 respectively.

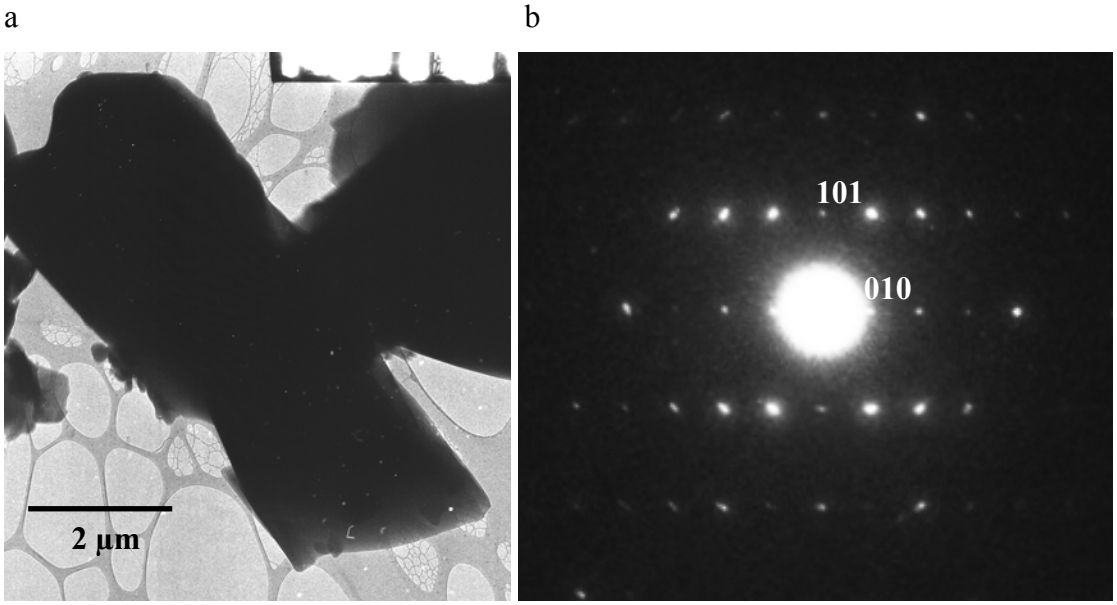

Figure 5.8 (a) Crystallites of ranitidine hydrochloride prepared by gently crushing larger crystals between two glass slides. (b) Corresponding selected area electron diffraction pattern of the <10-1> zone axis of ranitidine hydrochloride Form II.

5.3.2 Limiting Electron Beam Damage during TEM Analysis

Initial investigations into sample degradation in the electron beam were performed with p-terphenyl. The stability of this compound during TEM analysis had already been studied,[6] and so it provided a good benchmark with which to compare the electron beam sensitivity of crystals of pharmaceutical compounds. All work was conducted at 300kV, the maximum accelerating voltage of the TEM instrument that was used for the study, in order to minimise beam damage.

If an instrument set-up that would be typical for the analysis of inorganic samples was used (high beam flux), the electron beam caused rapid tearing and localised melting of the p-terphenyl crystals, and it was therefore necessary to control the flux of electrons through the sample. This was achieved by reducing the size of the condenser aperture, using a small spot size, working at low magnifications and spreading the electron beam. The flux was reduced until it was only just possible to visualise the sample on the instrument screen with the room lights switched off, preventing excessive localised heating of the sample.

Electron diffraction patterns of p-terphenyl were then recorded over time to monitor beam damage. The diffraction patterns in Figure 5.9 show p-terphenyl losing crystallinity in the electron beam. The initial diffraction pattern has many reflections, but after 20 minutes only a few strong reflections remain. This amorphisation is mainly caused by chemical degradation induced by the electron beam.

a b

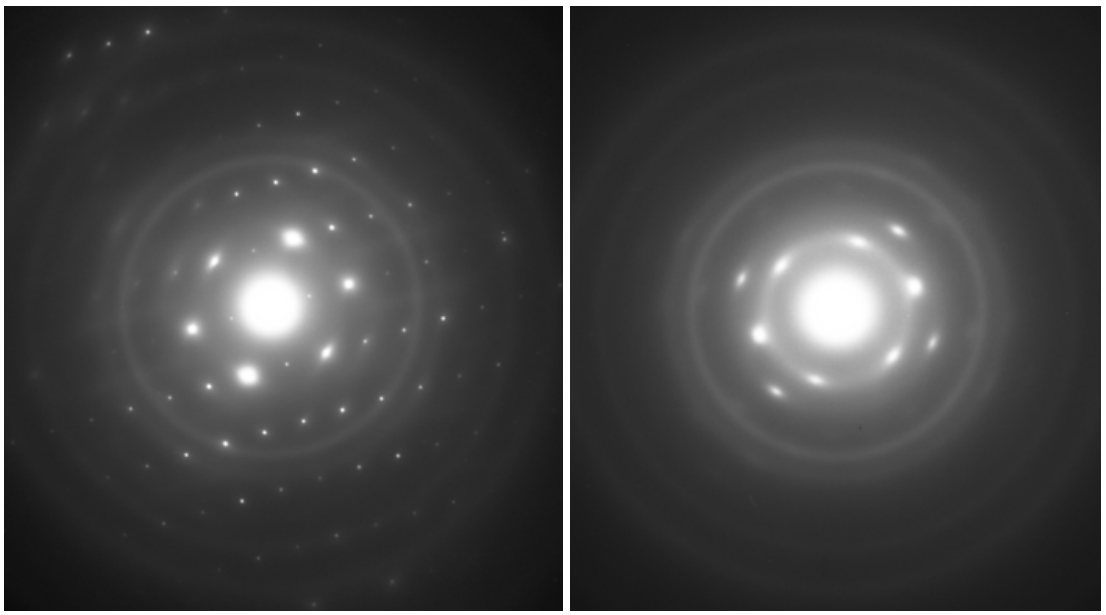

Figure 5.9 Selected area electron diffraction patterns showing beam damage in a sample of p-terphenyl at room temperature. (a) A <001> zone axis electron diffraction pattern of p-terphenyl. (b) The same pattern after approximately 20 minutes of beam exposure. The decrease in the number of diffraction spots indicates that the sample is becoming amorphous.

The beam lifetime of p-terphenyl (the time taken for a diffraction pattern to completely disappear, indicating complete amorphisation of the sample) was found to be approximately 30 minutes at ambient temperature. This is consistent with the previous study which found a beam lifetime of 22 minutes (with an accelerating voltage of 100 kV and a current density of 3.8 x 10^{-4} A.cm^{-2}).[6] Though it was not possible to measure the electron beam current density that samples were exposed to in the current study since the CM30 instrument that was used did not have a Faraday cup, the device required for this measurement, the current density is estimated to be 5 x 10^{-4} A.cm^{-2} (based on a comparison of the beam lifetimes of p-terphenyl in this study and the previous study, and an expected increase in beam stability at 300 kV).

Under similar low flux conditions, the stability of crystals of Form II of theophylline was found to be comparable to that of p-terphenyl. The beam lifetime was measured to be approximately 45 minutes at ambient temperature (slightly better than for p-terphenyl). The diffraction patterns in Figure 5.10 show loss of crystallinity in a sample of theophylline over time.

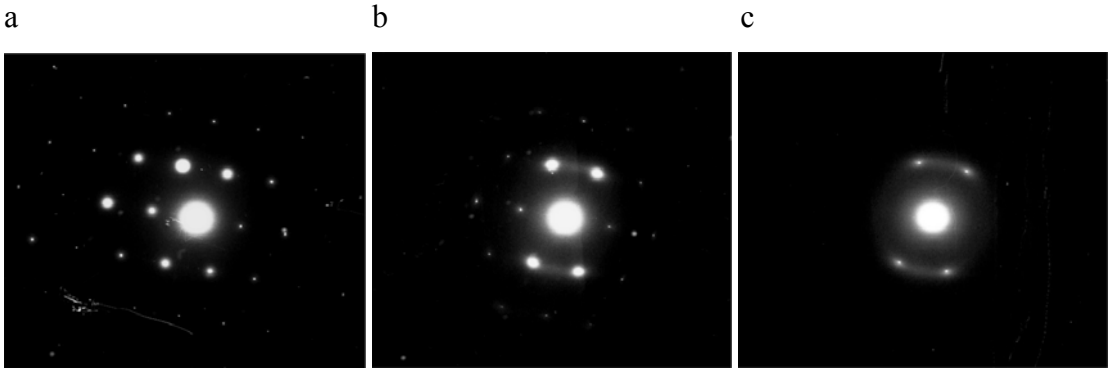

Figure 5.10 Selected area electron diffraction patterns showing beam damage in a sample of Form II of theophylline at room temperature (300 kV). Electron diffraction patterns of the <100> zone axis after (a) 2 minutes, (b) 20 minutes and (c) 40 minutes.

Though this beam damage in theophylline was found to be unavoidable, the rate of amorphisation is relatively slow. In most cases, it was found that beam damage did not significantly hinder analysis by TEM, as it was possible to record several images and diffraction patterns before significant sample degradation had occurred.

The relative stability of pharmaceutical compounds during TEM analysis was found to vary greatly. The stability of many compounds was comparable to that of theophylline, but other specimens rapidly degraded. For example, the beam lifetime of the RS-Ibuprofen:4,4-Bipy cocrystal was found to be less than 1 minute, just enough time to record an image or diffraction pattern. Sample degradation with aspirin was also much quicker than with theophylline. The TEM images in Figure 5.11 show degradation in a plate-like crystal of aspirin over a six-minute period. Bending in the sample was severe, shown by the rapid movement of bend contours across the crystal, and the crystal even shrank in size during analysis due to sublimation.

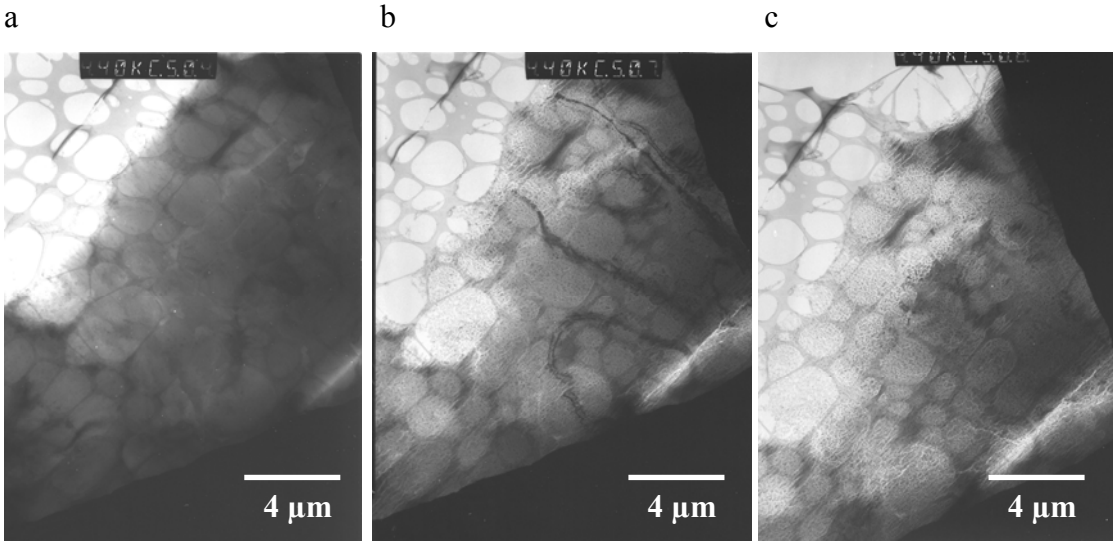

Figure 5.11 TEM images showing beam damage in a sample of Form I of aspirin at room temperature (300 kV). Images were recorded after approximately (a) 2 minutes, (b) 4 minutes and (c) 6 minutes. The sample has moved slightly between the recording of each image.

The rate of beam damage with aspirin crystals was significantly reduced by cooling the sample to -178 °C during analysis, using a liquid nitrogen sample holder. Crystals were stable for several minutes under these conditions allowing better images to be recorded (Figure 5.5a).

Another important consideration regarding the use of TEM as a tool for studying pharmaceutical materials is that samples are held under vacuum during analysis. This means that the characterisation of solvates and hydrates is not usually possible, especially at room temperature. This was demonstrated during the analysis of crystals of RS-ibuprofen sodium dihydrate by TEM. The TEM image in Figure 5.12 shows the effect of vacuum conditions on one of these crystals, the white lines indicating that the crystal has cracked. It is believed that water was lost from the crystal causing a change in crystal form, with an associated reduction in size of the crystal unit cell, and leading to the crack formation. The corresponding electron diffraction pattern could not be indexed to RS-ibuprofen sodium dihydrate, confirming that a form change (dehydration) had occurred. There is no reported crystal structure for anhydrous RS-ibuprofen sodium, so it was not possible to assess whether the electron diffraction patterns were consistent with this form.

a b

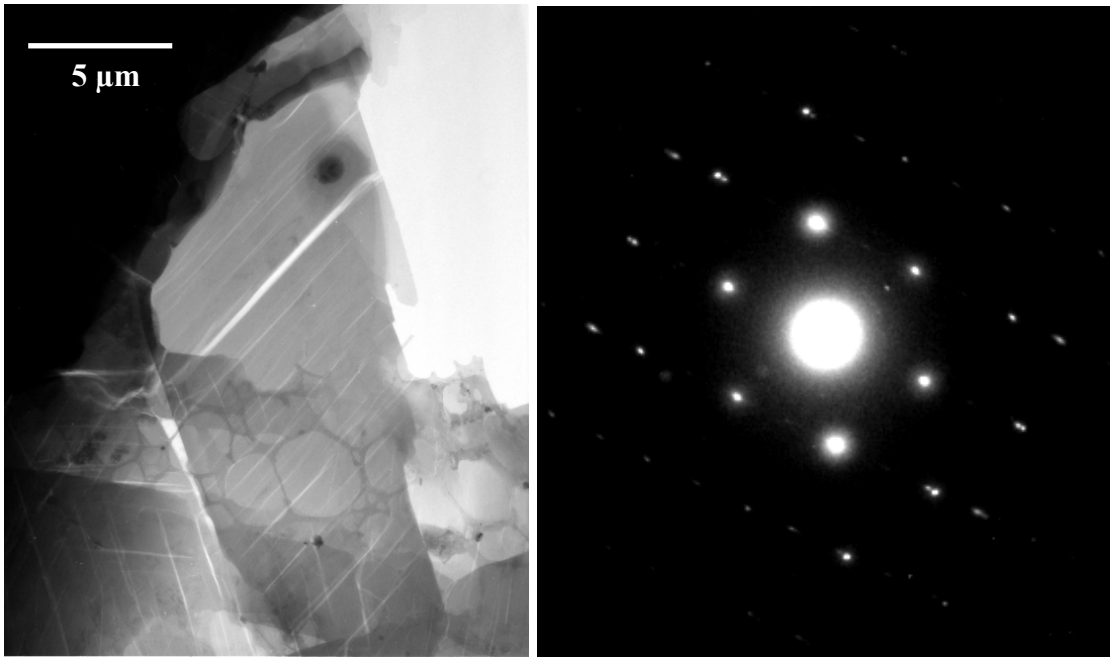

Figure 5.12 TEM analysis of a sample of RS-ibuprofen sodium 'dihydrate'. (a) An image of a crystal of RS-ibuprofen sodium. The white lines are cracks in the crystal, and are an indication that de-solvation has occurred in the TEM instrument. (b) A corresponding selected area diffraction pattern. The pattern could not be indexed to RS-ibuprofen sodium dihydrate, again suggesting that dehydration has occurred.

5.3.3 Comparison of TEM with Other Imaging Techniques

A TEM image of crystallites of Form II of theophylline is shown in Figure 5.13a. The crystals have an unusual triangular plate morphology and sizes ranging from 5 to 20 μm. Differences in brightness across the surface of the large crystal in the image show that it varies in thickness. The TEM sample support grid can also be seen in the image. The dark region to the bottom left is part of the copper grid, and the fainter network of pores seen clearly at the top of the image is the holey amorphous carbon support film on which the crystals are lying. Bend contours are evident on the crystals, and are disrupted in several regions (such as that marked with an asterisk) due to defects. In the region marked with a circle, many of the bend contours cross to form a bend contour pole. At the bend contour pole the electron beam is aligned with a crystallographic axis.

The electron diffraction pattern shown in Figure 5.13b was taken from the region of sample that is circled in Figure 5.13a. Analysis was confined to this region by using a selected area aperture. In this case, the region that was selected was 4 μm in diameter, but it was found to be possible to obtain good diffraction patterns from areas of less than 1 μm^2. All of the electron diffraction patterns presented in this thesis were recorded using a selected area aperture to highlight a region of interest.

a b